Analysis of the Beach and Dune Development in the Hoogheemraadschap Hollands Noorderkwartier Area

MSc Thesis Civil Engineering, Delft University of Technology

B. van Kessel

TU Delft

hoogheemraadschap Hollands Noorderkwartier

HKV LIJN IN WATER

Analysis of the Beach and Dune Development of the Hoogheemraadschap Hollands Noorderkwartier Area

by

B. van Kessel

to obtain the degree of Master of Science
at the Delft University of Technology,
to be defended publicly on 26 October 2022.

Project duration:	18 October, 2021 – 26 October, 2022	
Thesis committee:	Dr. Ir. S. de Vries	TU Delft
	C.O. van Ijzendoorn MSc	TU Delft
	Dr. Ir. J.A.A. Antolínez	TU Delft
	Dr. J.P. Aguilar-López	TU Delft
	C. Wegman MSc	HKV lijn in water B.V.
	Dr. J.K. Leenders	HKV lijn in water B.V.
	Ir. P. Goessen	HHNK

An electronic version of this report is available at `http://repository.tudelft.nl/`.

Cover picture by Inga on Unsplash, 2021

TU Delft

HKV LIJN IN WATER

hoogheemraadschap Hollands Noorderkwartier

Preface

This report of my MSc thesis research marks the completion of my Master's degree in Hydraulic Engineering at the Delft University of Technology. I carried out this research together with HKV Lijn in water and the Hoogheemraadschap Hollands-Noorderkwartier.

I would like to thank my committee members for their advice and support during this research. Thank you, Sierd de Vries for your enthusiasm and guidance during the project. Many thanks to José Antolinez, for helping me set up and learning the basics of a machine learning model. Thank you, Christa van Ijzendoorn and Juan Aguilar López for your useful feedback. Thank you, Carolien Wegman and Jakolien Leenders for your support and positivity that helped me through my research. Thank you Petra Goessen for showing me the practical side of the research and for the field trips to the research area.

Furthermore, I would like to thank HKV for giving me the opportunity to work at their offices and making me feel like part of the team. Special thanks to the colleagues at HHNK, Silvan Hoep for showing me the coast of Texel from a different perspective and Yaron Daniel for the excursion to the Hondsbossche Duinen.

Finally, I would like to thank my family and friends who supported me during my study at the Delft University of Technology. Thanks to my fellow students that made the final period of my Master's a great period and provided me with feedback on the research. I want to thank my friends and roommates for making my study time a great experience. And lastly, many thanks to my parents for providing me with the opportunity to study and obtain my Bachelor's and Master's degree and for giving me their full support.

B. van Kessel

Delft, June 2022

Summary

Dunes are the primary sea defence along the Dutch coast. This research investigated the development between 1965 and 2021 of the beaches and dunes of the Hoogheemraadschap Hollands Noorderkwartier (HHNK) area that stretches from IJmuiden to northern Texel. This research used an advanced data analysis on the annual coastal elevation data. The coastline of the HHNK area is maintained by several measures including nourishments, planting and removal of grass, placing reed fences and building regulations. The aim of this research was to relate the investigated developments of the beaches and dunes to these measures and natural processes.

A literature study was performed first, to get acquainted with the research area and the processes that drive the beach and dune development in the area. In four phases, the developments and their relationships with the drivers were investigated for several subsections of the research area that showed similar behaviour. In phase 1, the coastal profile data was collected for multiple transects spanning the research area. Characteristic parameters describing features of the dune and beach were derived from the coastal profile data. In phase 2, the collected profile data was decomposed into spatial and temporal patterns by a principal component analysis. In phase 3, the transects of the research area were categorised on the temporal development of their coastal profile using the spatial and temporal decomposition results. This created subsections of the coast that showed a similar morphological behaviour. In phase 4, the morphological behaviour of several subsections was investigated and related to the natural and human drivers. The relationships between the drivers and the developments were investigated for several subsections, varying in morphological behaviour and drivers, to gain insight into these relationships for the entire research area.

The coastal categorisation resulted in 36 subsections that were mainly continuous in space with the exception of four clusters. Seven subsections were studied in more detail, by investigating the development of several characteristic parameters derived from the coastal profiles, like dune volume, beach slope and shoreline location among others. The shoreline location and beach width showed a strong correlation with the nourishments. The beach slope and width were expected to influence the dune volume changes, which was not supported by the results. The beach width is assumed to be larger than the critical fetch length and the variations in beach slope had a marginal effect on the transport capacity. The presence of beach pavilions limited the dune growth in both height and volume, but regularly moving the pavilions did allow for a seaward migration of the dune front. The effect of small beach houses on the dune volume change was found negligible. Maintenance works of HHNK influenced the dune development locally. The placement of reed fences caused seaward migration of the dune front and the creation of blow-outs increased the dune volume behind the most seaward dune. The strongest dune volume increase was found at coastal areas behind shoals that reduced the incoming wave energy.

The coastal categorisation succeeded in grouping transects with a similar development of their modified coastal profiles. Several modifications were proposed to improve the categorisation of the original profiles and to take into account smaller scale processes. Nourishment was distinguished as most important driver for the development of the coastal area, which has maintained the shoreline location and caused a trend break in several other characteristic parameters. Human influences like buildings, coastal structures and reed fences have a strong local effect on the development of the beaches and dunes. Further research could take into account wave and wind climate, water level variations and grain size quantitatively to get a more comprehensive study of the relationships between the development and the drivers.

Contents

List of Figures

List of Tables

1 Introduction

The coastline of The Netherlands stretches for more than 400 kilometres along the southeastern part of the North Sea. A large part of the country lies below sea level and is protected by the primary sea defences along this coastline, which are shown in Figure 1.1. Consequently, the safety of many people depends on these sea defences and the Dutch government continuously works to maintain them. In 1990, the Dutch government implemented a new management policy 'dynamic preservation' which changed the maintenance strategy. In this current policy, sand nourishments are supplied to combat coastal erosion and on average the Dutch government supplies 12 million cubic metres of sand each year (Rijkswaterstaat, 2020).

This research focuses on the North Sea coastline of the management area of the Hoogheemraadschap Hollands Noorderkwartier (HHNK). The management area of HHNK covers a large part of the province of Noord-Holland and is shown in Figure 1.2. The North Sea coastline in the HHNK area stretches for 84 kilometres and is divided into two coastal sections, divided by the Texel inlet that connects the North Sea with the Wadden Sea. Coastal section 6 covers the island of Texel which is part of the Wadden coast and coastal section 7 stretches from Den Helder to IJmuiden and is part of the Holland coast. Maintenance work of HHNK guaranteed the flood safety of the low-lying hinterland. More insight into the effect of their maintenance work on the development of the coastline could improve their future strategy.

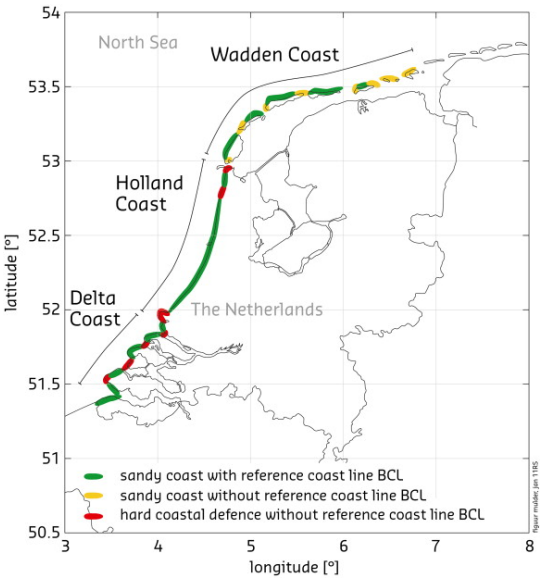

Figure 1.1: Overview of the Dutch coast, including the type of coast and the coastal zones (Mulder et al., 2011).

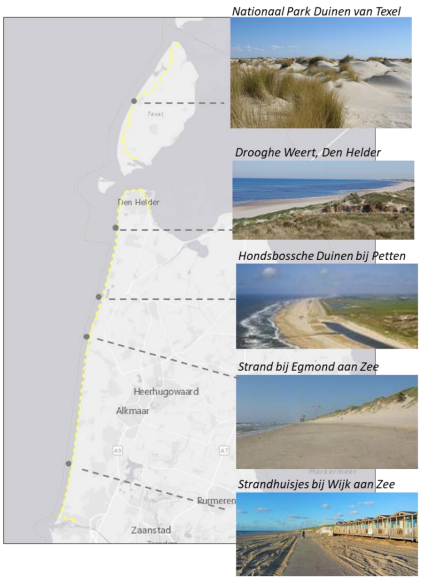

Figure 1.2: Area of the Hoogheemraadschap Hollands Noorderkwartier (Wegman and Leenders, 2020).

HHNK is a regional water authority that is responsible for water safety, water quality, the prevention of water scarcity and safe waterways in their management area (HHNK, 2018). The work of HHNK includes the monitoring, assessment and maintenance of primary and regional water defences to prevent flooding of the land. During dry periods HHNK distributes the water supply with weirs, locks and pumping stations to control the water levels in the management area. During high rainfall, flooding is prevented by improving the discharge rate and providing storage capacity. In addition, HHNK is responsible for 15 sewage treatment plants and the infrastructure that are used to clean the wastewater in the area. Furthermore, the water quality and waterways are maintained by HHNK and the water authority has a crisis management procedure to reduce the impact of calamities.

The dunes of the North Sea coastline are part of the primary flood defences that provide flood safety in the HHNK management area and HHNK is responsible for the monitoring, assessment and management of these dunes. HHNK uses a dynamic coastal management strategy to let the dunes grow with the rising sea level (HHNK, 2021). There are different management strategies for touristic or natural locations and for wide or narrow dunes. At locations where flood safety is not threatened, the transport of sand from the beach and most seaward dune into the dune area is stimulated to increase the ecological value and variation in habitats (Deltares, 2013). This is done by creating blow-outs and the removal of plants that trap the sediment. At locations where flood safety should be increased, HHNK plants grass or places reed fences to trap the sediment which is shown in Figure 1.3. At seaside resorts, there are buildings on the beach that limit the natural growth of the dunes. HHNK determines the location of the buildings and gives regulations for the buildings concerning the period of the year that they are allowed on the beach and the height of the poles supporting the buildings among others. Relocation of the buildings allows for a seaward migration of the dunes and raising the buildings on top of poles allows for the transport of sand below the buildings into the dunes. The large nourishment volumes supplied by Rijkswaterstaat increase the available sediment volume so that sand can be transported into the dunes (STOWA, 2010).

(a) (b)

Figure 1.3: Maintenance works by HHNK to trap sediment in front of the dunes by planting grass (panel a, source: HHNK) and by placing reed fences (panel b, source: Staatsbosbeheer).

Several organisations like HHNK, Rijkswaterstaat and Delft University of Technology have researched processes that affect the beach and dune development in the research area. Elias and Van Der Spek (2006) investigated the long-term development of the Texel inlet and its ebb-tidal delta, which have a large influence on the coastline of the research area. The effect of aeolian transport on the dune development was researched by Wittebrood et al. (2018). De Winter and Ruessink (2017) investigated the effect of sea-level rise on the dune erosion near Egmond and the effect of storms on the dune erosion at Egmond was researched by De Winter et al. (2015).

Since 1965, the Dutch government has done yearly measurements of the Dutch coast as part of the JarKus programme, creating a large dataset with surface elevation data of the Dutch coast. Coastal profiles were derived from the dataset for transects with a spacing of about 250 metres in

the alongshore direction spanning the entire Dutch coast, which was the main input data for this research. The coastal profiles consist of elevation measurements along the transects with a cross-shore interval distance of 5 metres. The large amount of data could lead to new insights into the developments of the Dutch coast. The dataset is used for monitoring the flood safety of the coast and for the determination of the nourishment strategy. Additionally, the dataset has been used for research on the dune volume change due to aeolian transport (de Vries et al., 2012) and the effect of nourishments on dune development (Hallin et al., 2019) among others.

Van Ijzendoorn (2021) developed a toolbox to derive characteristic variables from the JarKus dataset, that were used to describe the development of the beaches and dunes. These characteristic variables include the dune height, beach width and shoreline location among others. The development of the beaches and dunes is described by the temporal changes in these characteristic variables. Research has been done on the dune toe location using the characteristic variables obtained with the toolbox (van IJzendoorn et al., 2021). Figure 1.4 gives an example of the variables that are derived from the coastal profiles.

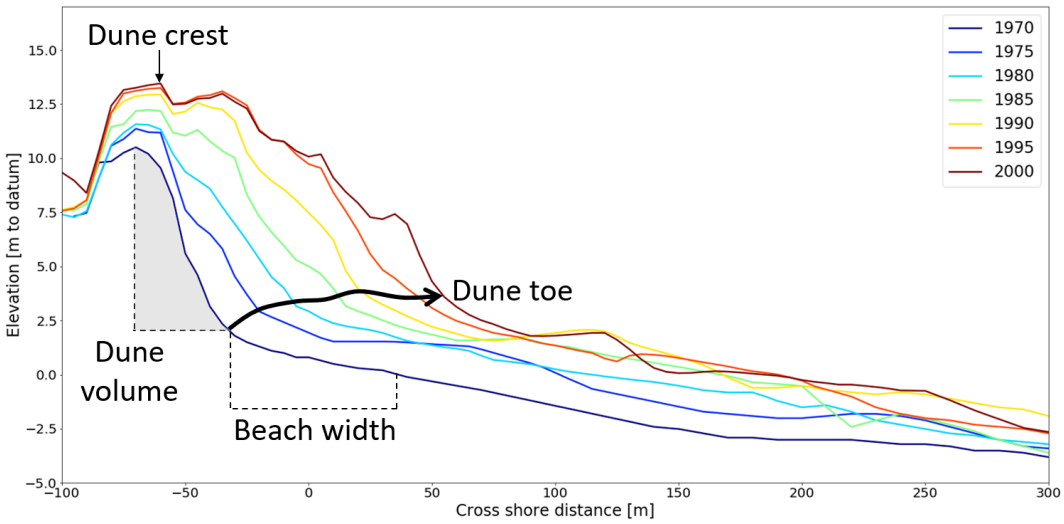

Figure 1.4: Example of the characteristic variables that were derived from the coastal profiles using the JarKus Analysis Toolkit (Van Ijzendoorn, 2021).

The development of the beaches and dunes is driven by several physical processes and human activities (Giardino et al., 2011). Drivers like waves, wind and human interventions act on different spatial and temporal scales and show different behaviour causing linear or cyclic variability of the coast (Stive et al., 2002). Understanding both the coastal behaviour and the processes that drive it is important to determine an efficient management strategy. The drivers are divided into two categories, natural drivers and human drivers. The natural drivers include climate variations, sea-level changes and tidal inlet cycles among others. Nourishments, coastal structures and coastal management are categorised as human drivers.

Since 1965, both computational power and the amount of data increased significantly, which allowed for more advanced data analyses of coastal areas. Research by Plant et al. (2016) coupled the shoreline change to sea-level rise and coastal morphology using a Bayesian network. The model was used to predict the impact of future sea levels based on forecast scenarios. Athanasiou et al. (2021) used a machine-learning algorithm to predict the effect of storms on the morphodynamics of dunes along the Dutch coast. The data was used to create several typological coastal profiles, that represent the Dutch coast. These profiles were used in a probabilistic model to predict dune erosion based on the most important drivers and achieved a good prediction skill.

Zwarenstein Tutunji (2021) used a clustering algorithm to group areas of the Hoogheemraadschap Hollands Noorderkwartier area that showed a similar coastal development. A clustering algorithm is a machine learning algorithm that groups similar samples in a dataset into different subsets (Madhulatha, 2012). The research of Zwarenstein Tutunji (2021) used a set of 29 characteristic variables obtained from the JarKus dataset to cluster different locations. Linear regression was used to analyse the trends of the characteristic variables and reduce the amount of input data. Eventually, five clusters were obtained with three subclusters. It was found that the clustering was mainly influenced by some dominant variables. All the dominant variables of the clustering were found in the foreshore part of the profile, while the management of HHNK focuses on the dry part of the profile. Due to the reduction of input data by linear regression, a lot of information on the development of the coastal profile was lost. In most cases, the coast did not show linear behaviour and human interventions like coastal structures changed the trend before and after the construction. More insight into the development could be found by looking at correlations between physical processes, human interventions and characteristic variables over the entire time series. Zwarenstein Tutunji (2021) did not succeed in coupling the outcomes of the machine learning algorithm with the physical processes that drive the coastal development.

Advanced data analyses of the JarKus dataset have not yet led to useful insights to improve the management strategy of the beach and dune development of the Hoogheemraadschap Hollands Noorderkwartier area. The possibilities of advanced data analysis on large data sets of coastal profiles have not been extensively studied yet. Applying advanced techniques like machine learning to the data set could lead to new insights into the relationships between the drivers and characteristic variables of coastal development.

1.1. Research objective

This research aims to gain more insight into the beach and dune development on the Dutch coast from IJmuiden to the Eierlandsegat, by analysing the JarKus data set with a machine learning algorithm and relating the outcomes to physical processes. The eventual goal is to improve the coastal management strategy with a better understanding of the coastal developments and the effects of human interventions. To achieve this the following main question will be answered:

> What is the expected development of the beaches and dunes of the HHNK area, based on relationships between physical processes and historical developments found with advanced data analysis of the JarKus data set?

The main research question is answered by first answering the following subquestions:

1. Which natural and artificial processes are drivers for the beach and dune development of the research area?
2. Which parts of the research area can be clustered together based on similarities in beach and dune development?
3. To what extent can the relationships between the drivers and the characteristic variables describe the observed beach and dune developments of the different clusters?
4. To what extent can the future development of the beaches and dunes of the research area be predicted based on relationships between physical processes and characteristic variables?
5. How can the insights into predicted future developments improve the coastal management strategy of the Hoogheemraadschap Hollands Noorderkwartier?

1.2. Thesis outline

This report starts with a detailed description of the research area in Chapter 2. A literature study was performed to get acquainted with the research area and its development over time. The chapter presents both the observed morphological developments of the area and some of the physical processes and human activities that affected the development.

Chapter 3 describes the method that was used to answer determine the relationships between the drivers and the beach and dune development. First, the collection of the required data and modifications of the data are described in Section 3.1. A principal component analysis, described in Section 3.2, was performed on the dataset to investigate the spatial and temporal variability in elevation in the research area. The coastal categorisation model and its input are reported in Section 3.3. The method to derive the relationships is described in Section 3.4.

Chapter 4 presents the results of the different phases. The first section gives an explanation and a graphical representation of the different modes derived by the spatial and temporal decomposition. Secondly, Section 4.2 gives an overview and evaluation of the identified clusters and their spatial distribution. The results of a more detailed analysis of several clusters are presented in Section 4.3. In addition, this section presents the relationships between the drivers and the development that were found in the clusters.

Chapter 5 presents a discussion of the results. The results of the spatial and temporal decomposition are discussed first in Section 5.1. The discussion of the obtained clusters and their spatial distribution is presented in Section 5.2 followed by the discussion of found relationships between the drivers and the beach and dune development in Section 5.3. A short discussion of the future development is presented in Section 5.4.

Finally, Chapter 6 gives the conclusions and recommendations for this research. This chapter reflects on the research questions and the answers that were found. Additionally, Section 6.2 gives recommendations for improvements on this research and further research on this topic

2

Research area

This chapter describes the research area and the drivers that influence the development of its beaches and dunes. The research area comprises the coastline of the Hoogheemraadschap Hollands Noorderkwartier (HHNK) area which covers coastal sections 6 and 7 of the Dutch coast (Rijkswaterstaat, 2021). The topography of the research area is shown in Figure 2.1. Section 2.1 presents information on the North Sea and the Wadden Sea that affect the coast of the research area. Section 2.2 gives an overview of coastal section 6, that covers the coastline of the barrier island Texel. Section 2.3 gives an overview of coastal section 7 that covers the coastline from Den Helder to IJmuiden. The different processes that drive the development of the beaches and dunes in the research area are presented in Section 2.4.

2.1. The North Sea and the Wadden Sea

The North Sea is a shallow sea with a mean depth of 80 metres and the northern part has a broad connection to the North Atlantic. In the South, it is connected to the Atlantic through the narrow Straight of Dover. Due to the shallow topography of the North Sea and the narrow strait at the southern end, storm surge levels can get very high in the Southern North Sea during a constant northerly wind (Sündermann and Pohlmann, 2011). The geometry of the North Sea resonates with a semi-diurnal tidal cycle and has tidal ranges over 4 metres. The bathymetry and tidal ranges are shown in Figure 2.2.

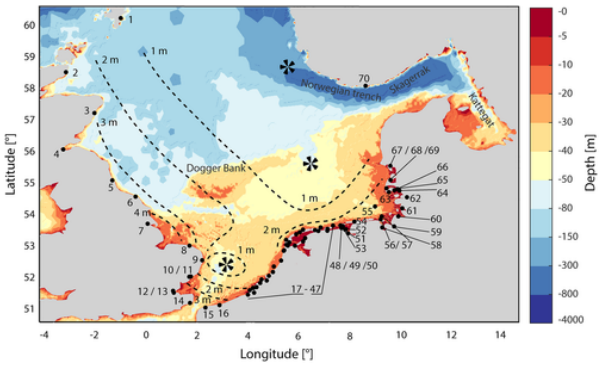

Figure 2.2: Bathymetry of the North Sea and the tidal ranges (Jänicke et al., 2021).

Figure 2.1: Altitude map of the research area, obtained from the coastviewer (Deltares, 2018).

The Wadden Sea lies behind several barrier islands and has a very shallow topography. During low tide, large mudflats in the Wadden Sea fall dry. Sea level rise and human interventions have caused a sediment demand in the Wadden Sea, which causes sediment import from the North Sea (Wang et al., 2012). The closure of the former Zuiderzee, through the construction of the Afsluitdijk in 1932, had a significant effect on the morphodynamics of the Wadden Sea (Oost and Kleine Punte, 2003). The tidal amplitude increased due to the decrease in basin length, which also caused an increase in the tidal prisms through the tidal inlets. Figure 2.3 shows the bathymetry in the Wadden sea.

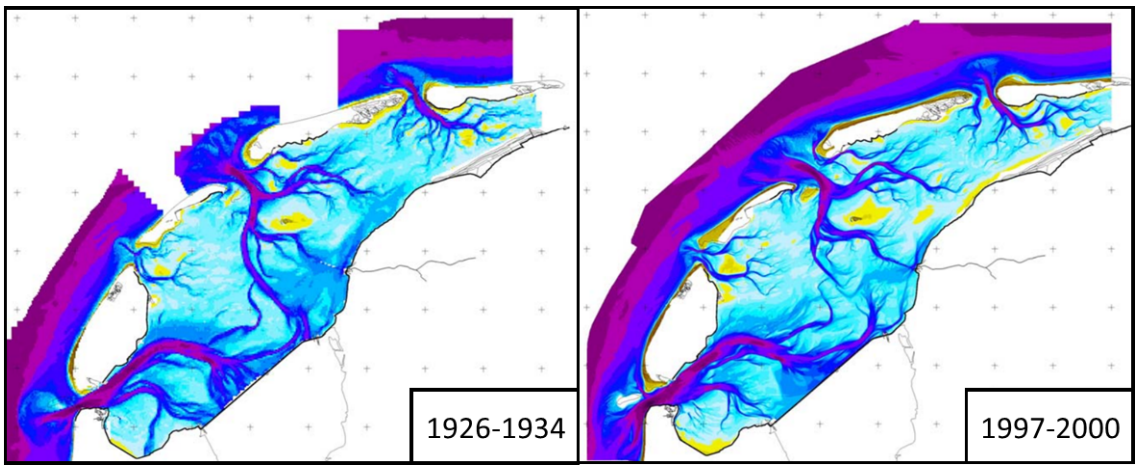

Figure 2.3: Historical development of the bathymetry of the Wadden Sea after the closure of the Zuiderzee (Oost and Kleine Punte, 2003).

The largest tidal inlet of the Dutch Wadden Sea is the Texel inlet (Elias and Van Der Spek, 2006). The Texel inlet separates the island of Texel from the mainland and is shown in more detail in Figure 2.4. The Helderse Zeewering, constructed around 1750, stabilises the southern embankment of the tidal inlet and increased flow velocities around the sea defence increasing the depth of the channel (Elias et al., 2014). The ebb-tidal delta of the Texel inlet stretches 10 km seaward and 25 km alongshore (Elias and Cleveringa, 2003). The ebb-tidal delta consists of northern and southern tidal channels separated by a large flat, the Noorderhaaks. The northern channel of the ebb-tidal delta is migrating landward causing erosion at the southern coast of Texel (Elias et al., 2014). The southern channels of the ebb-tidal delta stretch along the coast of Noord-Holland. In 1956 the main southern channel, Schulpengat, split into two channels, the western, flood-dominated channel Schulpengat and the eastern, ebb-dominated channel Nieuwe Schulpengat (van Santen, 1999). Landward migration of the Nieuwe Schulpengat caused coastal erosion on the coast of Noord-Holland. The flood-tidal delta of the Texel inlet is connected to another large inlet of the Wadden Sea, Zeegat van het Vlie, and the higher tidal amplitude of Zeegat van het Vlie causes a residual seaward flow through the Texel inlet (Ridderinkhof, 1988).

A smaller tidal inlet, Eierlandse Gat separates Texel from its neighbouring barrier island Vlieland. The tidal basin of the Eierlandse Gat has a much smaller tidal prism and surface area than the Texel inlet and Zeegat van het Vlie (Louters and Gerritsen, 1994), which can also be seen in Figure 2.3. The northern part of Texel, Eierland, experienced structural erosion of about 600 000 $m^3/year$ around 1990 which led to the construction of the Eierlandse dam (Van Heuvel, 1999). The 800 metres long Eierlandse dam was constructed in 1995 and caused large sediment depositions on both sides of the dam, ending the structural erosion of the northern coast of Texel.

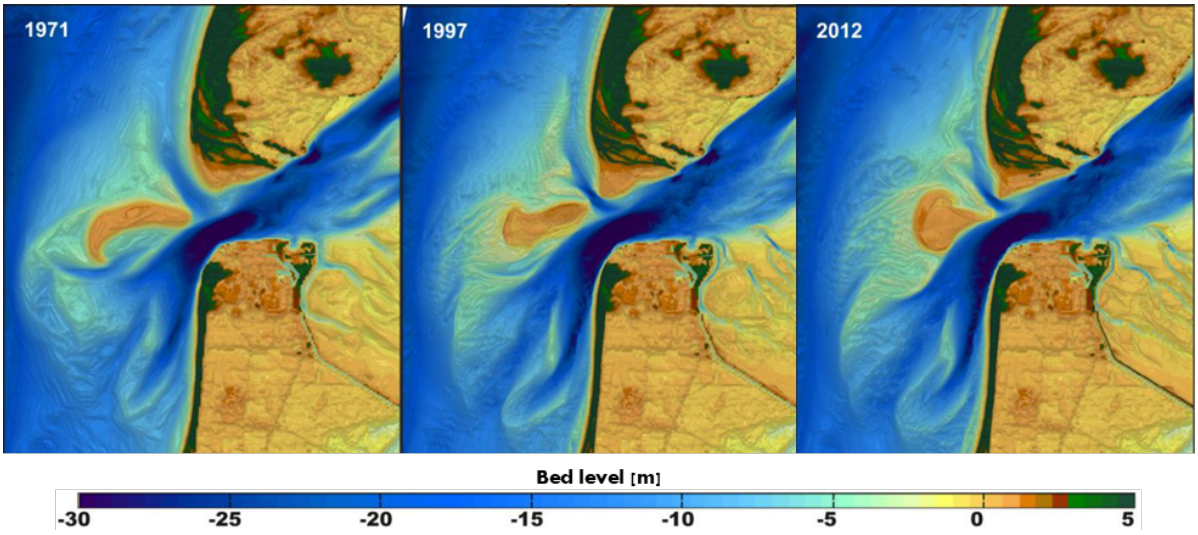

Figure 2.4: Development of the Texel inlet between 1971 and 2012 (Elias and Van Der Spek, 2006).

2.2. Texel

The barrier island Texel is the most northern part of the research area and is separated by the Eierlandse Gat and the Texel inlet as described above. The 'Beheerbibliotheek Texel' by Elias et al. (2014) was used to describe the observed coastal developments of Texel in this section. Elias et al. (2014) divided the island into three subsystems: Noorderlijke Uitlopers van de Noorderhaaks (NUN) and Hors (section A), the island coast and De Slufter (section B) and the region between De Slufter and Eierlandse gat (section C). The island of Texel and the locations of its subsystems are shown in Figure 2.5.

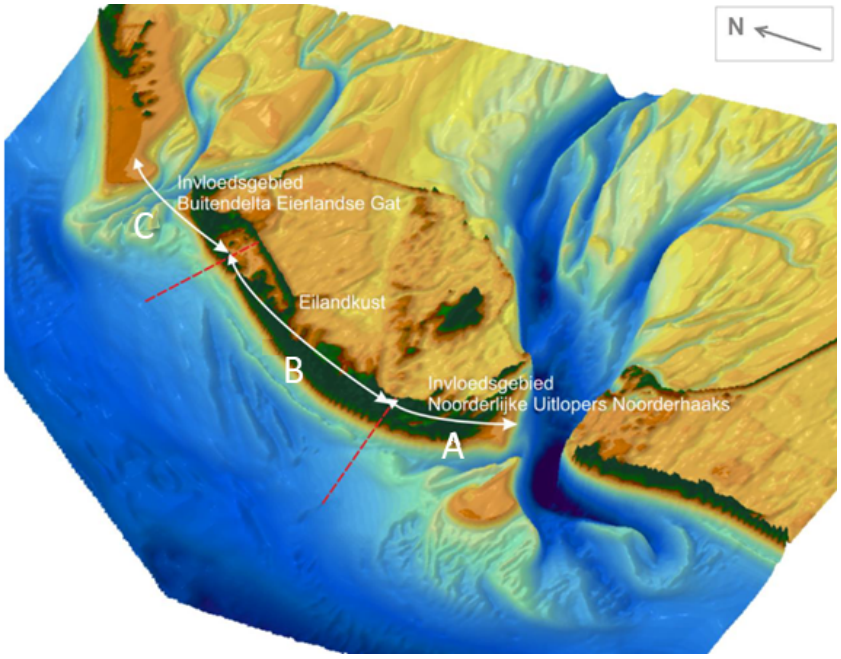

Figure 2.5: The island of Texel divided into three subsystems (Elias et al., 2014) A) Hors and Noorderlijke Uitlopers van de Noorderhaaks (NUN), B) Island coast and De Slufter, C) between De Slufter and Eierlandse gat.

A - Hors and Noordelijke Uitlopers van de Noorderhaaks

The southern part of Texel is mainly influenced by the Texel inlet and its ebb-tidal delta. An overview of subsystem A is shown in Figure 2.6. The figure shows three lines representing the mean high water line (dark blue), the dune foot position (brown) and the border of the sea defence (red). The Hors is the southern part of Texel and borders the Texel inlet. It has relatively broad beaches and is very dynamic. The dunes on the Hors have many blow-outs and sand can be easily transported through the most seaward dunes by aeolian transport. Rijkswaterstaat no longer has a base coastline for this part of the coast and no maintenance works are performed on this part of the coastline.

Between 1965 and 1990, a landward migration of the Marsdiep, the main tidal channel of the Texel inlet, was observed while the low water line of the southern part of the Hors migrated seaward. After 1990, the migration of the Marsdiep and the Hors changed in the opposite direction. The western part of the Hors is mainly influenced by the northern channel of the Texel inlet, the Molengat, which showed movements similar to the Marsdiep. Between 1965 and 1990 the Molengat increased in depth from -15m NAP to -24m NAP while migrating 500 metres landward. After 1990, it migrated in opposite direction with large sedimentation volumes in the deepest part of the channel causing a decrease in the depth of the channel and erosion at the Hors and the adjacent coastline. The landward movement of the Molengat created very steep slopes near the coast and is seen as the main reason for the recent structural erosion of the southern coast of Texel. The NUN is expected to meet the coast in the future increasing the sand volume near the coast. To counter the erosion of the coast north of the Hors, 22 groynes were constructed between 1957 and 1987 and the groynes have reduced but did not stop the coastal erosion in this area (Elias and van der Spek, 2017).

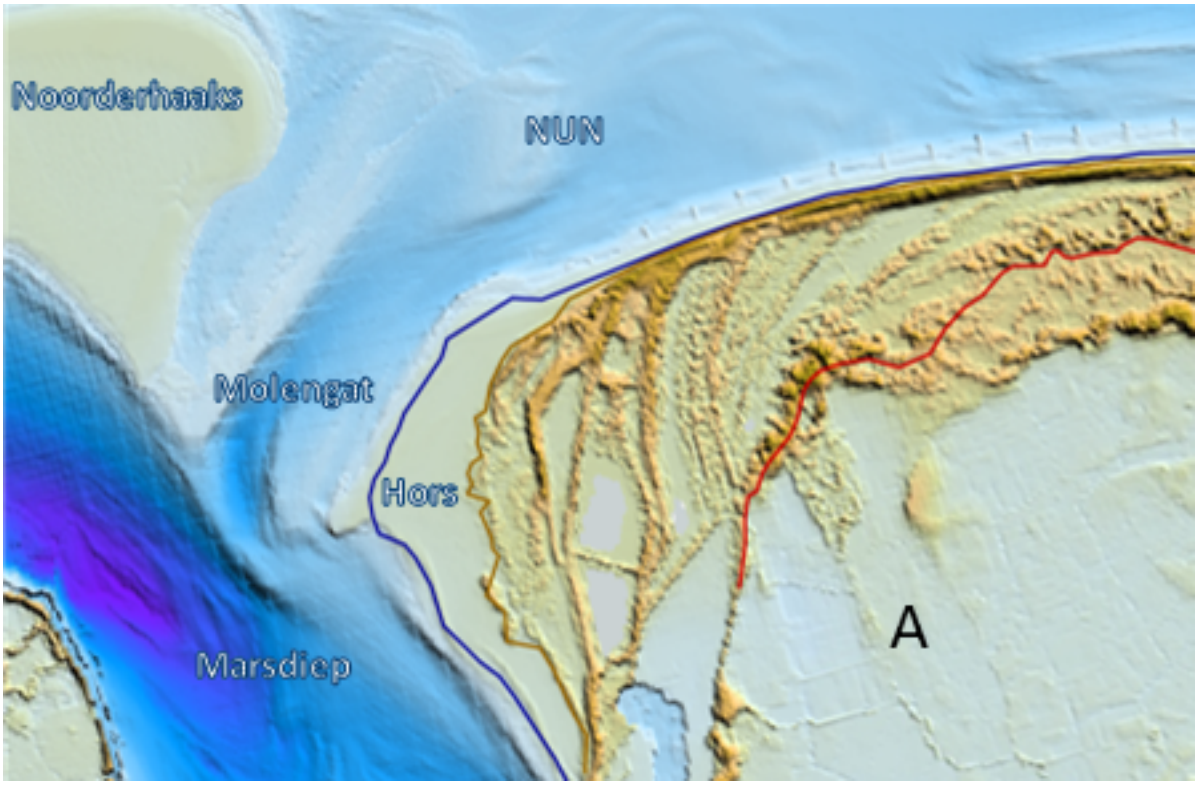

Figure 2.6: Overview of subsystem A, the Hors and the NUN, showing the mean high water line (dark blue), dune toe location (brown) and the border of the sea defence (red) (Deltares, 2018).

B - Island coast and De Slufter

The southwest coast of Texel is influenced by the ebb-tidal delta of the Texel inlet. Steijn and Jeuken (2000) modelled the sediment transport of southwest Texel by using numerical software which was investigated by Cleveringa (2001). A conceptualised visualisation of the sediment transport along the southwest coast of Texel is shown in Figure 2.7. Waves transport sediment from the Noorderhaaks northward along the NUN, this causes the NUN to move in the northern direction. Around beach pole 13, a divergence point is present due to the curved shape of the coastline, the average wave direction and the refraction caused by the shallow NUN. The sediment transport away from this divergence point results in structural erosion. The northern movement of the NUN changes the refraction of the waves and causes a northern shift of the divergence point. Some sediment from the NUN is also transported landwards over the NUN, but this sediment does not reach the southwestern coast of Texel as it is transported through the Molengat.

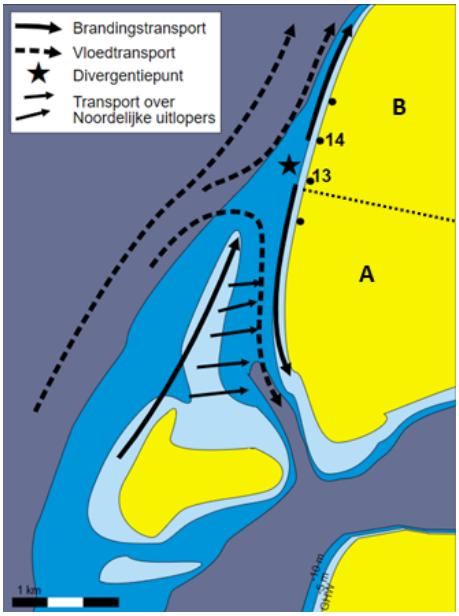

Figure 2.7: A conceptualised figure of the sediment transport directions along the coast of southwest Texel under yearly averaged wave conditions (Cleveringa, 2001).

The transport of sediment due to tidal flow is shown in Figure 2.7. During flood tide, sediment is transported through the Molengat towards the Wadden Sea, while sediment is transported northward along the Texel coast. The divergence point for the tidal transport lies around beach pole 11 which means that sediment is eroded around beach pole 11 during flood tide and sedimentation occurs during ebb tide. It is not clear whether the tidal currents cause net sediment transport.

The long rather straight stretch of coast from the NUN to De Slufter shows an erosive trend between 1965 and 2012. In volume measurements presented by Elias et al. (2014) it can be seen that both foreshore and beach sediment volumes decrease until 1990. In 1990, Rijkswaterstaat started with the dynamic preservation strategy and large nourishments were supplied to the coast. The graphs of the beach volumes of the straight coast (areas 3 and 4, shown in Figure 2.8) have a clear sawtooth caused by the nourishments, with an increase in volume due to the nourishments and a gradually decreasing volume until the next nourishment.

Around beach pole 25 the primary dune line is interrupted by a small inlet into De Slufter, a small dune valley and nature reserve. De Slufter is over a hundred years old and the area is continuously changing due to the forcing of the North Sea. The largest part of De Slufter is just above sea level

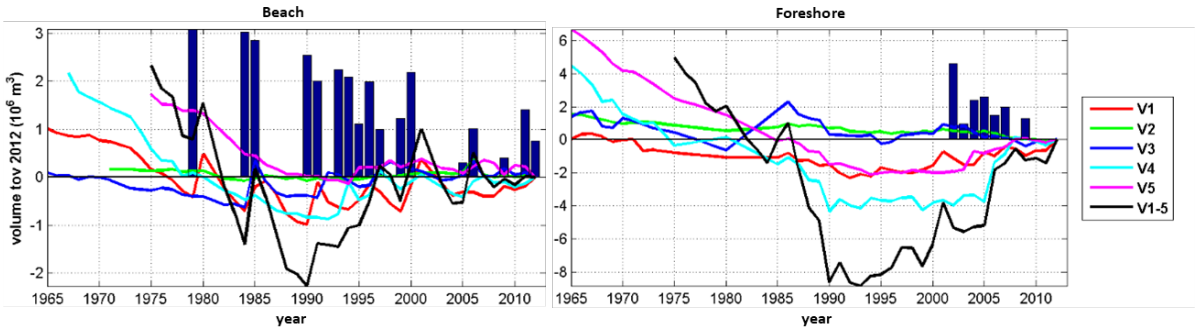

Figure 2.8: Beach and foreshore volume changes along the coast of Texel. Areas 3 and 4 cover the straight coast of Texel and nourishment volumes are shown by the blue bars (Elias et al., 2014).

and floods during storm surges and spring tides. One of its purposes is to reduce the incoming wave energy to protect the dunes behind it. The mouth of De Slufter is naturally moving northward and since 1973, the current position is maintained by human interventions. Broadening and movement of the mouth could increase the wave impact on the dunes and exceed the safety level during design storm conditions (van Rooijen and van Thiel de Vries, 2014). The foreshore near De Slufter shows fluctuations of sandbanks similar to the island coast. The dunes near De Slufter show a seaward trend and new foredunes have formed. The MCL had a landward trend and exceeded the BCL, but nourishments are not supplied to prevent De Slufter from silting up.

C - De Slufter to Eierlandse Gat

Subsystem C covers the northern coast of Texel and is influenced by the tidal inlet Eierlandse gat that separates Texel from Vlieland. The northern part of Texel was a separate island until it was connected with a sand dike in the 17th century. Bolwerk Robbengat and Bolwerk Eierland were constructed in 1948 and 1956 respectively, to reduce the southern migration of the southern channel of the Eierlandse Gat. In 1995 the northwestern point of Texel was reinforced by the construction of the Eierlandse Dam, which stretches 800 metres seaward perpendicular to the coast. The Eierlandse Dam captured sediment which created a wide beach and reduced the required amount of nourishments. An overview of the area is shown in Figure 2.9.

The coastline between De Slufter and the wide beach near the Eierlandse Dam had a landward migration until 1980. Intensive nourishing of the coastline caused the coastline to migrate seaward. The nourishments caused a sawtooth signal with the coastline migrating seawards after nourishment and gradually migrating landward until the next nourishment was supplied.

The coast on the south side of the Eierlandse Dam showed a clear trend of landward migration until 1995. Nourishments supplied in this area did not reduce the landward migration significantly. After the construction of the Eierlandse Dam, the coastline migrated seaward and the broad beach remains stable to date. The dune foot location remained stable around the location of Bolwerk Eierland. The north side of the Eierlandse Dam showed similar developments, a landward migration of the coastline before construction and a seaward migration after. The northeast side of Texel, around Bolwerk Robbengat, has a steep slope towards the channel of the flood-tidal delta. Before 1997 the channel increased in width and depth, while the location of the channel remained stable.

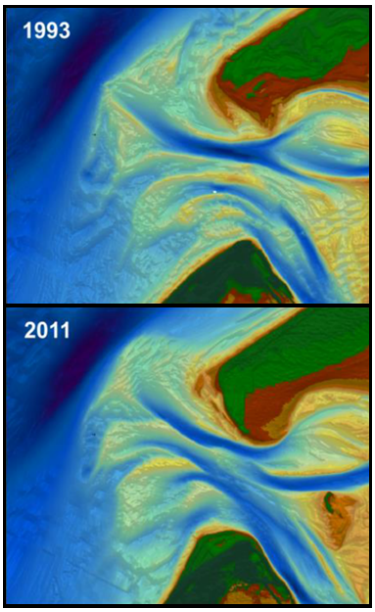

Figure 2.9: Development of the Eierlandse Gat after construction of the Eierlandse Dam (Elias et al., 2014).

2.3. Noord-Holland coast

The Noord-Holland coast (coastal section 7) is shown in Figure 2.10 and stretches from Den Helder to IJmuiden. The information to describe the research area of the Noord-Holland coast was obtained from (Elias and Bruens, 2013). The southern border of the area is the port of IJmuiden, a breakwater protecting the port from waves blocks the longshore transport creating a physical border with coastal section 8. The biggest coastal structures along the Noord-Holland coast are described first followed by a description of several subsections of the coastal section. Elias and Bruens (2013) used the subsections defined by Van Rijn (1997) to describe the observed developments of the Noord-Holland coast. The information in this section made use of the work of Elias and Bruens (2013) and is therefore described using the same subsections of the Noord-Holland coast.

Coastal structures

The coastline was reinforced by the construction of multiple groynes between the Hondsbossche en Pettemer Zeewering (HPZW) and Den Helder, the construction of these groynes finished in 1935. The effectiveness of the groynes was studied by Verhagen and van Rossum (1990) and they stated that the groynes did not reduce the erosion of the coast. Since 1990 the coastline is maintained by supplying sediment to the coast.

The most northern part of the Noord-Holland coast is protected by the Helderse Zeewering. In the 17th century, wooden poles and fascine mattresses were used to reduce the coastal erosion near the sea dike. In the 18th century, the coast was reinforced by a stone sea defence, which stopped the southward migration of the Texel inlet. After construction the depth of the tidal channel increased as the sediment at the toe of the structure was eroded. Erosion of the channel decreases the stability of the Helderse Zeewering and therefore it was periodically reinforced by dumping stones at the toe. In 2007 a large nourishment was placed on the landward side of the channel to guarantee the stability of the sea defence.

Part of the Noord-Holland coast, near Petten, was protected by a sea dike, Hondsbossche en Pettemer Zeewering (HPZW) instead of dunes. The HPZW was constructed to fill the gap in the dune system that was created by storms in the past. Groynes were constructed to reduce erosion at both ends of the dike. The HPZW was reinforced in 2015 when the Hondsbossche Duinen were created using a total of 35 million cubic metres of sand to create new dunes that serve as primary sea defence (Bodde et al., 2019).

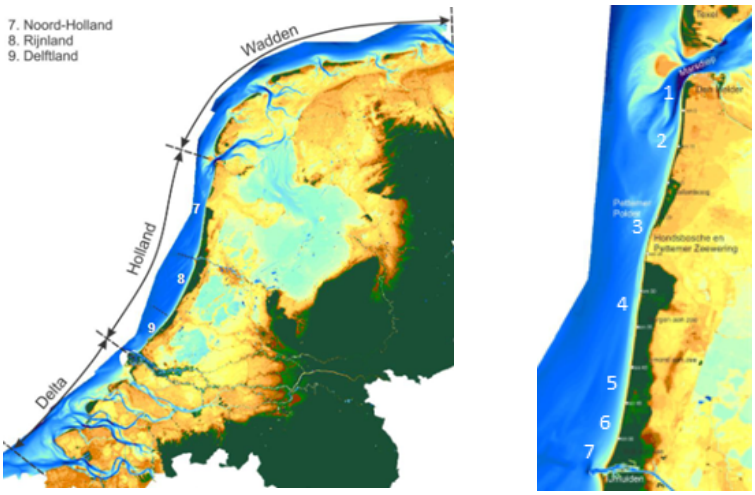

(a) (b)

Figure 2.10: Overview of the Dutch coast with the three different coastal regions and the three coastal sections of the Holland coast (a). A more detailed overview of coastal section 7 in (b) (Elias and Bruens, 2013).

Subsection 1 (km 0 - 8.1)

Subsection 1 stretches from the Texel inlet to Julianadorp and is mainly influenced by the Nieuwe Schulpengat (Figure 2.11, left). The northern part of this subsection has a very steep slope because the tidal channel Breewijd lies directly against the coast. Nourishments supplied since 1990 cause the MCL to migrate seaward, but erosion rates are increased after the nourishment. The high erosion rate requires frequent nourishment to maintain the coastline. Further to the south, the coast is eroding due to the landward migration of the Nieuwe Schulpengat. A platform at -12m NAP separated the Nieuwe Schulpengat from the coast, but this platform is no longer present due to erosion. The platform can still be seen further south around km 6. The southern part, from km 6, shows a seaward migration while the nourishment volumes in this area were limited.

Subsection 2 (km 8.1 - 16.3)

Subsection 2 stretches from Julianadorp to Zwanenwater and is outside the ebb-tidal delta of the Texel inlet (Figure 2.11, centre). Morphological changes in this area are smaller than in subsection 1 which is influenced by the inlet. This subsection of the coast shows only slight alongshore differences. It has a relatively shallow nearshore and it is protected by groynes stretching 200 metres seaward. The coast is characterised by a single sandbank which shows alternating seaward and landward trends. Intensive nourishment in the area caused seaward migration of the MCL in most parts of the subsection. The most southern part shows a negative trend and the supplied nourishments have not effectively moved the MCL seaward of the BCL.

Subsection 3 (km 16.3 - 28)

Subsection 3 covers the coastline that is protected by the Hondsbossche en Pettemer Zeewering (HPZW) and the developments in this area are influenced by the interaction with the HPZW (Figure 2.11, right). This subsection is characterised by a single sandbank with a relatively stable location of around 200m-250m RSP (RSP is a local reference line along the Dutch coast). Many nourishments were supplied in this subsection which also affected the sandbank cycles. The nourishments effectively maintained the coastline and the MCL did not exceed the BCL. The sandbanks south of the HPZW showed a different behaviour, sandbanks in this area migrated seaward and damped out, and new sandbanks were formed near the coastline creating a cycle.

In 2015, new dunes were created to reinforce the HPZW by supplying a total of 35 million cubic metres of sand to the coast in this subsection, see Figure 2.12. By creating new dunes, the government and other involved parties hope that the dunes would grow along with the sea level rise to guarantee flood safety. According to Leenders et al. (2018) the dunes were expected to grow by about 35 $m^3/m/year$ in the first three years due to aeolian sand transport. Observations in the three years after the construction of the dunes show an average dune growth of 33 $m^3/m/year$, close to the expected value. The secondary goals of the project were to create favourable conditions for nature and increase the amenity value (Bodde et al., 2019).

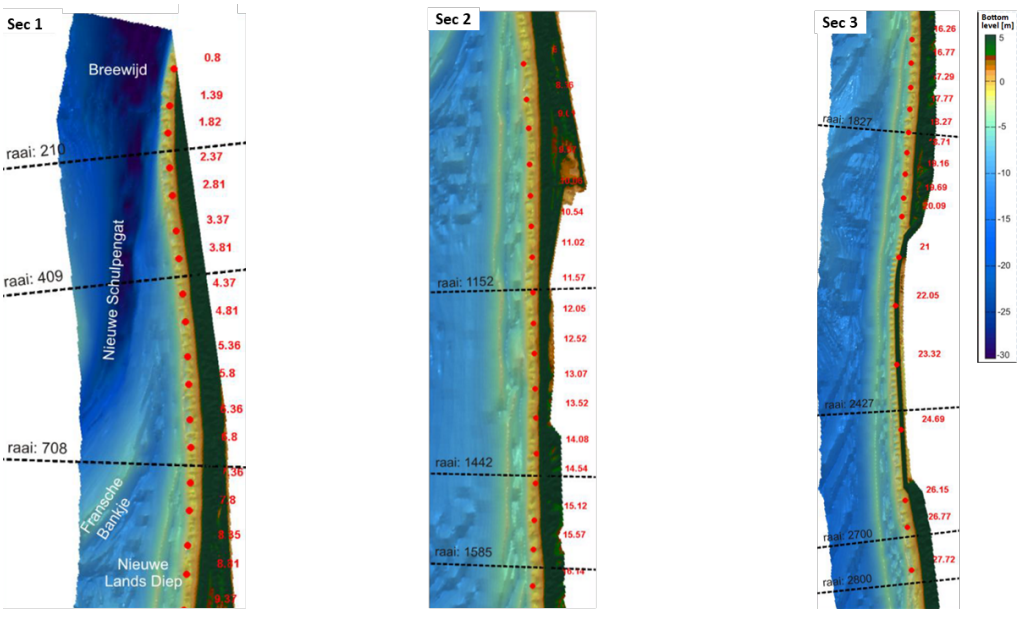

(a) (b) (c)

Figure 2.11: Overview of subsections 1 (a), 2 (b) and 3 (c) of coastal section 7, Noord-Holland coast. The figure shows the topography observed in 2012 (Elias and Bruens, 2013).

Figure 2.12: Image of the newly constructed Hondsbosche Duinen next to the HPZW (Picture by: Rini van der Pol).

Subsection 4 (km 28 - 39)

Subsection 4 stretches from Bergen to Egmond and is shown in Figure 2.13. Bergen and Egmond are tourist locations and the beaches of these villages were frequently nourished hindering beach recreation (Boers, 1999). Both villages also have buildings close to the beach that limit the width of the dune area and produce additional safety requirements. The additional safety requirements cause a seaward shift of the BCL around the villages compared to the rest of this coastal section. According to Boers (1999) erosion rates around these villages are higher due to the further seaward-extending coastline and the rip currents. Because the shoreline extends further seaward a lot of sediment is transported to the adjacent coast restoring the natural position of the shoreline.

The entire coastline of subsection 4 shows multiple sandbanks during the entire measurement period between 1965 and 2012. Before nourishing the coastline the sandbanks mainly showed a seaward migration while the shoreline showed an erosive trend with an erosion rate of about 0.2 million $m^3/year$. Since 1990, the sandbanks show cyclic behaviour and the sedimentation rate of the coastline increased to about 0.5 million $m^3/year$.

Subsection 5 (km 39 - 47)

Subsection 5 stretches from Egmond to Castricum (Figure 2.13, centre). The subsection is very stable and its developments are dominantly influenced by the movement of the sandbanks. The coastline shows a cyclic fluctuation caused by the seaward migration of the sandbanks. The subsection shows a positive trend in sand volume over the entire measurement period between 1965 and 2012. Sedimentation volumes are the largest in the northern part of the subsection, which is probably caused by the large nourishment volumes at the coast of Egmond.

Subsection 6 and 7 (km 47 - 55)

Subsections 6 (Figure 2.13, right) and 7 stretch from Wijk aan Zee to IJmuiden and the developments in these subsections are mainly influenced by the breakwater of the port of IJmuiden. The coast of subsection 6 and the port of IJmuiden are shown in Figure 2.14. The breakwater was constructed between 1867 and 1876 and the coastline is still migrating towards the new equilibrium. The breakwater interrupts the longshore sediment transport which led to the deposition of large volumes of sediment close to the breakwater which can be seen in Figure 2.14. The MCL had a maximum seaward migration of 285 metres at the breakwater between 1965 and 2012. The accretion area stretches up to 3 kilometres north of the breakwater. The coastline showed an erosive trend further north of the accretion area, but the erosion volumes were significantly smaller than the sedimentation volumes in the accretion area.

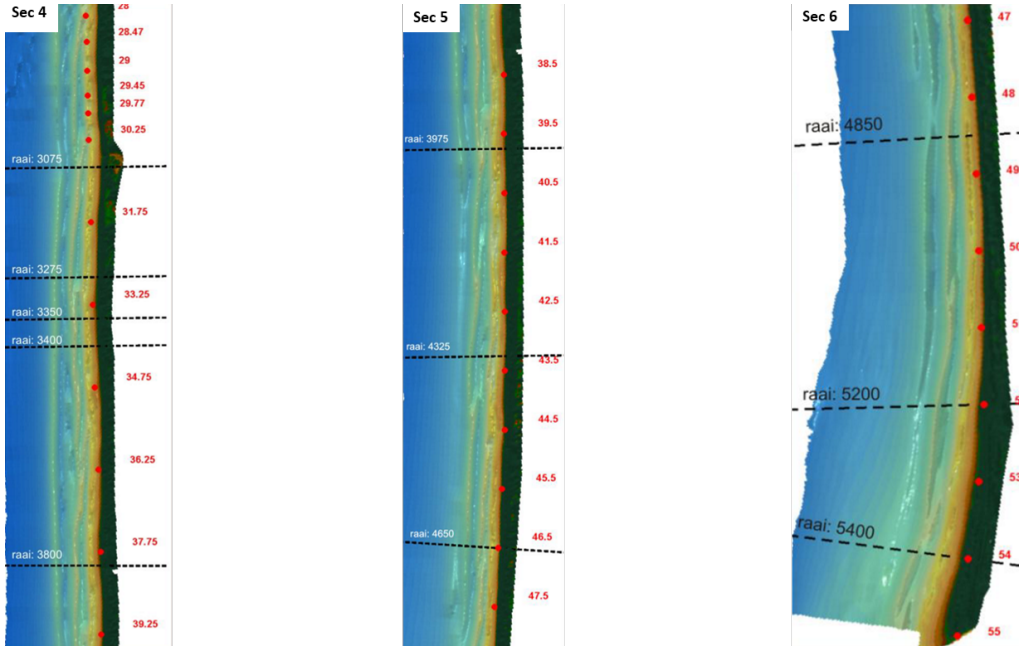

(a) (b) (c)

Figure 2.13: Overview of subsections 4 (a), 5 (b) and 6 (c) of coastal section 7, Noord-Holland coast. The figure shows the topography observed in 2012 (Elias and Bruens, 2013).

Figure 2.14: Picture taken in 1993 showing the coastline north of the port of IJmuiden, which clearly shows the large sedimentation area next to the breakwater. (source `https://beeldbank.rws.nl/`)

2.4. Drivers

The first step in answering the research questions was identifying the processes that drive the beach and dune development in the research area. This section presents the relevant drivers for this research that were identified by a literature study. This research used the JarKus dataset that contained annual measurements of the coastal profiles for 57 years. Therefore, the relevant drivers, that are observable in the dataset, act on a time scale in the range of several years to several decades. The drivers were divided into two categories, the natural drivers described in Subsection 2.4.1 and the human drivers described in Subsection 2.4.2.

2.4.1. Natural drivers

The most important natural drivers of shoreline change were described by Stive et al. (2002) and are shown in Table 2.1. The investigated drivers act on a timescale ranging from several years to several decades which corresponds to the long-term and middle-term timescales in Table 2.1. This subsection gives a short description of aeolian transport that affects dune growth (Durán et al., 2011) and several drivers in the long-term and middle-term timescales. The tidal inlet cycles of the Texel inlet and the Eierlandse Gat were described in Section 2.1.

Table 2.1: Most important natural drivers and typical evolutions for shore and shoreline variability and their timescales. Obtained from Stive et al. (2002).

Scale	Natural causes/factors	Typical evolutions
Very long term (time scale: centuries to millenia; space scale: ~ 100 km and more)	⇒ 'sediment availability' ⇒ relative sea-level changes ⇒ differential bottom changes ⇒ geological setting ⇒ long-term climate changes ⇒ paleomorphology (inherited morphology)	⇒ (quasi-)linear trends ⇒ trend changes (reversal, asymptotic, damping) ⇒ fluctuations (from (quasi-) cyclic to noncyclic
Long term (time scale: decades to centuries; space scale: ~ 10–100 km	⇒ relative sea-level changes ⇒ regional climate variations ⇒ coastal inlet cycles ⇒ 'sand waves' ⇒ extreme events	⇒ (quasi-)linear trends ⇒ fluctuations (from (quasi-) cyclic to noncyclic) ⇒ trend changes (reversal, asymptotic, damping)
Middle term (time scale: years to decades; space scale: ~ 1–5 km)	⇒ wave climate variations ⇒ surf zone bar cycles ⇒ extreme events	⇒ fluctuations (from (quasi-) cyclic to noncyclic) ⇒ (quasi-)linear trends ⇒ trend changes (reversal, asymptotic, damping)
Short term (time scale: hours to years; space scale: ~ 10 m–1 km)	⇒ wave, tide and surge conditions ⇒ seasonal climate variations	⇒ fluctuations (from (quasi-) cyclic to noncyclic) ⇒ (quasi-)linear trends ⇒ trend changes (reversal, asymptotic, damping)

Aeolian transport

Aeolian transport is the transport of sediment by wind action and is the main driver for dune growth (Durán et al., 2011). Sand particles are set in motion by the wind when a certain velocity threshold is exceeded. The sediment is deposited in the dunes, due to an increase in surface roughness caused by the vegetation and an increase in slope. Wind speed and direction mainly influence the transport fluxes and the average wind speed and direction of the research area are shown in Figure 2.15. Besides wind speed and direction several other factors affect the transport rates, like the beach slope, grain size, moisture content and shell layers among others.

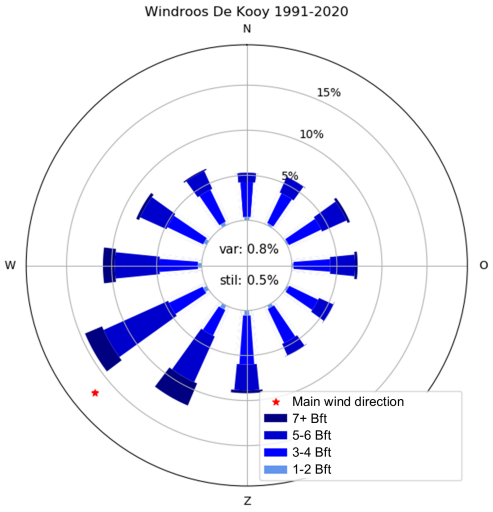

Figure 2.15: Wind rose of De Kooy, near Den Helder, showing the average wind speed and direction between 1991 and 2020. (KNMI, 2022b)

Aeolian transport occurs when the shear stresses caused by the wind speed exceed the critical shear stress of the sediment. The critical velocity depends on the grain diameter (d), the density of the grains and the air (ρ_s and ρ), the gravitational acceleration (g) and an empirical coefficient (A) and is given by Equation 2.1 (de Vries et al., 2012). This equation is only valid if the conditions of the beach are constant in time, while most conditions of the beach vary in time.

$$u_{t*} = A\sqrt{dg(\rho_s - \rho)/\rho} \tag{2.1}$$

One of the time-varying conditions is the beach slope, which affects the critical velocity (Iversen and Rasmussen, 1999). The weight force of grains on an inclined surface can be broken into two components, one perpendicular to the surface and one parallel to the surface in the downward direction. The parallel component can increase or decrease the critical velocity depending on the wind direction. When sand particles are transported from the beach to the dunes, they have to move upward on the slope and therefore the critical velocity increases. Hardisty and Whitehouse (1988) provided a slope correction factor (B) that should be applied to the critical velocity which can be calculated by Equation 2.3, where i is the internal friction angle and b the bed slope. A similar reduction factor (A) was provided for the transport rate, which can be calculated using Equation 2.2.

$$A = \left(\frac{\tan i}{\tan i - \tan b}\right)^7 \tag{2.2}$$

$$B = \sqrt{\frac{\tan i - \tan b}{\tan i}\cos b} \tag{2.3}$$

The transport flux could be limited by the beach width when the fetch length is lower than the critical fetch length. Wind coming from the sea does not contain any sediment yet and some distance is required to reach a fully saturated transport flux. The fetch length required to reach transport saturation is called the critical fetch length. Erosion occurs when the transport flux is lower than the saturated flux and sedimentation occurs when the transport flux is higher than the saturated flux (Durán et al., 2011). When the critical fetch length is larger than the beach width, the transport flux can not reach its maximum saturation level which could limit the transport to the dunes.

Transport fluxes that deposit sand in the dunes might be blocked by structures on the beach. Commercial structures like beach pavilions and small beach houses are present along the Dutch coast. The number and size of the structures have increased over time and might influence the growth of the dunes at multiple locations. Poppema et al. (2022) studied the deposition patterns of sediment by aeolian transport around structures. Their research showed that the transported sediment is deposited on two tails behind the sides of the structures and some erosion occurs between the two tails directly behind the structure. The effect of buildings is explained in more depth in Subsection 2.4.2.

Sea level rise

The sea level is rising globally which can cause a retreat of the coastline. The rate of sea level rise (SLR) increased from 1.8 $mm/year$ before 1993 to a rate of 2.4 $mm/year$ after 1993 (Baart et al., 2019). The effect of SLR on the coast was most commonly assessed using the Bruun Rule (Bruun, 1962). The Bruun Rule predicts a coastline retreat based on the conservation of mass and is given by Equation 2.4 where R is the coastal recession, L the horizontal distance to the depth of closure, S

the SLR, B the berm or dune elevation and h the depth of closure. The depth of closure represents the boundary between the landward morphologically active region and the seaward inactive region and lies around -5 to -8 m NAP for the Dutch coast (Hinton and Nicholls, 1998). The Bruun Rule is described in more detail by the schematic shown in Figure 2.16.

$$R = \frac{L \cdot S}{B + h} \tag{2.4}$$

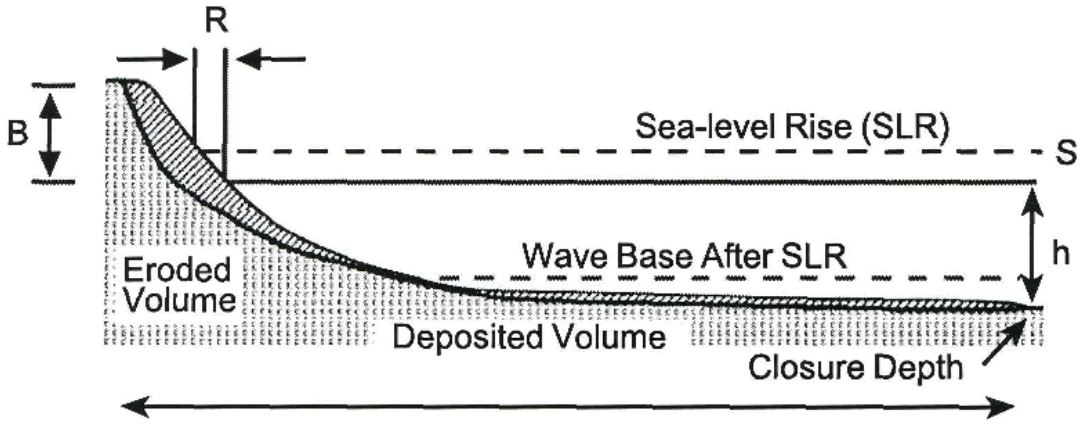

Figure 2.16: A schematic of the Bruun Rule, which is used to calculate the effect of sea level rise on coastal recession. (Cooper and Pilkey, 2004)

The Bruun Rule has been and is being used to determine coastal recession, but recent studies show that the Bruun Rule does not accurately predict the coastal recession due to SLR (Cooper and Pilkey, 2004; Ranasinghe et al., 2012). The Bruun Rule does not include any accretionary component, while coastlines have accreted under SLR. Van IJzendoorn et al. (2021) showed that the vertical dune toe translation outpaced the SLR along the Dutch coast, caused by the nourishments along the coast.

Although the dunes along the Dutch coast have grown in spite of the increased sea level, it does have an effect on coastal erosion. The shoreline migrates landward and more waves can reach the dunes when the water level is increased. Furthermore, sediment is imported by the Wadden Sea from the North Sea to compensate for the SLR which decreases the available sediment for the North Sea coast (Wang et al., 2018).

Wave climate and water level variations

Waves play an important role in the development of beaches and dunes. Most waves along the Dutch coast come from the West-southwest direction while the largest waves come from the north-west due to a longer fetch (Hoekstra and Stolk, 1990). Waves are generally largest around January with a mean wave height of 1.8 metres. Winter et al. (2012) studied the effect of climate change on the wave climate near the Dutch coast and predicted that the wave height will not increase due to climate change. According to Winter et al. (2012), the mean wave height and direction will be similar, only the direction of extreme events is expected to come from the West-southwest more frequently.

Extreme events with return periods larger than once a year can cause significantly more dune erosion than waves during mild storms. Waves under normal conditions do not reach the dune toe, while waves can attack the dune toe during storms due to storm surge and a larger incoming wave energy. The surge level increases inversely with the water depth and therefore increases in water level can be very large in a shallow sea like the North Sea (Gornitz, 2005). Due to the increase in water level, waves can reach the dune front and the collision of waves on the dune front causes the

dune slope to steepen. When the dune slope reaches a critical steepness it collapses and large lumps of sediment slide down the slope. The lump of sand deposited at the dune foot temporarily shields the dune front from direct wave impact. Offshore-directed return flows transport the sediment at the dune foot further seaward extending the foreshore (Roelvink et al., 2009).

The erosion volume of a storm depends on multiple factors. Hydrodynamic conditions like the storm surge level, wave height and wave period determine the forcing conditions on the dune. As the sediment is transported gradually, the duration of the storm influences the erosion volume. According to Kriebel and Dean (1993), the new storm profile mainly depends on the storm surge level. The increased water level gives a new equilibrium profile and the wave forcing determines the rate at which the profile moves towards this new equilibrium.

2.4.2. Human drivers

This subsection describes the effect of human interventions in the research area. Stive et al. (2002) provided an overview of the most important human drivers of shoreline change which are shown in Table 2.2. First, a more detailed description of the effect of nourishments is given, followed by a description of buildings on the beach and their impact on beach and dune development. The effect of the closure of the Zuiderzee by the Afsluitdijk was described in Section 2.1 and the effect of other coastal structures on Texel and the Noord-Holland coast were described in Section 2.2 and Section 2.3 respectively.

Table 2.2: Most important human drivers and typical evolutions for shore and shoreline variability and their timescales. Obtained from Stive et al. (2002).

Scale	Human causes/factors	Typical evolutions
Very long term (time scale: centuries to millenia; space scale: ~ 100 km and more)	⇒ human-induced climate change ⇒ major river regulation ⇒ major coastal structures ⇒ major reclamations and closures ⇒ structural coastal (non)management	⇒ (quasi-)linear trends ⇒ trend changes (reversal, asymptotic, damping) ⇒ fluctuations (from (quasi-)cyclic to noncyclic)
Long term (time scale: decades to centuries; space scale: ~ 10–100 km	⇒ river regulation ⇒ coastal structures ⇒ reclamations and closures ⇒ coastal (non)management ⇒ natural resource extraction (subsidence)	⇒ trend changes (reversal, asymptotic, damping) ⇒ (quasi-)linear trends ⇒ fluctuations (from (quasi-)cyclic to noncyclic)
Middle term (time scale: years to decades; space scale: ~ 1–5 km)	⇒ surf zone structures ⇒ shore nourishments	⇒ trend changes (reversal, asymptotic, damping) ⇒ fluctuations (from (quasi-) cyclic to noncyclic)
Short term (time scale: hours to years; space scale: ~ 10 m–1 km)	⇒ surf zone structures ⇒ shore nourishments	⇒ trend changes (reversal, asymptotic, damping) ⇒ fluctuations (from (quasi-)cyclic to noncyclic)

Nourishments

Since 1990, the Dutch government has been supplying large volumes of sand to oppose coastal erosion. The nourishment volumes have increased over time and currently, on average 12 million cubic metres of sand are supplied annually. Figure 2.17a shows three different types of nourishments, beach, shoreface and channel wall, that are being used to maintain the Dutch coast. Channel wall nourishments are mainly supplied near the tidal inlets near the Wadden Sea. Beach nourishments were most common when the dynamic preservation policy was implemented, while shoreface nourishments have become more common over the years due to lower costs per volume and more available research on their effectiveness (Laustrup et al., 1996).

Brand et al. (2022) studied the effects of the different types of nourishments on the sand volumes in the coastal profiles. Their research investigated the percentage of volume from the nourishments that was present in the momentary coastline (MCL) for each year after the nourishment. Beach nourishments are immediately visible in the MCL, as they are placed directly in front of the dune toe in the beach zone. Shoreface nourishments can not immediately be seen in the MCL as they are supplied underwater and it takes some time to be transported to the beach zone. Figure 2.17 shows a diagram of these nourishment volumes in the MCL over time. It can be seen that the effect of shoreface nourishments on the MCL lasts longer than beach nourishments. Beach nourishments are therefore currently mainly used when additional flood safety is directly required.

A larger sediment budget in the active profile might also increase the dune volume by aeolian transport and by reducing the erosion due to waves. Bakker et al. (2012) investigated where the sediment that was supplied to a part of the Dutch coast ended up in the new coastal profile. Most of the sand was found in the profile derived from nourishments between 2000 and 2005 when there were no significant storm surges causing erosion. Aeolian transport of the sand to the dunes was almost always significant because enough sediment was available on the dry beach. Furthermore, the grain size of the nourished sand affects the aeolian transport rate as larger grains need higher wind speeds to be transported.

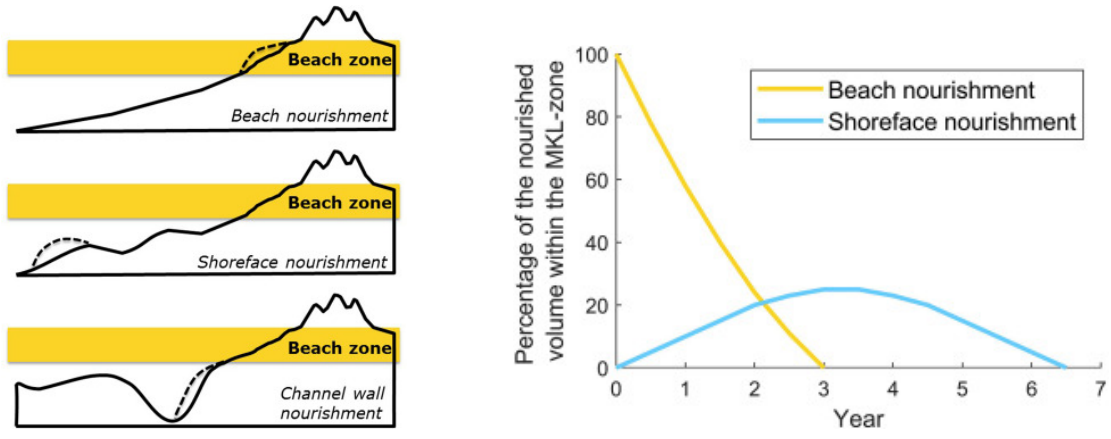

(a) (b)

Figure 2.17: Panel a shows the three different types of used nourishments and Panel b shows the effect of the shoreface and beach nourishments on the beach volumes over time. Figures obtained from Brand et al. (2022).

Buildings on the beach

Buildings on the beach can influence beach and dune development by obstructing wind flow and sand transport. Local differences in aeolian transport, created by structures, can cause significant variability in landforms on a small spatial scale (Jackson and Nordstrom, 2011). Many commercial buildings are present along the Dutch coast, which are mainly concentrated around several isolated

coastal resorts (Nordstrom and Arens, 1998). Figure 2.18 shows one of the coastal resorts at Wijk aan Zee. The buildings on the beach include large beach pavilions and smaller beach houses. Other large coastal resorts in the research area are located at Castricum, Egmond aan Zee, Bergen aan Zee, Callantsoog, Julianadorp and De Koog. The water authority HHNK determines the locations of the buildings in the research area, which are moved when this is required for the growth of the dunes. Additionally, the water authority makes demands for the buildings regarding their presence during the winter season and the obstruction of sand transport during the winter season.

Figure 2.18: Aerial picture of the coast of Wijk aan Zee. This coastal area includes many buildings on the beach like beach pavilions and beach houses. Picture obtained from Deltares (2018).

Obstruction of the aeolian transport by the buildings on the beach limits the dune growth (Smith et al., 2017). Several factors influence the consequences of the buildings on the dune growth, like building size and orientation, the distance between the buildings and the time and duration of the building placement (Poppema and Mulder, 2020). Flow patterns around a building depend on the width, length and height of the building, which therefore influence the sediment depositions around the building. When multiple buildings are located close to each other it increases the negative effect on the dune growth, this effect is only significant when the distance between the buildings is very small which is the case for many of the small beach houses in the research area (Hoonhout and Van Thiel de Vries, 2013).

In addition to the influence on the aeolian transport, human activities around the buildings affect the beach and dune development. Bulldozers create flat artificial berms around the pavilions to provide more dry beach area near the pavilion (Nordstrom and Arens, 1998). Furthermore, most commercial buildings are supplied on the landward side of the building and sand is removed from the dune toe to create access routes.

3

Methodology

This chapter describes the method that was used to answer the research questions. The method of this research was divided into four phases shown in Figure 3.1, which are described in more detail in Sections 3.1 through 3.4.

In phase 1, all available coastal data of the research area was retrieved from the JarKus dataset. Gaps in the dataset were filled by several operations which resulted in the modified dataset that was used in further analyses. The JarKus Analysis Toolkit developed by Van Ijzendoorn (2021) derived characteristic variables from the dataset that described the coastal profiles and gave a better understanding of the morphological changes.

In phase 2, the modified dataset was decomposed into spatial and temporal modes by means of a principal component analysis. The spatial and temporal modes give insight into the spatial and temporal behaviour of the surface elevation in the research area. The temporal modes display the trends and cycles in the dataset and the spatial mode displayed the alongshore and cross-shore differences in elevation variability.

In phase 3, the transects in the research area were categorised based on the development of their coastal profile. Morphological changes of transects that showed similar behaviour were expected to be driven by the same processes. Transect categorisation made it possible to study the relationships between drivers and the observed morphological behaviour for several subsections of the research area. The categorisation used features extracted from the spatial modes to describe the changes in elevation over time. The transects were clustered by an unsupervised clustering algorithm after the assignment of weights to the different features.

Finally, the relationships between the drivers and the observed morphological behaviour were investigated. Several clusters were selected with differences in morphological behaviour, nourishment volumes, beach slope and dune slope. For each cluster, the observed changes in dune volume and height and the cross-shore migration of the shoreline and dune toe were linked with the drivers. In addition to the drivers described in Section 2.4, variables like foreshore slope, beach slope and width were also considered as drivers. Understanding of these relationships for different subsections of the research area gave insight into these relationships for the entire research area.

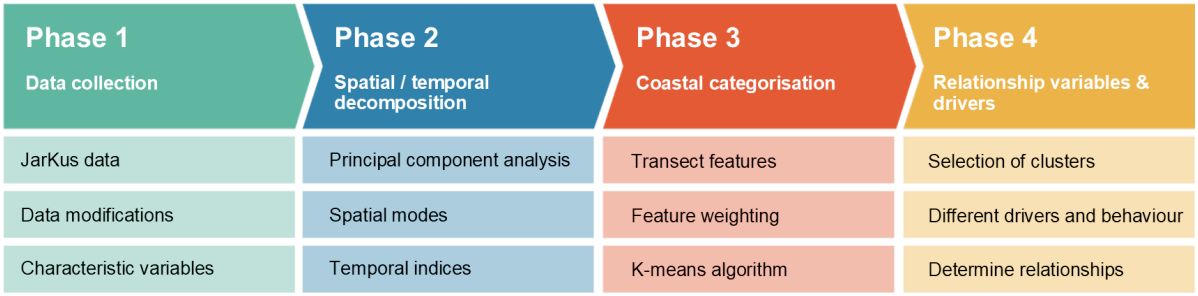

Figure 3.1: Flowchart of the four phases of this research.

3.1. Phase 1: Data collection

This research used the JarKus dataset containing the profiles of 2344 transects measured between 1965 and 2021. This research used the transects in the HHNK area which is shown in Figure 3.2. The research area comprises Texel, coastal section 6 counting 207 transects (blue) and Noord-Holland, coastal section 7 counting 294 transects (red). The retrieved data is not completely continuous in time and space as the measurements did not cover the entire research area for some years. Furthermore, multiple measured profiles do not include the entire profile from the dunes to the foreshore, while some of the performed analyses required full coverage of the beaches and dunes. Because this research mainly focused on the beaches and dunes, only a part of the cross-shore range was used. The extracted profiles of Noord-Holland stretched from RSP -1000m to RSP +800m and the profiles of Texel stretched from RSP -1500m to RSP +1100m. These ranges were chosen to include both the primary dune and the shoreline of all the profiles. Altitude samples were collected with cross-shore intervals of 5 metres above sea level and 10 metres below sea level. Figure 3.3 presents an overview of missing altitude samples within the above-mentioned cross-shore range.

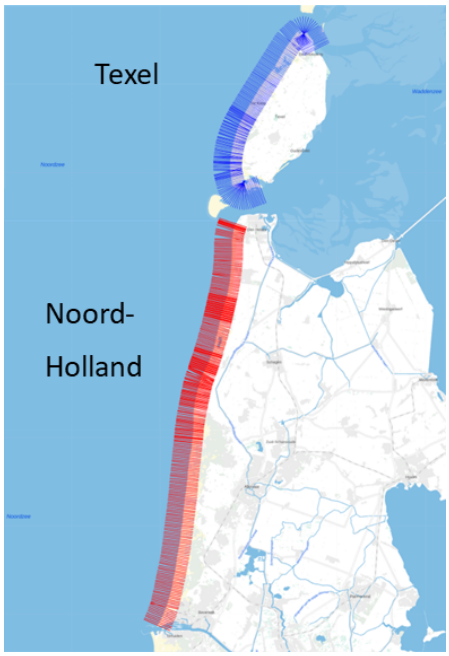

Figure 3.2: Overview of the transects in the JarKus dataset. Coastal section 6 (Texel) is shown in blue and coastal section 7 (Noord-Holland) is shown in red.

The elevation samples were measured separately for the dry part and the wet part and at varying times of the year. Planes using photogrammetry or laser altimetry measured the topography of the dry parts of the coast and the bathymetry of the wet parts was measured using ships (Vermaas, 2012). The dry and wet parts of the profile are not measured simultaneously, but they are still combined into one coastal profile. The month in which the profiles are measured is varying each year. Figure 3.4 shows the percentage of measured profiles per month. Because the measurement month is varying each year, seasonal fluctuations could influence the differences between the coastal profiles of the different years.

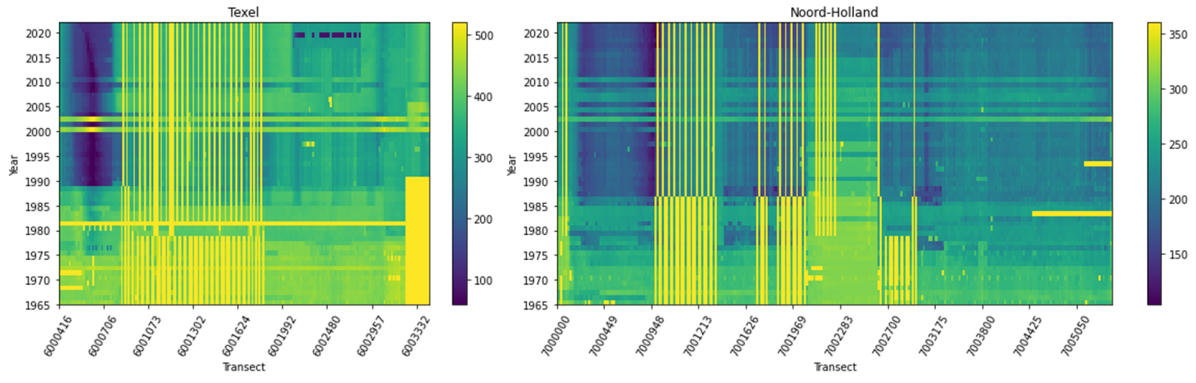

(a) (b)

Figure 3.3: Overview of the missing altitude samples per transect (x-axis) and year (y-axis) for Texel (a) and Noord-Holland (b). The blue-yellow colour map shows the number of missing elevation samples in the cross-shore range.

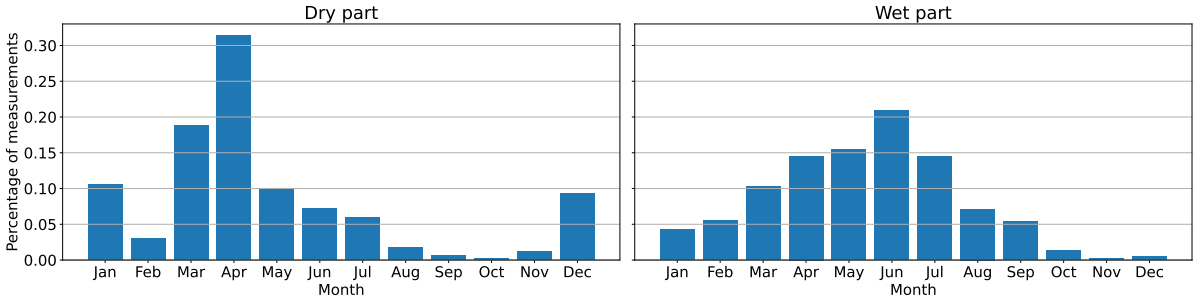

(a) (b)

Figure 3.4: Distribution of the measurement dates of the coastal profiles in the JarKus dataset for coastal sections 6 (Texel) and 7 (Noord-Holland). The dry part (a) and wet part (b) are measured separately and are therefore shown in separate figures.

Several modifications were performed to make the the dataset homogenous and uniform several, which was required for the principal component analysis applied in phase 2. Gaps in the profile data caused by the difference in cross-shore intervals for the wet and dry part of the profiles were filled during the first step of the data modification process. The transect data has an across-shore interval of 5 metres for the dry part and 10 metres for the wet part. Linear interpolation between samples in the wet part reduced the interval to 5 metres.

The next step of the data smoothing dealt with temporal gaps in the data of up to 5 years. Linear interpolation of the profile data of adjacent years gave an approximation of the missing elevation data. Linear interpolation of large gaps in the data increases the linearity of the dataset which also affects the outcomes of the PCA. Therefore missing data in temporal gaps larger than 5 years were not filled during this step.

A centred moving average in space smoothed the data over a short distance and created new equidistant transects, with an interval of 500 metres, spanning the entire research area. The profiles of the new transect were calculated using all valid profiles of the same year within a distance of one kilometre. The profiles were weighted based on their distance to the new transect, decreasing linearly from one to zero for distances between zero and one kilometre. The new profile was found by averaging the weighted profiles.

The last transformation shifted the profiles in the cross-shore direction to align the temporal mean dune toe locations of the transects. The dune toe location was chosen as reference point as it is the transition between the beach and the dune, which this research focused on. The location of the dune toe was determined using the NAP +3m method described in Subsection 3.1.1. Figure 3.5 shows an example of an elevation map that resulted from the above-mentioned modifications.

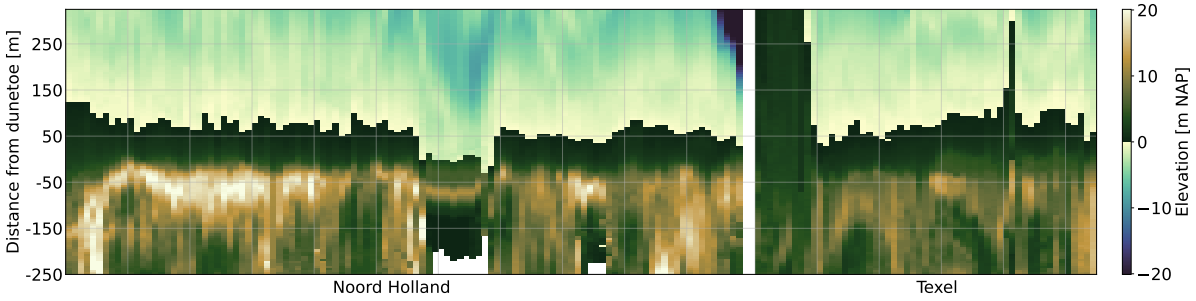

Figure 3.5: Elevation data for the research area in 1986 after all transformations. The southern part is shown on the left, the white gap represents the Texel inlet and the northern part is shown on the right. The colormap shows the elevation of the locations, with a different colour for areas above mean sea level (positive values) and areas below mean sea level (negative values). The y-axis shows the cross-shore distance from the temporal mean dune toe location.

3.1.1. Characteristic variables

Information about the profiles can also be described by a few characteristic parameters of the profiles, like dune height, dune toe location and shoreline location among others. The derivations of these parameters were based on the JarKus Analysis Toolkit (Van Ijzendoorn, 2021) and are described below. Figure 3.7 gives an overview of a coastal profile with all the derived characteristic variables.

Dune toe

The dune toe is located at the transition between the beach and the dune. Vegetation usually starts from the dune toe and there is a clear change in the slope of the profile. This research used two different methods to determine the dune toe location, the NAP +3m method and the second derivative method. The NAP +3m has been used since the start of the JarKus programme and defines the location of the dune foot as the most seaward intersection of the profile with the NAP +3m line. This method does not take the shape of the profile into account and assumes that the height of the dune foot remains constant over time. The NAP +3m method was used to align the temporal mean dune toe locations of the profiles in the modified dataset.

Diamantidou et al. (2020) proposed a different method taking into account the shape of the profile and with a variable height. The method makes use of the first and second derivatives of the profile and is referred to as the second derivative method. The method searches for the dune toe location within the seaward and landward constraints, where the most seaward intersection with the high water level defines the seaward constraint and the first dune top defines the landward constraint. For dune tops higher than NAP +6m, the landward constraint is shifted towards the most seaward intersection with the NAP +6m line. The first and second derivatives of the profile describe the slope and change in slope of the profile. By applying a threshold on both the first and second derivatives, long, flat stretches are removed from the profile section. The threshold removes cross-shore locations with a first derivative larger than -0.001 or a second derivative smaller than 0.01. The most seaward location of the remaining profile section gives the dune toe location. Figure 3.6 shows an example of the second derivative method. Analyses on the development of the dune toe in this research made use of the second derivative method.

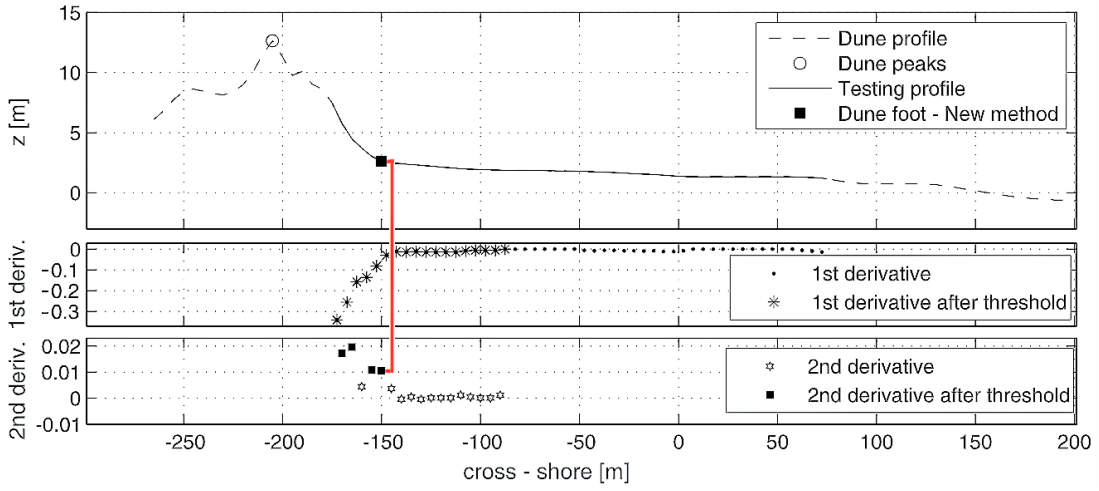

Figure 3.6: Overview of the second derivative method used to find the dune toe location. The top panel shows the coastal profile with the highlighted profile section between the seaward and landward constraints. The centre and bottom panels show the application of the threshold on the first and second derivatives respectively. (Diamantidou et al., 2020)

Dune top

The dune top locations and changes in dune top locations give useful insights into the flood safety of the hinterland. The primary dune top is the most seaward local maximum in the profile and was found using the python function $scipy.signal.find\_peaks$. The function finds the local maxima above a user-defined threshold height and prominence. This research used a minimum peak height of $5m + NAP$ and a minimum prominence of 2. When multiple peaks exceeded these threshold values, the most seaward peak was selected.

Shoreline

The shoreline location is defined as the intersection of the profile with the mean sea level. In some cases, there were multiple intersections with the mean sea level and this required some additional steps. For the location of the shoreline, only intersections seaward of the primary dune were considered. The shoreline location was selected from the filtered intersections at the most seaward intersection within 100 metres from the most landward intersection. This filtering prevented the selection of landward intersections behind the dunes and seaward intersections with shoals as shoreline locations.

Other variables

Additional variables were derived from the profiles using the above-mentioned variables. The dune volume was calculated using a landward boundary and the location of the dune toe (NAP +3m method) as shown in Figure 3.7. The landward boundary was defined as the first point landward of the dune top with a temporal variance lower than the threshold of 0.1 metres. The beach is regarded as the area between the shoreline location and the dune toe location and the beach width and beach slope were determined from these locations. The slope of the dunes was calculated in a similar manner using the dune toe and dune top location.

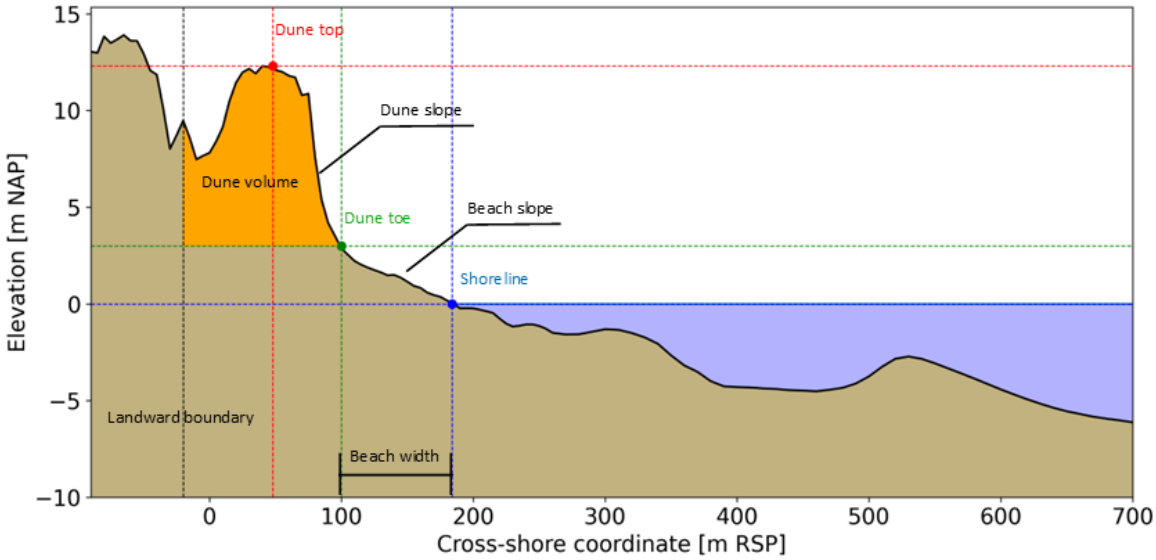

Figure 3.7: Overview of a coastal profile with all the extracted characteristic parameters. The red dot shows the dune top, the green dot shows the dune toe, the blue dot shows the shoreline and the black line shows the landward boundary.

3.2. Phase 2: Spatial and temporal decomposition

This section describes the application of a principal component analysis (PCA) on the modified dataset. PCA is a statistical method used to investigate the variability in a dataset. This research used a PCA to describe different spatial and temporal patterns of elevation variability through empirical orthogonal functions (EOFs) and temporal indices. The resulting spatial modes and temporal indices were used to describe the development over time of the different alongshore locations and were used as features for the coastal categorisation described in Section 3.3. Larson et al. (2003) used a similar approach to study the variability in surface elevation at the coast of Terschelling. Several other applications of PCA have been used to investigate the variability in cross-shore coastal profiles (Houser et al., 2008) and the variability of the coastline (Fairley et al., 2009; Hapke et al., 2016; Miller and Dean, 2007). The statistical method that decomposed the modified dataset into the EOFs and temporal indices is described below.

The modified dataset X_{raw} contained elevation data for 57 years spanning the entire research area. The PCA only investigated the variability in elevation and therefore the temporal mean elevation at every location was removed from the dataset. A $(m \times n)$ elevation matrix X was computed for the research area, where m is the number of years in the dataset and n is the number of elevation sample locations. This step is also shown for one example transect in Figure 3.8. The upper graph shows the elevation data from one transect obtained from the modified dataset. The bottom figure shows the elevation anomaly of the transect, which was computed by subtracting the mean elevation from each cross-shore location.

$$\mathbf{X} = \mathbf{X}_{raw} - mean(\mathbf{X}_{raw}) \tag{3.1}$$

$$\boldsymbol{X} = \begin{bmatrix} \boldsymbol{x}_1 & \boldsymbol{x}_2 & \dots & \boldsymbol{x}_n \end{bmatrix}, \quad \boldsymbol{x}_1 = \begin{bmatrix} x_{1,1} & x_{2,1} & \dots & x_{m,1} \end{bmatrix}^T \tag{3.2}$$

The first step in the PCA is to compute the covariance matrix. The covariance matrix is a $n \times n$ matrix, containing the covariances between all n dimensions in the matrices. The covariance matrix explains for every location how the elevation varies with respect to the other locations and if there is any relationship between the locations.

$$\boldsymbol{C} = \begin{bmatrix} Cov(\boldsymbol{x}_1, \boldsymbol{x}_1) & \cdots & Cov(\boldsymbol{x}_1, \boldsymbol{x}_n) \\ \vdots & \ddots & \\ Cov(\boldsymbol{x}_n, \boldsymbol{x}_1) & & Cov(\boldsymbol{x}_n, \boldsymbol{x}_n) \end{bmatrix} \tag{3.3}$$

An eigenanalysis was performed on the covariance matrix and as the covariance matrix is a real square symmetric matrix, all eigenvectors are real and orthogonal. The eigenvectors ($\mathbf{v}_i$) of the covariance matrix provide the spatial modes of the elevation variance and their eigenvalues (λ_i) describe the importance of the spatial modes. The eigenvectors are then sorted on their eigenvalues in descending order so that each eigenvector describes more variance than the succeeding eigenvectors.

$$eigenanalysis(\boldsymbol{C}) \rightarrow \begin{cases} \mathbf{V} = \begin{bmatrix} \mathbf{v}_1 & \mathbf{v}_2 & \dots & \mathbf{v}_{57} \end{bmatrix} \\ \boldsymbol{\lambda} = \begin{bmatrix} \lambda_1 & \lambda_2 & \dots & \lambda_{57} \end{bmatrix} \end{cases} \qquad \lambda_1 > \lambda_2 > \ldots > \lambda_{57} \tag{3.4}$$

The relative importance of each eigenvector (r_i) was calculated by dividing its eigenvalue by the sum of all eigenvalues. Because the dataset contains only 57 samples, one for each year, the first 57 eigenvectors can be used to describe the variance in the dataset. As every eigenvector maximized the explained variance and the eigenvectors were sorted in decreasing order of explained variance, it was expected that a significant amount of the remaining 57 eigenvectors could be neglected in further analyses.

$$r_i = \lambda_i \Big/ \sum_{j=1}^{57} \lambda_j \tag{3.5}$$

A transformation of the data by the matrix operation in Equation 3.6 gave insight into the temporal variability of the different spatial modes. The data for each year was projected onto the spatial modes to obtain the temporal indices (**T**). The temporal indices contained trends and cyclic behaviour of the dataset that gave useful insights into the development of the area. The spatial modes and temporal indices were derived mathematically and do not necessarily contain any physical meaning. The first five modal shapes of the example transect are shown in the left graph of Figure 3.9 and their corresponding temporal indices are shown in the right graph. Higher values in the modal shape mean that the elevation at that cross-shore location changes stronger with the temporal indices of that mode. The left figure shows for example that the -60m to 0m area of this transect strongly responds to the first mode. The rather linear increasing trend of mode 1 would mean a linear increase in elevation in the -60m to 0m area, which can also be seen from Figure 3.8. The results of the spatial and temporal decomposition are further explained in Section 4.1.

$$\mathbf{T} = \mathbf{X} \cdot \mathbf{V} = \begin{bmatrix} \mathbf{t}_1 & \mathbf{t}_2 & \cdots & \mathbf{t}_{57} \end{bmatrix} \tag{3.6}$$

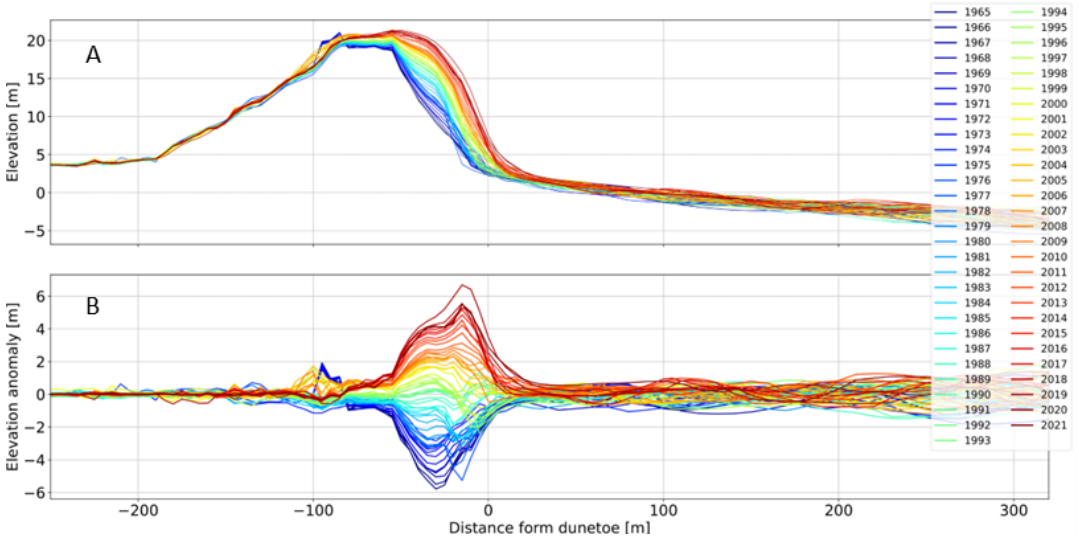

Figure 3.8: Elevation data of a transect from the modified dataset after the smoothing operations, where the profiles of different years are shown with different colours. Panel A shows the profile data and Panel B shows the relative elevation to the mean elevation of the transect.

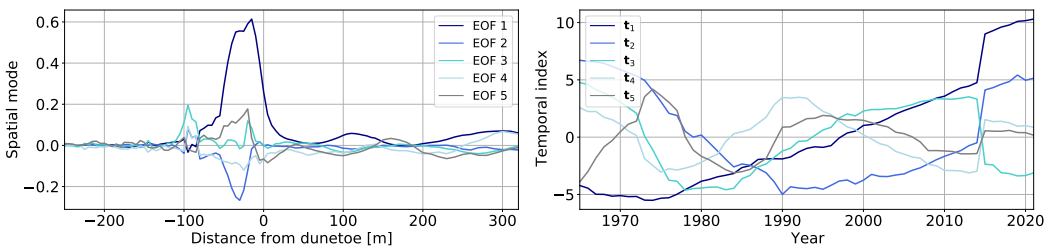

(a) Modal shapes.

(b) Temporal indices.

Figure 3.9: Modal shapes and temporal indices of the first 5 modes for an example transect of the modified dataset.

3.3. Phase 3: Coastal categorisation

This section describes the clustering approach that was used to categorise the transects in the research area into different clusters. The transects are categorised into clusters to create subsections of the research area that show similar morphological behaviour. The drivers that cause the observed morphological behaviour can then be investigated for each subsection of the research area. Similar clustering techniques have been applied to coastal profiles. Zwarenstein Tutunji (2021) used a set of characteristic variables to cluster transects of the Noord-Holland coast and the dominant variables mainly described the wet part of the coastal profiles. This research did not succeed in linking the outcomes of the clustering algorithm with morphological processes. Another research by Athanasiou et al. (2021) created topological profiles using a clustering algorithm to predict the response of the Dutch coast to storms.

The selection of the clustering features, that are used to describe the morphological behaviour, is explained in Subsection 3.3.1. Subsection 3.3.2 describes the weighting of the different clustering features. The clustering algorithm that categorised the transects into different clusters is explained in Subsection 3.3.3. Subsection 3.3.4 describes the used evaluation methods that evaluated the clustering results.

3.3.1. Feature selection

The coastal categorisation was used to cluster transects that showed similar behaviour over time. The clustering was done by comparing several features of the transects and finding representative cluster centres that best describe the complete dataset. These features describing the morphological behaviour could be entire profiles, characteristic variables or features based on the modal decomposition. Several approaches with different features were examined to find a suitable method.

The first approach used all elevation samples, every year and all cross-shore locations, of the transects as features to describe the development of the transects. Application of this approach on the modified dataset did categorise transects with a similar profile but did not properly take into account the development over time. The second approach used the characteristic variables described in Subsection 3.1.1 as features. The profiles of the modified dataset did not always represent the original profile shapes which resulted in large deviations in the characteristic parameters. The original dataset contained multiple missing profiles and therefore the transects could not be compared using the full set of variables. The development of the variables could be compared by fitting polynomials on the data similar to the approach of Zwarenstein Tutunji (2021), but the development of the variables showed different types of non-linear behaviour which could not be described with low-order polynomials.

A third approach was used, which used clustering features based on the modal shapes of the transects to include the temporal behaviour of the transects. The temporal indices of the EOFs described different trends in the dataset. The modal shape of a transect described how each part of the profile corresponded with the trend and therefore described a part of the morphological behaviour over time. The development over time of the transects could then be compared by comparing several modal shapes. The mean profile of the transect was not described by the modes and was therefore added as an additional feature.

The amount of input data was reduced by selecting only the first twelve modes, which together explained 95% of the variance. Using all the modes required more computation time while the first 12 modes already describe the development of the profiles accurately. Furthermore, the discarded modes mainly described noise in the dataset and were therefore not relevant for long-term development. The mean profiles and the 12 modal shapes derived from the empirical orthogonal functions made up the features for each transect. The final feature matrix had 164 samples (rows) equal to the number of transects in the modified dataset. The first 115 features (columns) consisted of the

heights of the mean profile at the 115 cross-shore locations. The next 115 features were taken from the first EOF, by selecting the 115 cross-shore samples in the spatial mode at the location of the transect which gives the modal shape of the transect. This process was repeated for the remaining 11 EOFs which resulted in the final input matrix **K** with 164 samples and 1495 features. The steps to compose the input matrix are described visually in Figure 3.10.

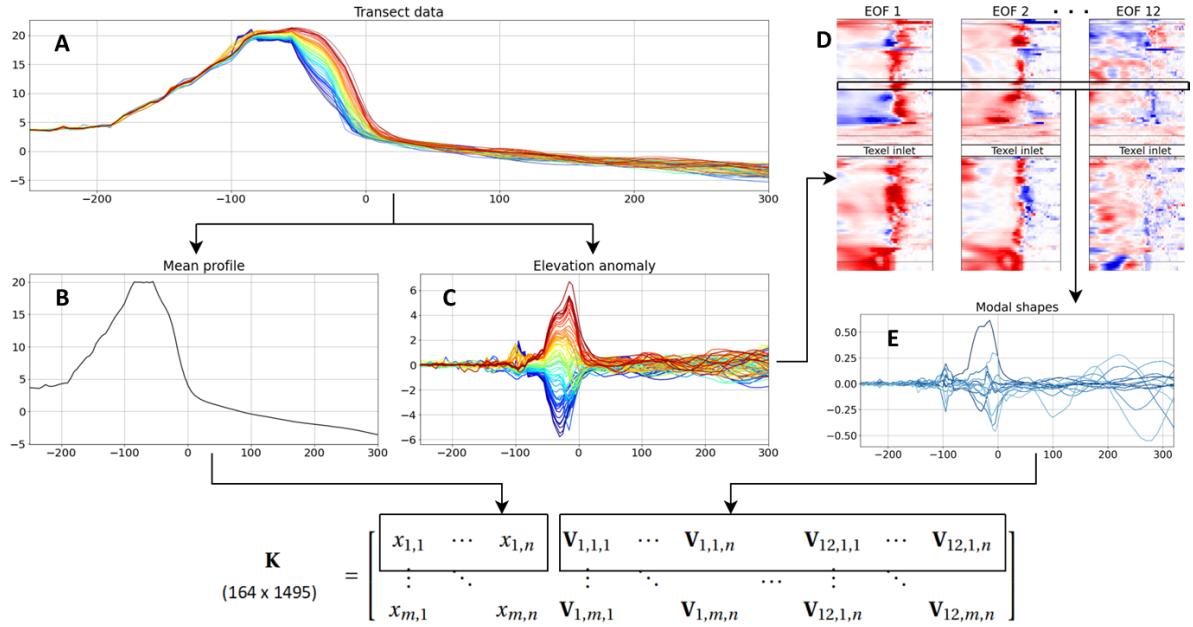

Figure 3.10: Schematic of the composition of the feature matrix for the clustering algorithm. The process starts with the modified profile data of every transect (A), which is divided in the mean profile (B) and the elevation anomaly (C). The 115 elevation samples of the mean profile are inserted in the first 115 columns of input matrix **K**. The elevation anomalies of the profiles are decomposed into spatial modes (D). For each transect, the modal shapes (E) of the first 12 modes are derived which consist of 115 values each. The 115 values of mode 1 are inserted in the second 115 columns of the input matrix **K** and this is repeated for the remaining 11 modes.

3.3.2. Feature weighting

The importance of the different features is not equal as each EOF is more important than its subsequent EOF. Therefore weights were given to the different modes and cross-shore locations to take this into account. Before weights are applied, data should be normalised or standardised so that the weights of the features are not determined by their magnitude. Standardisation is preferred on data that has a normal distribution and therefore a Shapiro-Wilk test was performed on the features to check whether they could be normally distributed. The results showed that 88% of the features had a p-value lower than 0.05 for a normal distribution which meant that it was not normally distributed and therefore normalisation was preferred. The normalisation was done with a min-max feature scaling for each column of the feature matrix **K**, which is described by Equation 3.7. First, the minimum value of a column was subtracted from all the column values. The values were then divided by the difference between the maximum value and the minimum value so that all column values were in the range of 0 to 1.

$$k_{i,j,norm} = \frac{k_{i,j} - min(\mathbf{k}_j)}{max(\mathbf{k}_j) - min(\mathbf{k}_j)} \tag{3.7}$$

After normalisation, two different weights were applied. The first weight increased the importance of the cross-shore locations that described the dune front and the beach because this research fo-

cused on the dry part of the coastal profile. Thus, the weights for the cross-shore locations between -150m and +100m from the dune toe, see Figure 3.11, were increased by a factor of 3. This weight was applied on columns 20 through 70 for the mean profile and columns 20+115n through 70+115n for the 12 EOFs with $n = (1, 2, ..., 12)$. The second weight was applied to the different modes and the mean profile, based on the variance ratios of the modes. Because the variance ratio of the first few modes is much higher and some useful information could be stored in the lower modes, the weights were scaled by taking the cubic root of the variance ratio and dividing it by the sum of the roots, Table 3.1 shows the resulting weights. The weight of the mean profile was equal to the average weight of the EOFs and therefore made up one-thirteenth of the total weight. The weight of the mean profile was applied on the first 115 columns of **K**, the weight of EOF 1 on columns 116 through 230 and this is repeated for the remaining EOFs on the remaining columns. The configuration of the weights was determined by comparing the outcomes of several configurations. The final configuration resulted in small intra-cluster variance around the dune toe and the smallest differences between the profiles in a cluster and their development over time, which was observed by manually inspecting animations of the profiles over time.

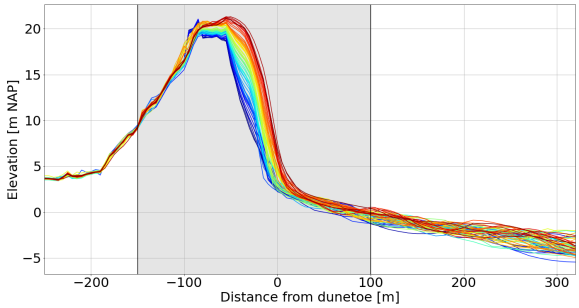

Figure 3.11: Weights of the cross-shore locations in the shaded area, between $-150m$ to $100m$, were multiplied by a factor of three for the clustering algorithm.

EOF	Weight [%]	EOF	Weight [%]
1	18.53	7	5.63
2	14.56	8	5.12
3	10.29	9	4.86
4	8.18	10	4.38
5	6.89	11	4.11
6	5.74	12	3.99

Table 3.1: Weights of the different EOFs, based on the explained variance ratio. The remaining 7.7% was assigned to the mean profiles.

3.3.3. K-Means clustering algorithm

The transects of the research area were categorised into different clusters using the K-Means algorithm. The algorithm does not require much computation time or memory (Yedla et al., 2010). K-Means clustering is an unsupervised data analysis method that partitions data samples into a predefined number of clusters. The algorithm creates initial cluster centres which iteratively move through the data set to optimise the outcome. The learning process of the algorithm is controlled by several hyper-parameters that are defined by the user. The number of cluster centres that are initially created is one of these hyper-parameters. The optimum number of clusters depends on the purpose of the clustering and in this case, the number of clusters should be as low as possible for easier interpretation while keeping the intra-cluster differences at a reasonable level.

When the K-Means algorithm is initialised, it places the imposed number of cluster centres randomly in the data set. Using a distance function, all the samples are assigned to the closest cluster centre. The distance function used here is the Euclidean distance (Equation 3.8), where k is a sample and c is the cluster centre. When all the samples are assigned to a cluster, the new cluster centre is computed by the mean values of all the samples in the cluster. The samples are then assigned to the new cluster centres and these steps are repeated until the cluster centres no longer move.

$$|k_i - c_i| = \sqrt{\sum_{j=1}^{n} (k_{i,j} - c_{i,j})^2} \tag{3.8}$$

The K-Means algorithm greatly depends on the initial locations of the cluster centres as they can move to a local minimum. Therefore, the algorithm was initialised multiple times to find the outcome with the smallest sum of squared errors. The number of initialisations is another hyperparameter that is imposed on the algorithm by the user. The higher the number of initialisations the larger the chance that the global minimum is found. However, using more initialisations requires more computational time and therefore a different amount of initialisations was used in the different stages of the research. The number of initialisations used, varied in the different between 200 for quick estimates and 30.000 for the final results.

3.3.4. Evaluation methods

The K-Means clustering algorithm is unsupervised and there was no supervised data available to validate the results. However, several internal evaluation methods exist, where the clustering is only evaluated using the results themselves. The K-Means clustering algorithm was used for classification an therefore the intra-cluster variance was optimised. Most of these evaluation methods make use of properties like the compactness of a cluster and the separation between clusters.

This research used the silhouette index that computes a score for each sample which describes the distance to its cluster compared to its neighbouring cluster. The silhouette score (S_i) takes two variables, the mean intra-cluster distance (a_i) and the mean nearest-cluster distance (b_i) and is given in Equation 3.9. The mean intra-cluster distance was calculated by taking the average Euclidean distance to all the samples in the same cluster. The mean nearest-cluster distance was calculated similarly, using the distances to the samples in the nearest cluster. The difference between the distances was divided by the largest of the two distances so that the scores lie in the range of -1 to +1. A negative score means that the sample is poorly matched and a high score means that it is well matched.

$$S_i = \frac{b_i - a_i}{max(a_i, b_i)} \tag{3.9}$$

Besides a mathematical method, the results were also evaluated visually. Static plots were made describing the intra-cluster variance and the number of clusters was increased when the intra-cluster variance was too high. Additionally, animations were used to evaluate the clustering of the development over time. The animations showed a time-lapse of all the profiles of transects that belonged to a cluster. The number of clusters was reduced until the intra-cluster differences in these animations became too large.

3.4. Phase 4: Relationships characteristic variables and drivers

This section describes the last phase of the research, which investigated the relationships between the drivers and the observed morphological behaviour, described by the characteristic variables. The coastal categorisation resulted in several subsections of the research area that showed similar morphological behaviour. Several clusters were selected, aiming at a set of clusters varying in the most important drivers and morphological behaviour, so that the relationships could be determined from this set of clusters. The set of clusters included differences in the location and orientation, the development of the dune volume and height, the cross-shore migration of the shoreline and the dune toe, the nourishment volumes and frequency, the beach width and slope and the presence of

blow-outs in the dunes.

For each cluster, several characteristic variables like dune volume, dune height, shoreline location and dune toe location were plotted in the alongshore direction for different years to observe the changes over time. Spatial differences in the cluster were examined and compared to the locations of the nourishments and the structures, which gave insight into the relationship between these drivers and the observed development.

The natural drivers, aeolian transport, sea-level rise and wave-climate variations, were assumed to be spatially constant within the clusters. Therefore, the effect of these drivers was only investigated on the mean temporal changes in the clusters. The measurement period of the coastal profiles varied per year which affected the characteristic variables by including the seasonal differences. Therefore, a moving average of the characteristic variables was used to determine the temporal development, filtering out the short-term developments that were beyond the scope of this research.

4
Results

This chapter describes the results of the principal component analysis and the clustering algorithm. The results of the PCA are presented in Section 4.1. Section 4.2 shows the spatial distribution of the clusters and the results of the evaluation methods. Section 4.3 gives a more detailed description of several clusters and their development over time. Similar clusters are compared in this section and some correlations between the characteristic variables and the drivers are displayed.

4.1. Spatial and temporal decomposition

The principal component analysis described in Section 3.2 decomposed the modified dataset into 57 spatial modes and their associated temporal indices. The spatial modes were sorted based on the amount of variance that they explained. Table 4.1 gives an overview of the importance of the first 12 spatial modes.

Table 4.1: Explained variance of the first 12 spatial modes (EOFs) of the research area that were derived using a principal component analysis.

EOF	Explained variance [%]	Cumulative	EOF	Explained variance [%]	Cumulative
1	49.57	49.57	7	1.39	91.76
2	24.03	73.59	8	1.04	92.81
3	8.48	82.08	9	0.90	93.70
4	4.27	86.35	10	0.66	94.36
5	2.55	88.90	11	0.54	94.90
6	1.48	90.37	12	0.50	95.40

The first 12 spatial modes already explain more than 95% of the variance in the dataset. The remaining EOFs each have an explained variance ratio lower than 0.5% and therefore do not contain any helpful information. The explained variance drops rapidly from the first EOF and therefore only the first three EOFs are presented in this section, the other EOFs can be found in Appendix A. Figure 4.1a shows the first three spatial modes and their temporal indices are shown in Figure 4.1b. The colours on the map show the spatial variability of elevation within the EOF and the graph shows the temporal variability of the spatial mode. A positive trend in the temporal indices indicates an increase in elevation in the red areas and a decrease in the blue areas. The spatial modes are all scaled to a range of -1 to 1 so that the magnitude of the variance is mainly described by the temporal indices. The large jump in the temporal indices in 2015 was caused by the creation of the Hondsbossche Duinen.

The temporal indices for the first spatial mode show a clear increasing trend which means that the elevation was rising in most parts of the research area except just north of IJmuiden and on the

western coast of Texel. The second mode shows a decreasing trend in the temporal indices before 1990 and an increasing trend after 1990. Most of the elevation variance in this mode is located around the HPZW, the dune crests and near the Texel inlet. The third mode shows a somewhat cyclic temporal behaviour and a cyclic spatial pattern in the wet part of the area. Most of the variance is located around the HPZW and the dune front.

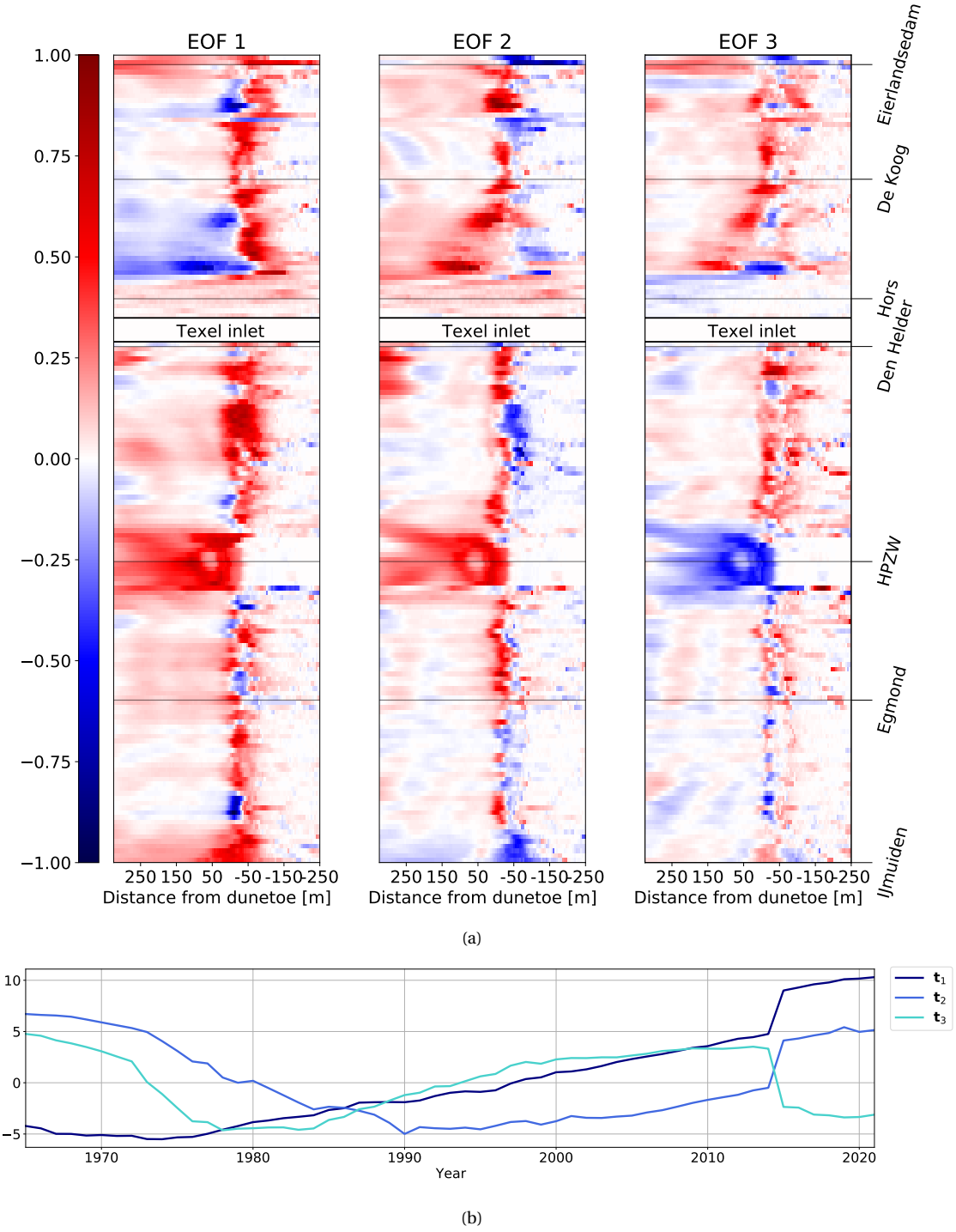

Figure 4.1: The first three spatial modes (a) showing the spatial distribution of elevation variance in the different modes across the research area. The elevation variance within the mode of every location is directly proportional to the corresponding temporal index with a proportionality coefficient equal to the values indicated by the colours. The first three temporal indices (b) show the temporal development of the elevation of each mode.

4.2. Coastal categorisation

This section describes the overall results of the clustering algorithm and the evaluation methods. The spatial distribution of the clusters is shown along with the intra-cluster variances. A lattice of the cluster centres, created by a self-organising map, illustrates the similarities between the clusters.

The results of the clustering algorithm mainly depended on the specified number of clusters. The elbow method provided an initial guess for the preferred number of clusters and Figure 4.2 shows the results of the elbow method and the silhouette scores. The sum of squared errors of the samples to their cluster centre was plotted against the number of clusters to find the elbow point, which was found at 41 clusters. The optimal number of clusters found with the elbow method lies close to the number of clusters with the best silhouette score. All different amount of clusters that were investigated resulted in overall silhouette scores lower than 0.3.

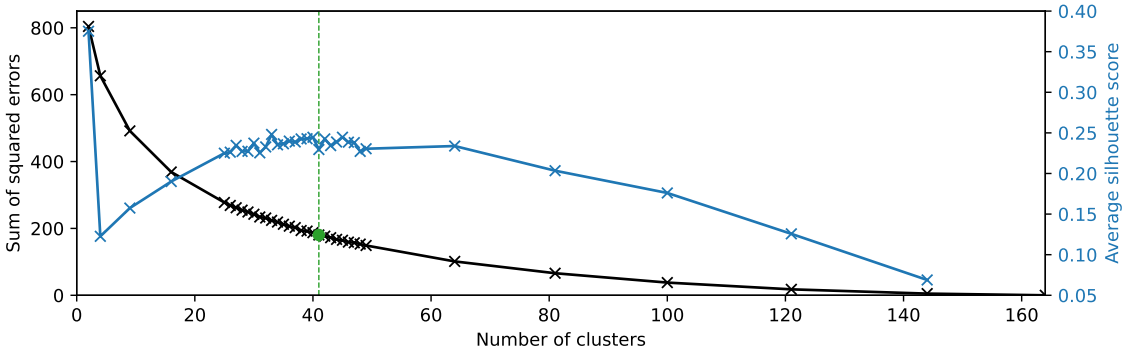

Figure 4.2: The inertias (black) and silhouette scores (blue) for simulations with different numbers of clusters. The vertical line shows the elbow point that was used as an initial guess for the preferred number of clusters.

Due to the low silhouette scores for all simulations, an additional model was created to check whether a new model with fewer features would yield better silhouette scores and more distinct clusters. The model used only 6 EOFs as input and used averaged values of 5 cross-shore locations to reduce the number of cross-shore locations. The results of the elbow method and silhouette scores are shown in Figure 4.3. The graph shows that the reduction of features increased the silhouette score around the optimal number of clusters by approximately 0.05. The optimal number of clusters according to the elbow method and silhouette score was found at 39 clusters, which is slightly lower than the 41 clusters found with the original model.

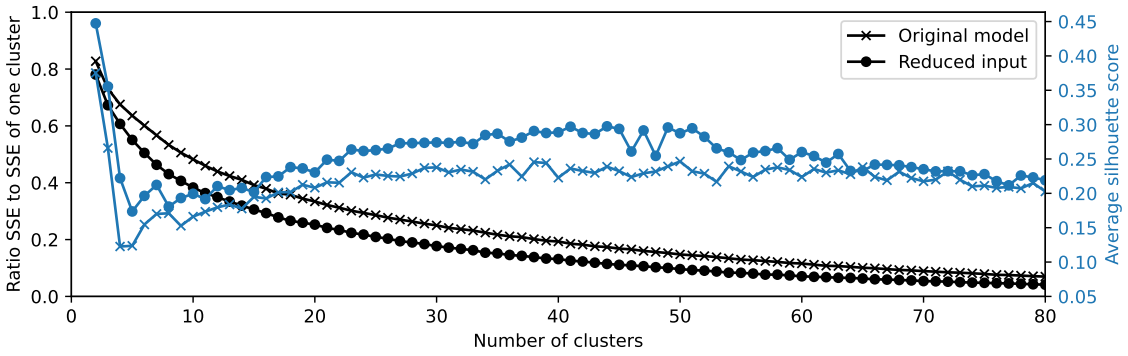

Figure 4.3: Comparison of the inertias (SSE, shown in black) and the silhouette scores (shown in blue) of the original model indicated by the crosses and the model with a reduced number of features indicated by the circles. The figure only shows the data up to 80 clusters to display the area of interest more clearly.

The results of the clustering algorithm with 41 clusters were inspected visually to check whether the transects in a cluster behaved similarly over time. The number of clusters was reduced until the intra-cluster differences in profile shape and development became too large. When the number of clusters was decreased to 35, too large differences occurred and therefore the final results were obtained with 36 clusters. Figure 4.4 gives an example of how the visual inspection of a cluster was performed. For clarity reasons, the example figure only shows the profiles for three different years instead of the 57 profiles used for the animations that were used for the actual inspection. The dashed lines in the figure show the transect that was added to the cluster when the number of clusters decreased from 36 to 35. The figure shows an increase in dune height for the transects in the cluster, which is significantly larger than the increase in dune height of the highlighted transect.

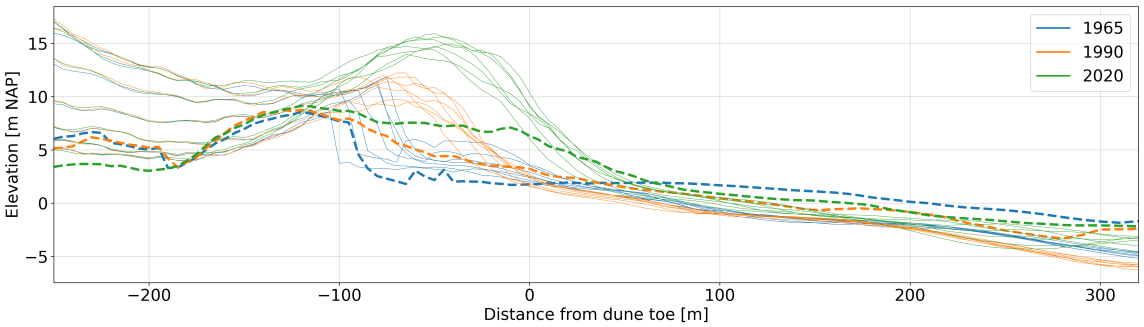

Figure 4.4: Profile data for the transects in a cluster for 3 different years. The dashed line shows the profiles for a transect that was added to the cluster when the number of clusters decreased from 36 to 35. Animations of the same figure showing the profiles of 57 years subsequently were used for inspection of the intra-cluster variance.

A simulation with 36 clusters and 30,000 random initialisations of the cluster centres gave the final results for the clustering of this research. Figure 4.5 gives an overview of the spatial distribution of the clusters. Most of the clusters consist of a set of bordering transects which are alternately shown in blue and dark blue and these clusters are numbered 1 to 30. Two clusters contain a single transect, the first cluster (31) at the border between the Hors and the southwest coast of Texel and the second cluster (32) at the Eierlandsedam. Four clusters contain transects from separate areas which are numbered 33 to 36 and are shown in red, orange, pink and green respectively. The height of the bars indicates the silhouette scores of each sample which describes the distance to its cluster relative to the distance to its nearest cluster. Figure 4.5 shows that the transects in the middle of the cluster generally have a higher silhouette score than the transects near the cluster borders where all negative silhouette scores can be found. The low silhouette scores at the cluster borders indicate that the borders between the clusters are not distinct.

A self-organising map sorted the 36 cluster centres on a six-by-six grid where similar cluster centres are placed near each other. The algorithm only used the distances between the computed cluster centres and did not compare the different transects of the clusters. Figure 4.6 shows the resulting lattice where the colours of the clusters match with Figure 4.5. The text below the cluster numbers describes the stretch of coast that the cluster covers in RSP coordinates. The coordinate system for Noord-Holland, denoted here as NH, starts at Den Helder and therefore the positive direction is to the South, which is left in Figure 4.5. The positive direction for Texel is to the North, which is right in Figure 4.5.

There are groups of clusters that are close together both on the lattice and in space. The bottom left corner of the lattice consists of clusters 5 through 10 which cover the HPZW and the adjacent coasts that are affected by the mega nourishment in 2015. The clusters in the top left corner (16, 17, 18 and 31) are all located near the Texel inlet and the clusters in the bottom right corner cover the northern part of Texel except cluster 19 which comprises the Hors.

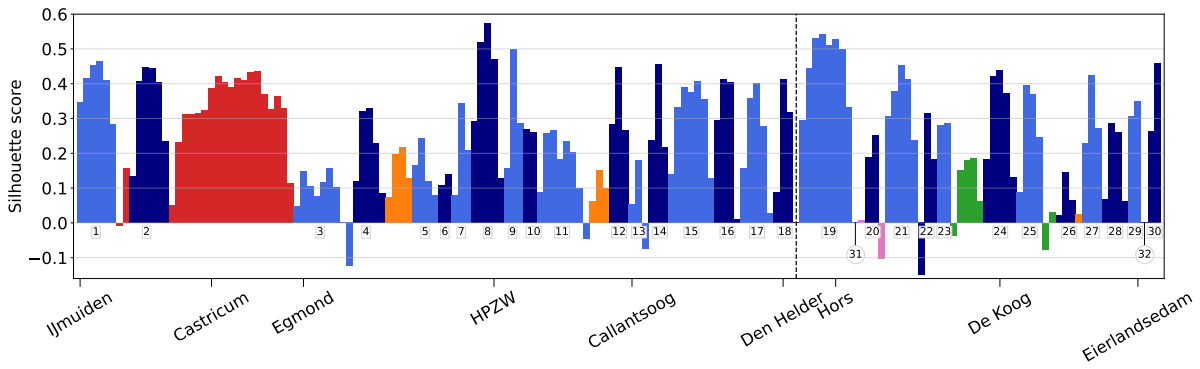

Figure 4.5: Spatial distribution of the clusters with the silhouette scores of the samples. Each bar represents a transect and the numbers indicate the cluster number. Clusters that are continuous in space are shown in blue and clusters that are discontinuous in space have been given a distinct colour. clusters 31 and 32 are made up of one transect and therefore do not have a silhouette score. The dashed line represents the Texel inlet.

Cluster 31 TX: 8.25—8.75	Cluster 17 NH: 1.75—4.25	Cluster 1 NH: 51.75—54.75	Cluster 22 TX: 13.25—14.75	Cluster 23 TX: 14.75—15.75	Cluster 20 TX: 9.25—10.25
Cluster 18 NH: 0.00—1.75	Cluster 16 NH: 4.25—6.25	Cluster 26 TX: 23.75—25.25	Cluster 15 NH: 6.25—9.75	Cluster 21 TX: 10.75—13.25	Cluster 35 TX: 8.75 — 9.25 TX: 10.25—10.75
Cluster 12 NH: 12.75—14.25	Cluster 33 NH: 38.25—47.75 NH: 50.75—51.75	Cluster 34 NH: 14.25—15.75 NH: 29.25—31.25 TX: 25.25—25.75	Cluster 36 TX: 15.75—18.25 TX: 22.75—23.75	Cluster 14 NH: 9.75—11.25	Cluster 25 TX: 20.75—22.75
Cluster 3 NH: 33.75—38.25	Cluster 2: NH: 47.75—50.75	Cluster 11 NH: 15.75—19.75	Cluster 4 NH: 31.25—33.75	Cluster 24 TX: 18.25—20.75	Cluster 13 NH: 11.25—12.75
Cluster 8 NH: 22.25—24.75	Cluster 5: NH: 27.25—29.25	Cluster 10 NH: 19.75—20.75	Cluster 28 TX: 27.25—29.25	Cluster 19 TX: 4.25—8.25	Cluster 32 TX: 30.25—30.75
Cluster 7 NH: 24.75—26.25	Cluster 9 NH: 20.75—22.25	Cluster 6 NH: 26.25—27.25	Cluster 27 TX: 25.75—27.25	Cluster 29 TX: 29.25—30.25	Cluster 30 TX: 30.75—31.75

Figure 4.6: A lattice of the clusters was created by a self-organising map, displaying the similarities between different clusters. The text in each cell describes the stretch of coast that the cluster contains. The letters indicate the area, NH for Noord-Holland and TX for Texel, and the numbers give the start and end coordinates in km RSP.

4.3. Highlighted clusters

This section presents more detailed results of seven selected clusters and some of the drivers that contribute to the development of the beaches and dunes in these clusters. Some information on the median values and distribution of the characteristic parameters across the research area is given so that the differences between the clusters and the average values in the research area become clear. Figure 4.7 shows the research area with the locations of the seven clusters that are described in more detail. The RSP line, which is used as a reference line in the figures below, is shown in green. The alongshore RSP coordinates start at the Texel inlet, indicated by the dashed line, and the positive direction is directed away from the Texel inlet as indicated by the black arrows. The cross-shore dimension of each transect is directed perpendicular to the RSP line with the origin on the RSP line and the positive direction seaward. The selected clusters vary in beach and dune developments, nourishment volumes, location and orientation so that the effects of different contributing factors on the beach and dune developments can be compared.

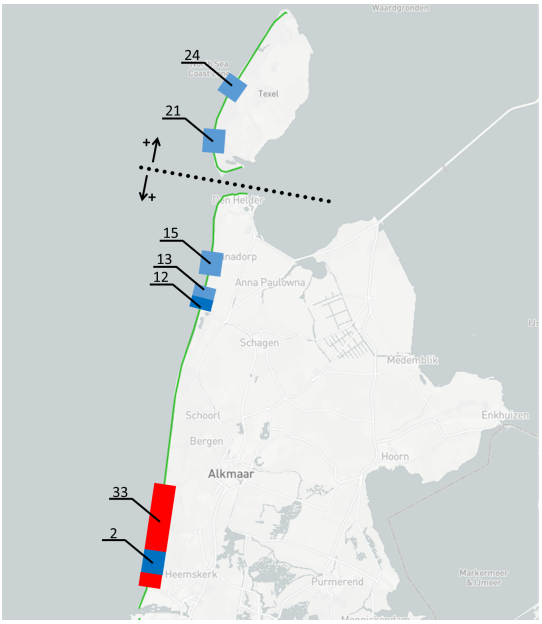

Figure 4.7: Map of the research area that shows the locations of the selected clusters. The RSP line is shown in green and the arrows indicate the positive direction of the RSP coordinates.

The characteristic parameters were determined for every available profile in the JarKus dataset. The parameters describing the beach and dune development are presented in this section. Figure 4.48 shows the development of the dune height and volume of the entire research area with respect to the temporal mean value of each transect. The dune volume of the entire research area shows a clear increasing trend after 1990, with a slight increase in the rate of change. The dune height showed an increase over the entire time span, but the rate of change decreased to approximately zero.

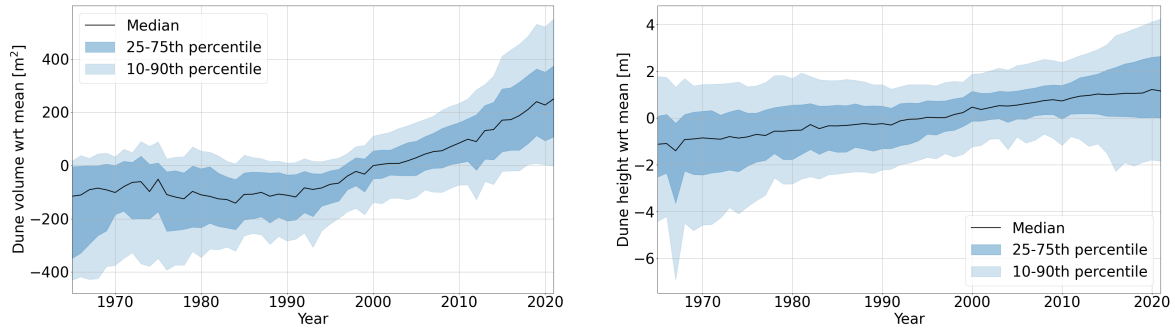

(a) Dune volume

(b) Dune height

Figure 4.8: Temporal development of the dune volume (a) and the dune height (b) in the entire research area. The graph shows the median dune volume and height of all transects relative to their temporal mean value.

The distributions of the values that were found for the characteristic parameters describing the beach and dune development across the entire research area are shown in Figure 4.9. The distribution of the dune volumes is not shown because the landward boundary used to determine the

dune volumes has no physical meaning. The figures show the median value of the characteristic parameters and the 10-90th percentile range. Most beach slope values lie between 0.016 and 0.049, with several outliers with beach slopes steeper than 0.1, around Den Helder, the HPZW and the northeastern part of Texel. The beach width is shown in Figure 4.9b and had large outliers that are not shown in the graph with a maximum of 2015 metres. Most values lie in the range of 50 to 170 metres with a median value of 85 metres. The large values are not shown to make the distribution of the values within the 10-90th percentile range clearly visible. The values for the dune slope are quite uniformly spread in the 10-90th percentile range (0.07-0.41). There are a few outliers with slopes steeper than 0.5 which are spread over the entire research area and timespan. The dune heights in the research area mainly lie in the range of 8.62 to 20.58 metres, with a median value of 14.21 metres. The largest dune heights (>22 metres) were all found in coastal section 7.

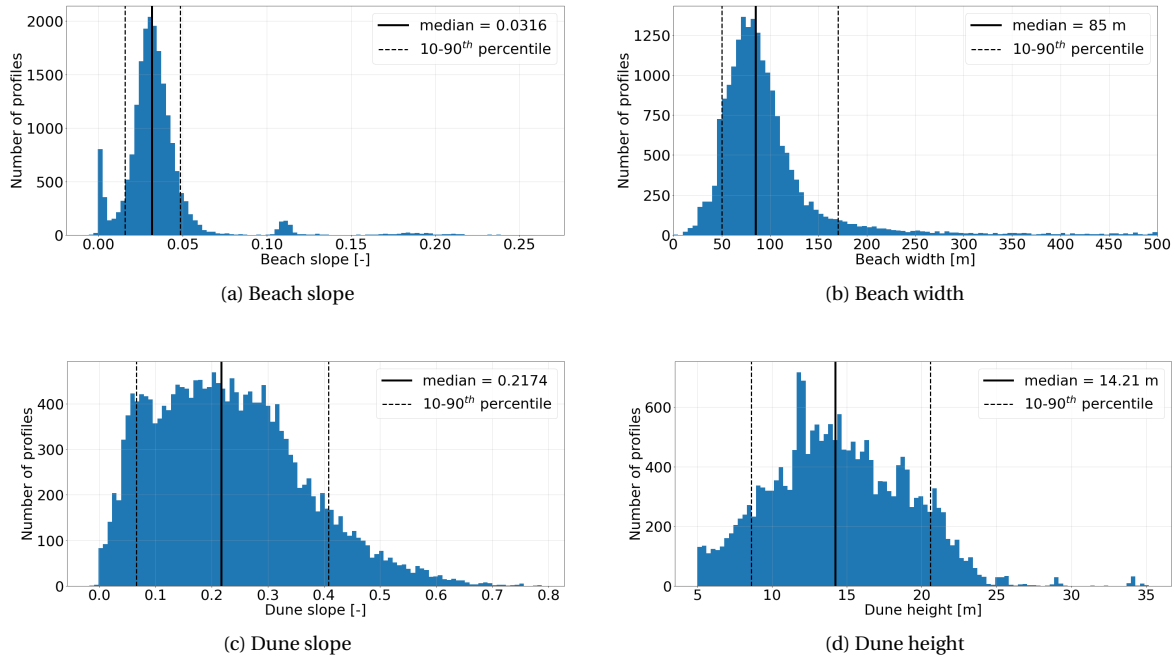

(a) Beach slope

(b) Beach width

(c) Dune slope

(d) Dune height

Figure 4.9: Distribution of values for the beach slope (a), beach width (b), dune slope (c) and dune height (d) of all transects and for every year. The lines indicate the median value and the 10-90th percentile range.

4.3.1. Cluster 33: Egmond - Wijk aan Zee (38.25-47.75 & 50.75-51.75km RSP)

This subsection describes cluster 33, which stretches from Egmond to Wijk aan Zee, in more detail. Cluster 33 is one of the four clusters that are not continuous in space as it is interrupted by cluster 2. Figure 4.10 gives an overview of the areas that cluster 33 comprises. Pavilions and small beach houses, shown in red, are present in parts of this cluster near Egmond, Castricum and Wijk aan Zee. The figure only shows the buildings in the current situation. The number of buildings in the area and the period in which seasonal buildings are present varies for the different years. Figure 4.11 shows the supplied nourishments in the area. The figure shows that only the most northern part of the cluster received nourishments frequently while a part of the cluster did not receive any nourishment. Before 2000 most nourishments were supplied on the beach, while after 2000 the nourishments were mainly supplied to the foreshore.

Figure 4.12 shows the locations of the shoreline in cluster 33 for four years relative to the shoreline location in 1976. Between 2005 and 2019, the shoreline shows a seaward migration which is strongest between 39 $km\ RSP$ and 42.5 $km\ RSP$ and around 45 $km\ RSP$. These locations both received nourishments after 2005.

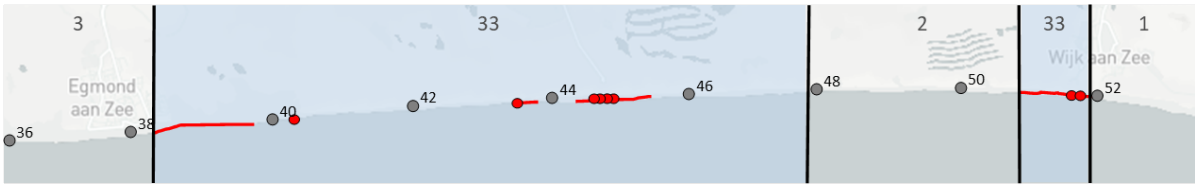

Figure 4.10: Overview of cluster 33 located in the southern part of Noord-Holland. The cluster boundaries are indicated by the black lines and the cluster numbers are shown at the top of the figure. The numbered circles show the beach poles along the Dutch coast and the buildings on the beach are shown in red.

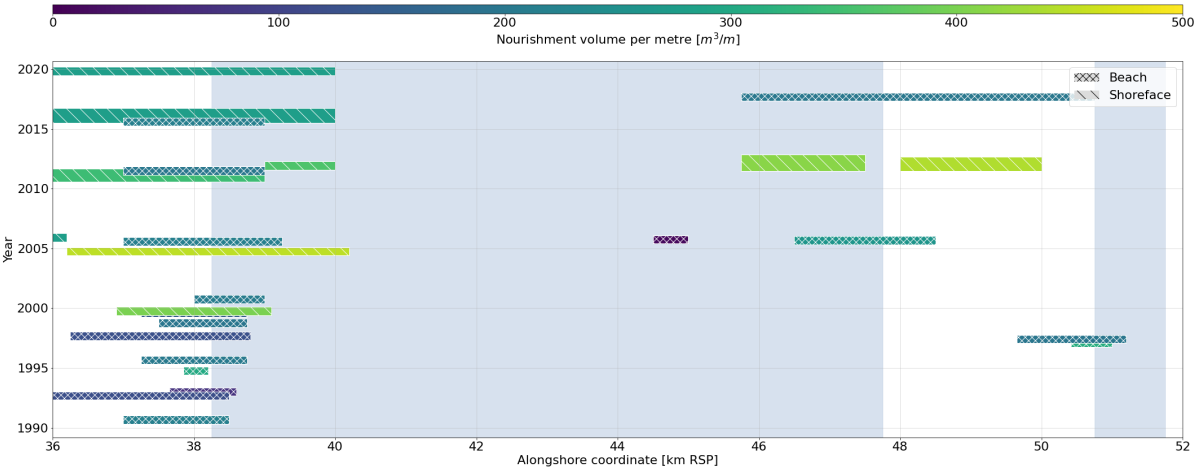

Figure 4.11: Overview of the nourishments in and around cluster 33. The colours indicate the nourishment volumes and the type of nourishment is indicated by the hatch of the boxes.

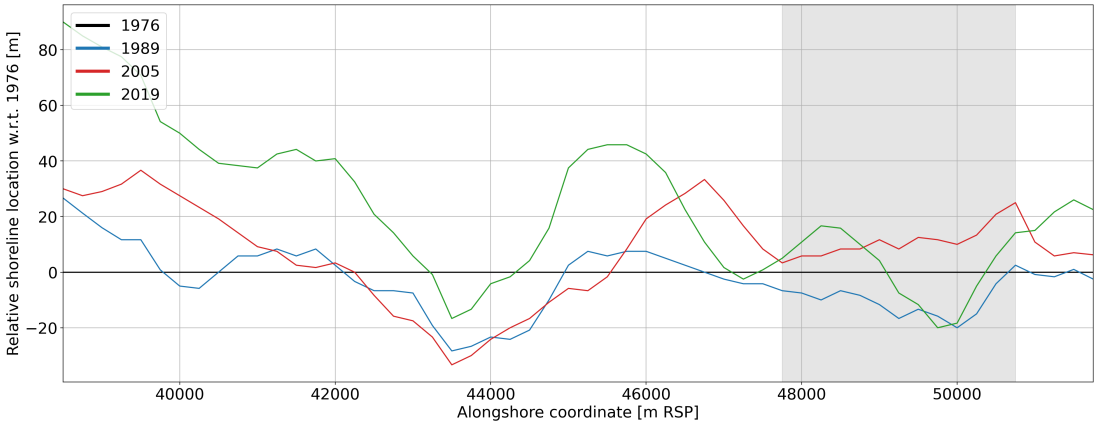

Figure 4.12: Spatial plot of the shoreline locations of cluster 33 for three different years, relative to the shoreline location in 1976. The shaded area does not belong to this cluster but to cluster 2.

Figure 4.13 shows that the dune volume has increased from 1976 to 2020 in every part of the cluster. Between 2005 and 2019 most locations show an increase in dune volume or dune height (shown in Figures 4.13 and 4.14). The highlighted transects at 44.75 $km\ RSP$ and 51.5 $km\ RSP$ cross beach pavilions that have both been present since 2007 and were opened year-round. Both transects show a slight decrease in dune height and a constant dune volume since 2005. The remaining transects of the cluster mainly show an increase in dune height from 1979 to 2020. The temporal changes in median dune volume and height are shown in Figures 4.15a and 4.15b. Both the dune volume and the dune height show an increase since 1970, where the rate of the dune volume increased over time

and the rate of the dune height decreased. The temporal behaviour of the shoreline is described in Figure 4.15c and shows a slight seaward migration from 2005.

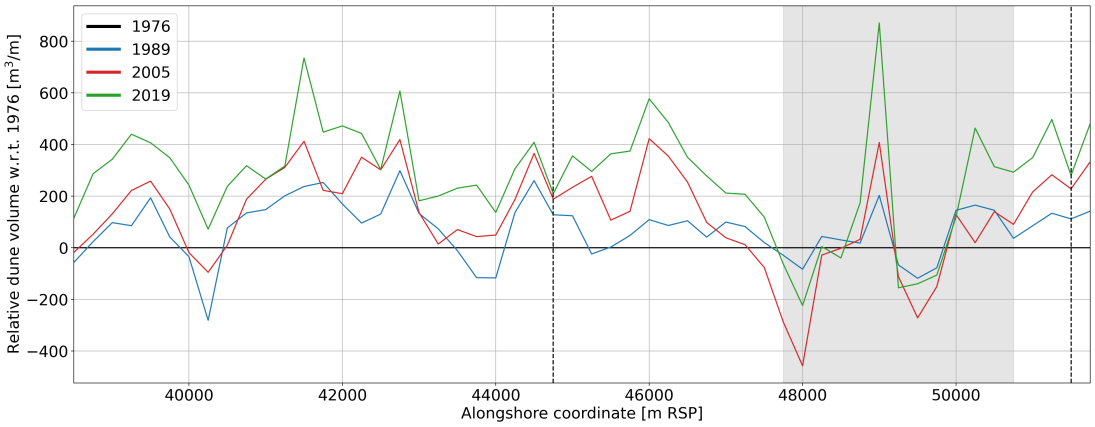

Figure 4.13: Spatial plot of dune volumes of cluster 33 for three different years, relative to the dune volumes in 1976. The shaded area does not belong to this cluster but to cluster 2.

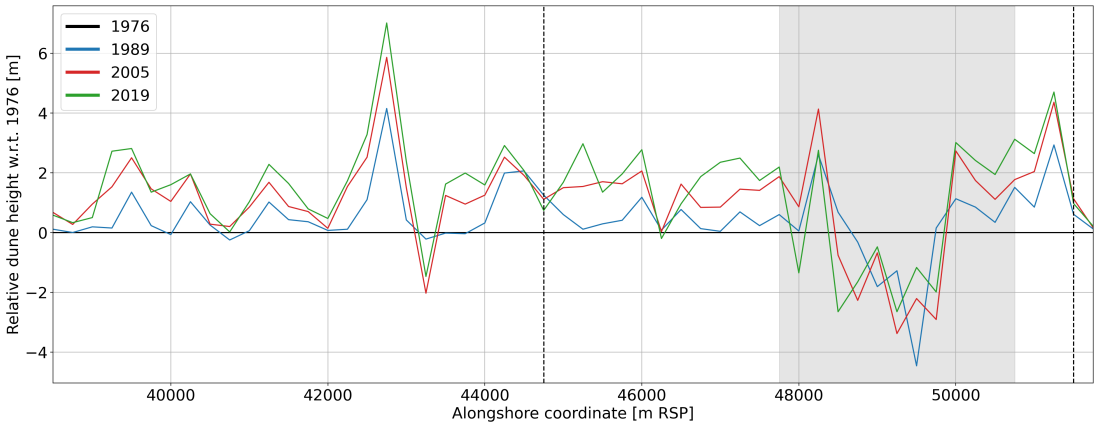

Figure 4.14: Spatial plot of dune heights of cluster 33 for three different years, relative to the dune heights in 1976. The shaded area does not belong to this cluster but to cluster 2.

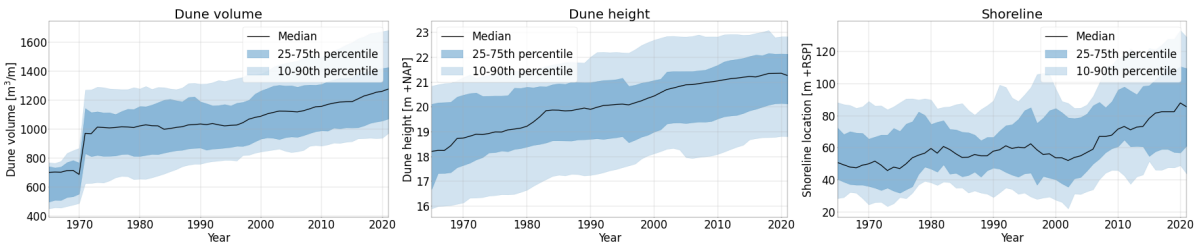

(a) (b) (c)

Figure 4.15: Temporal development of the dune volume (a), dune height (b) and shoreline location (c) of all transects in cluster 33.

4.3.2. Cluster 2: Heemskerk (47.75-50.75km RSP)

This subsection describes cluster 2, which is highlighted in Figure 4.16, in more detail. Cluster 2 is located in the southern part of the research area and stretches from 47.75 $km\,RSP$ to 50.75 $km\,RSP$. The cluster lies close to the breakwater of IJmuiden and the dunes in this cluster contain several blow-outs, which can be seen in Figure 4.18. The cluster received five nourishments with volumes ranging between 150 and 450 m^3/m and they are shown in Figure 4.17. There was one beach pavilion in this cluster and several small beach houses, which are indicated by the red circle and red line in Figure 4.16 respectively.

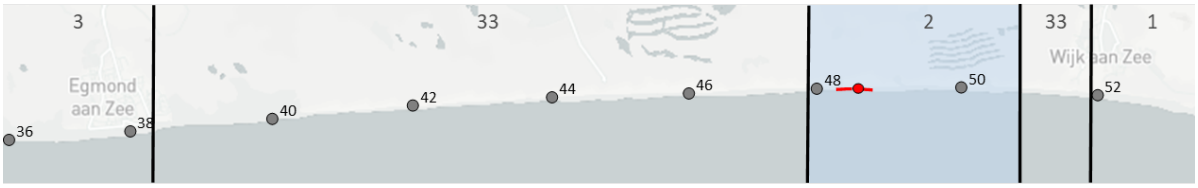

Figure 4.16: Overview of cluster 2 located in the southern part of Noord-Holland. The cluster boundaries are indicated by the black lines and the cluster numbers are shown at the top of the figure. The numbered circles show the beach poles along the Dutch coast and the buildings on the beach are shown in red.

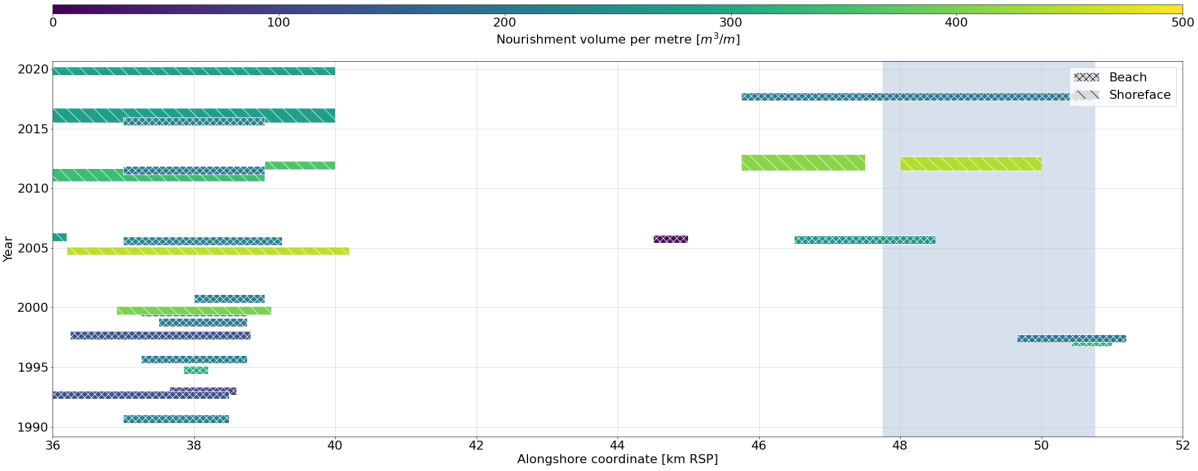

Figure 4.17: Overview of the nourishments in and around cluster 2. The colours indicate the nourishment volumes and the type of nourishment is indicated by the hatch of the boxes.

Figure 4.18: Aerial picture of the dunes of cluster 2. Transects directly crossing a blow-out are highlighted and the number shows the alongshore RSP coordinate in metres. Picture obtained from Coastviewer (Deltares, 2018).

Figure 4.21a shows the development of the dune toe location over time for the transects in the cluster. The dune toes in the cluster had a strong landward migration until 2007. The landward migration of the dune toe is strongest in the northern part of the cluster and the dune toes in the most southern part had a slight seaward migration, which can be seen in Figure 4.19. The figure shows a clear difference in dune toe migration between cluster 2 and the bordering cluster 33.

The median dune volume in the cluster remained constant over the entire time span, while Figure 4.20 shows a large alongshore difference. Two transects, 49000 and 50250 showed a large increase in dune volume between 2005 and 2019. Most of the volume increase of these transects was found behind the most seaward dune. These transects directly crossed the blow-outs shown in Figure 4.18.

The beach width of the cluster varied between 60 and 120 metres, which lies around the average of the research area. Between 1990 and 2010, the beach width remained rather constant, while it shows a strong increase around 2012 from 80 to 100 metres. Furthermore, this cluster had an average beach slope of 0.03 and a very steep dune slope which varied between 0.35 and 0.55.

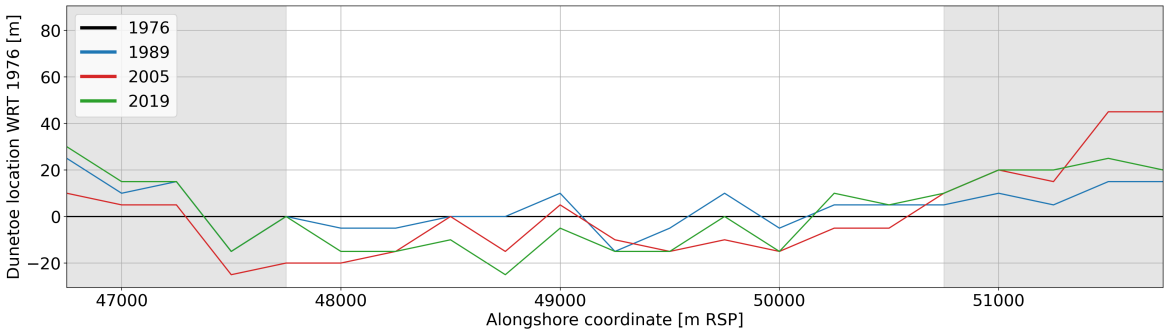

Figure 4.19: Spatial plot of the dune toe locations of cluster 2 for three different years, relative to the dune toe location in 1976. The shaded grey area is not part of cluster 2.

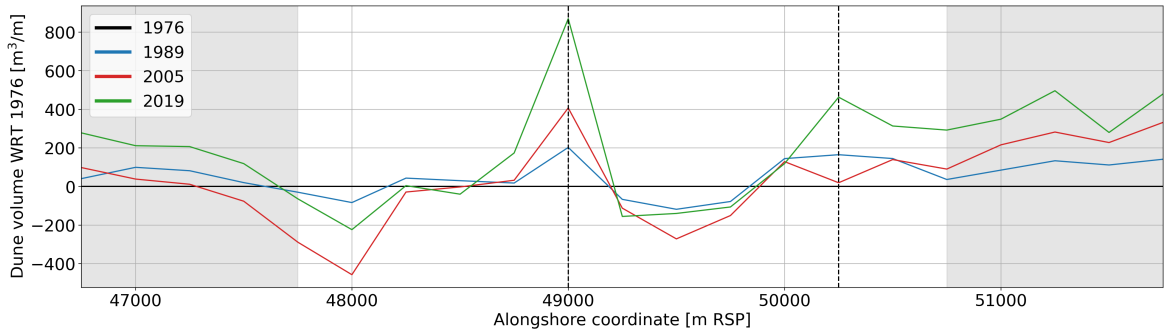

Figure 4.20: Spatial plot of the dune volumes of cluster 2 for three different years, relative to the dune volumes in 1976. The shaded grey area is not part of cluster 2.

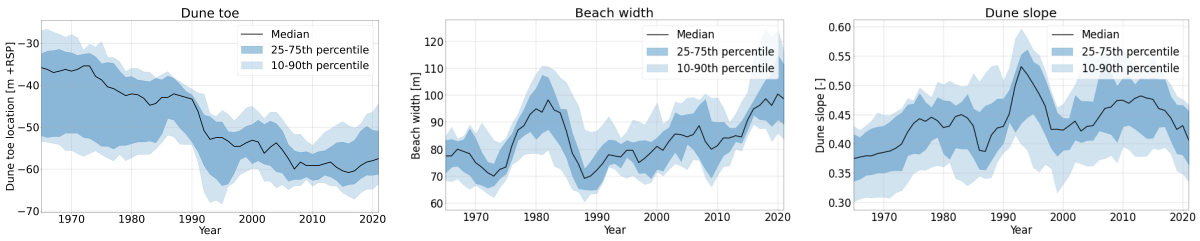

(a) (b) (c)

Figure 4.21: Temporal development of the dune toe location (a), beach width (b) and dune slope (c) of all transects in cluster 2.

4.3.3. Clusters 12 and 13: Callantsoog (12.75-14.25 & 11.25-12.75 km RSP)

This subsection describes clusters 12 and 13 in more detail and Figure 4.22 gives an overview of the area. These clusters are located in the northern part of the Noord-Holland coast, approximately 12 kilometres south of the Texel inlet. These clusters are described together to assess the quality of the coastal categorisation. The SOM placed these clusters far from each other on the grid, while the cluster centres were very similar.

Figure 4.23 shows the supplied nourishments in the area of these two clusters. Both clusters received frequent nourishments with a total volume of 3586 and 3391 m^3/m for clusters 12 and 13 respectively. The first two nourishments in 1977 and 1979 were supplied in the dune, which was no longer done after 1990. Nourishments after 1990 were supplied on the beach and the shoreface, where the shoreface nourishments had significantly higher volumes than the beach nourishments.

The vegetation of the most seaward dunes of clusters 12 and 13 show a large difference, which is shown in Figure 4.24. It can be seen that the first row of dunes in cluster 13 has less vegetation than the dunes in cluster 12. The most seaward dunes with less vegetation in cluster 13 were newly developed embryo dunes, which were formed around 2005. In addition, Figure 4.24a shows the buildings on the beach in cluster 12 and the village behind the dunes. The presence of the village limits the width of the dunes on the landward side.

The dune volumes of these clusters were computed for four different years and Figure 4.25 shows the alongshore differences in dune volume over time relative to the dune volumes in 1987. It shows that the dune volumes have increased over the entire stretch of the coast, with the largest increases in cluster 12. The lowest volume increases were found behind the buildings on the beach, where no embryo dunes were formed.

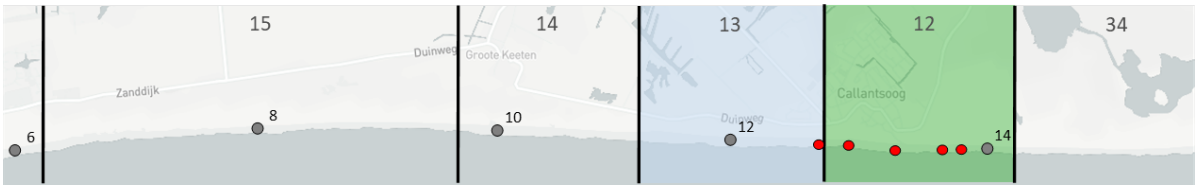

Figure 4.22: Overview of clusters 12 (green) and 13 (blue) and the surrounding area, located in the northern part of the Noord-Holland coast. The cluster boundaries are indicated by the black lines and the cluster numbers are shown at the top of the figure. The beach poles are shown by the numbered circles and the red circles indicate the beach pavilions in the two clusters.

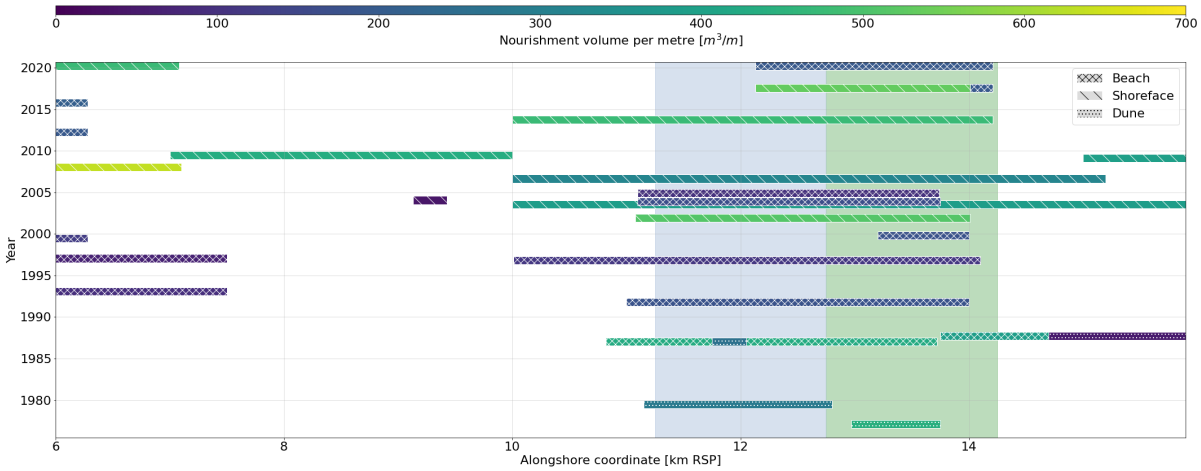

Figure 4.23: Overview of the nourishments in and around clusters 12 (green) and 13 (blue). The colours indicate the nourishment volumes and the type of nourishment is indicated by the hatch of the boxes.

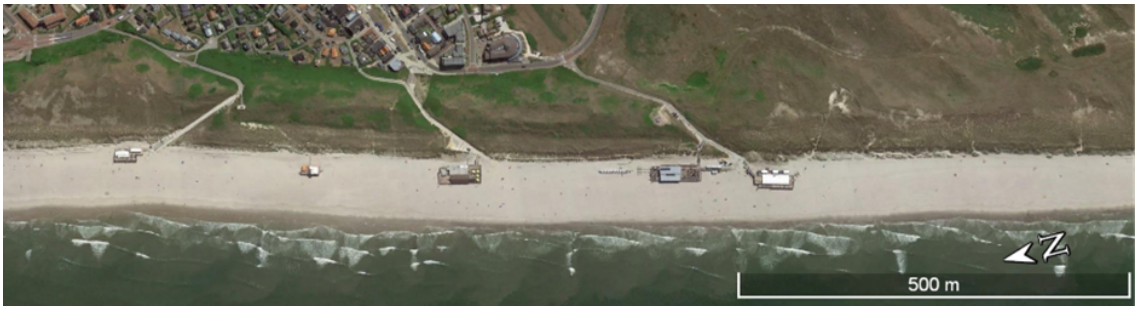

(a) Cluster 12

(b) Cluster 13

Figure 4.24: Aerial picture of the dunes of cluster 12 (a) and cluster 13 (b), showing the difference in vegetation density and the presence of buildings on the beach. Picture taken in June 2017, obtained from Google Earth.

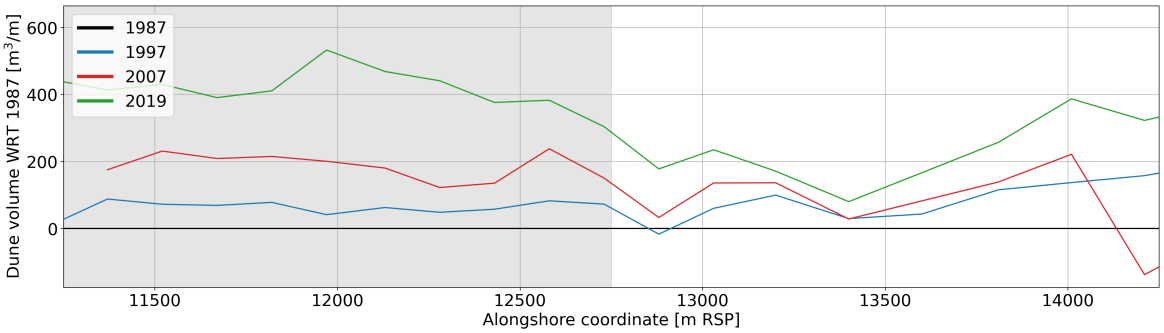

Figure 4.25: Spatial plot of the development of the dune volumes in clusters 12 (white area) and 13 (grey area) over time, relative to the dune volumes in 1987.

The increase in dune volume over time is displayed in more detail in Figures 4.26a and 4.27a. The first jump in the dune volumes was caused by a lack of data for the transects in the clusters and the second jump in the dune volume of cluster 13 was caused by a change in transect locations for which the data was stored. After large fluctuations in the dataset, both clusters showed an increasing dune volume from around 1990. The rate at which the dune volume grew was very constant in cluster 12 while the rate of cluster 13 increased between 1990 and 2000. The development of the dune heights of clusters 12 and 13 are shown in Figures 4.26b and 4.27b respectively. Both clusters showed an increase in dune height around the time of the dune nourishments. After 1990, the dune heights remained constant in both clusters. Figures 4.26c and 4.27c show the development of the beach width over time. The beach width does not show any correlation with the development of the dune height and dune volume. The beach widths of both clusters showed a large increase from 2000 to 2008 and from 2012 and 2020. The accretion periods were simultaneous with periods of large nourishment volumes (>1000 m^3/m) and preceded by erosion periods with lower nourishment volumes (<100 m^3/m).

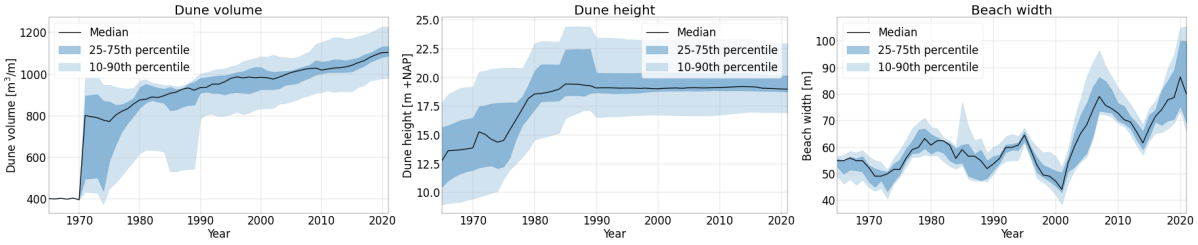

(a) (b) (c)

Figure 4.26: Development over time for three characteristic variables (a) dune volume, (b) dune height and (c) beach width, of cluster 12.

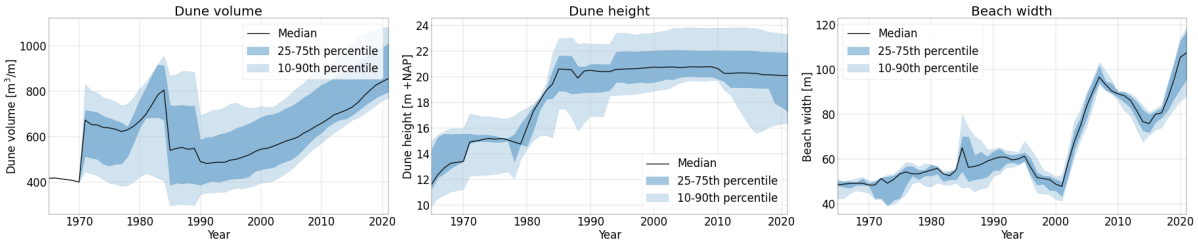

(a) (b) (c)

Figure 4.27: Development over time for three characteristic variables (a) dune volume, (b) dune height and (c) beach width, of cluster 13.

4.3.4. Cluster 15: Julianadorp (6.25-9.75km RSP)

This subsection describes cluster 15, shown in Figure 4.29, in more detail. This cluster covers the coast near Julianadorp that stretches from 6.25 $km\ RSP$ to 9.75 $km\ RSP$. Julianadorp lies on the northern part of the Noord-Holland coast, close to the Texel inlet. Two tidal channels lie in front of this part of the coast, Nieuwe Lands Diep and Nieuwe Schulpengat, which are separated by a shoal called Franse Bankje that shields the coast from the incoming waves. Figure 4.28 shows the bathymetry of the area in more detail. There were no buildings present on the beach of this cluster and the entire stretch of coast has groynes with a spacing of about 200 metres.

Figure 4.30 shows the nourishments that were supplied in the area. The nourishments in this cluster were mainly supplied in the northern part and one nourishment in 2009 covered a large part of the cluster. The nourishment volumes and frequency in cluster 15 were lower than on the adjacent coast south of this cluster. Nourishments in this cluster before 2000 were beach nourishments and the nourishments after 2000 were shoreface nourishments with larger volumes than the beach nourishments.

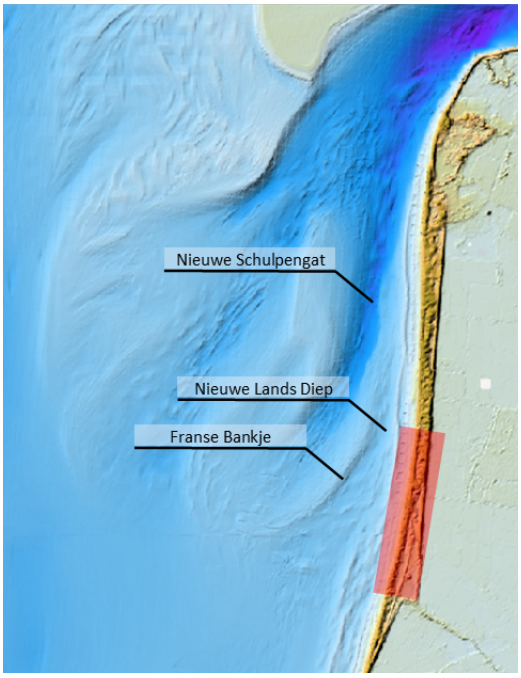

Figure 4.28: Bathymetry of the area around cluster 15, which is highlighted by the red area. Map obtained from Coastviewer (Deltares, 2018).

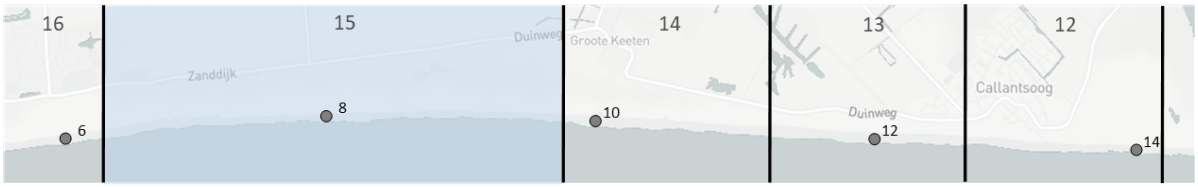

Figure 4.29: Overview of cluster 15 located in the northern part of Noord-Holland. The cluster boundaries are indicated by the black lines and the cluster numbers are shown at the top of the figure. The numbered circles show the beach poles along the Dutch coast.

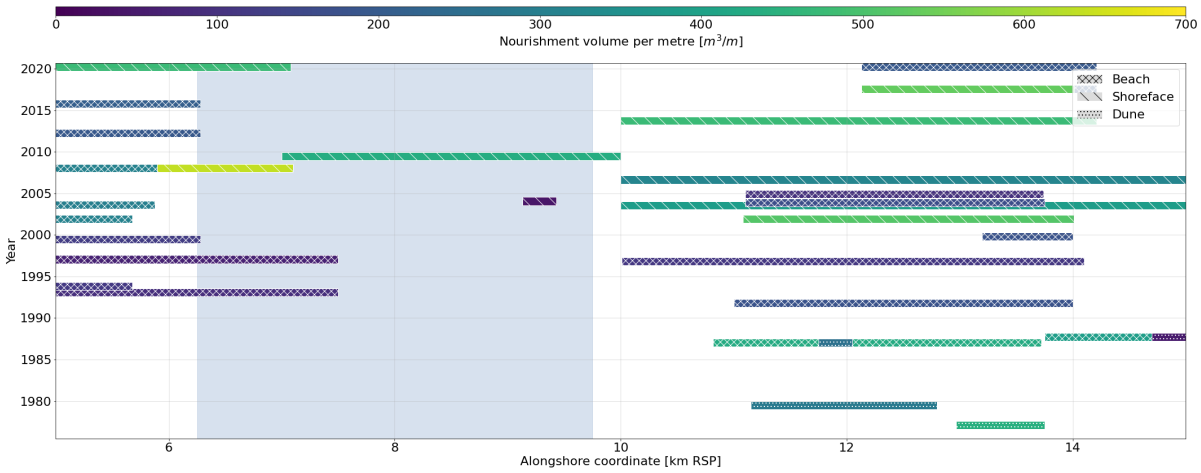

Figure 4.30: Overview of the nourishments in and around cluster 15. The colours indicate the nourishment volumes and the type of nourishment is indicated by the hatch of the boxes.

Figure 4.31 shows the alongshore differences in the development of the dune volumes in the cluster. The entire stretch of coasts showed a significant increase in dune volume without much alongshore variability. The development over time is displayed in more detail in Figure 4.32a. The dune volume increased monotonically with a slight decrease in the rate of change around 2015. The development of the dune height is shown in Figure 4.32b and shows a similar increasing trend. The rate of change of the dune top height decreases earlier, around 2005.

The beach width of this cluster shows an erosive trend with a strong decrease in beach width until 1985. Around 2008, the beach width showed a slight increase which coincides with the large foreshore nourishment that was supplied at a large part of the cluster. The dune slope ranged between 0.1 and 0.2, which is below the average of the research area and the beach slope varied between 0.0275 and 0.0375 which lies around the average value for the research area.

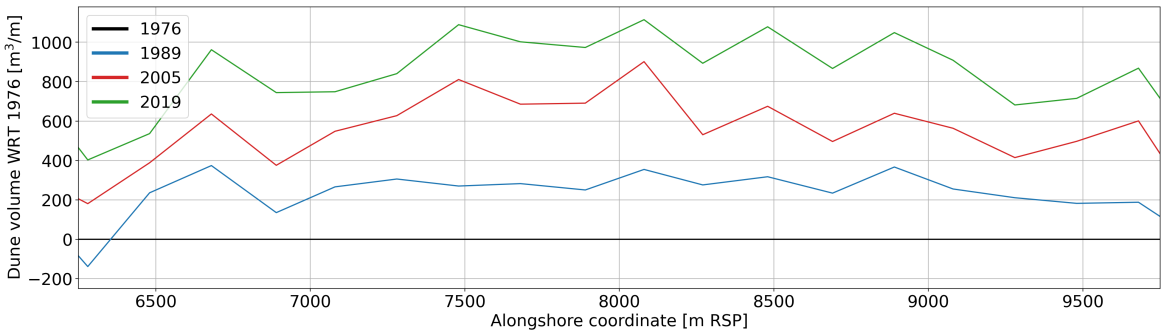

Figure 4.31: Development of the dune volumes in cluster 15 over time, relative to the dune volumes in 1976.

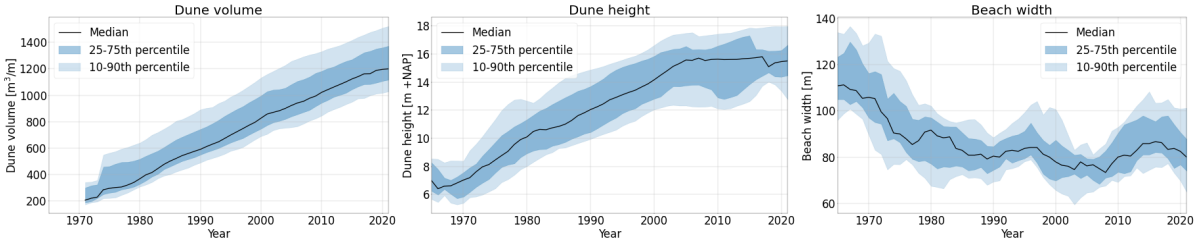

(a) (b) (c)

Figure 4.32: Development over time for three characteristic variables (a) dune volume, (b) dune height and (c) beach width, of cluster 15.

4.3.5. Cluster 21: South West Texel (10.75-13.25km RSP)

This subsection describes cluster 21 in more detail. Figure 4.33 gives an overview of the cluster, which is located in southwest Texel and stretches from 10.75 $km\ RSP$ to 13.25 $km\ RSP$. The cluster lies close to the Texel inlet and is influenced by the ebb-tidal delta. The entire coastline of this cluster is protected by groynes with a spacing of approximately 400 metres, which were constructed between 1957 and 1987. There are several buildings on the beach of this cluster, which are shown by the red circle (pavilion) and red lines (small beach houses). The pavilion remains on the beach year-round while the small beach houses are only present during spring and summer.

Figure 4.34 shows the nourishments in the cluster. Most nourishments before 2005 were supplied on the beach and after 2005 a combination of beach and foreshore nourishments was used to reinforce the coastline. The adjacent coastlines received similar amount of nourishment, but the nourishment volumes north of the cluster were generally larger than the nourishment supplied in the cluster.

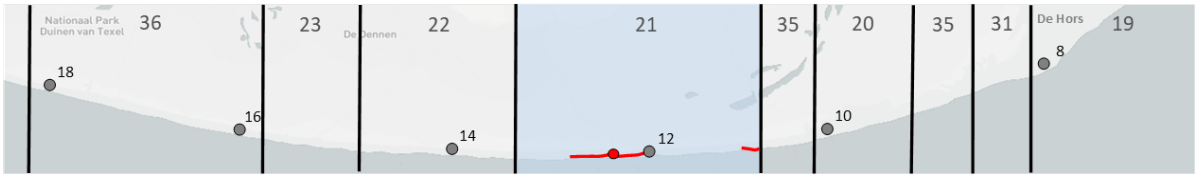

Figure 4.33: Overview of cluster 21 located in the southwestern part of Texel. The cluster boundaries are indicated by the black lines and the cluster numbers are shown at the top of the figure. The numbered circles show the beach poles along the Dutch coast and the buildings on the beach are shown in red.

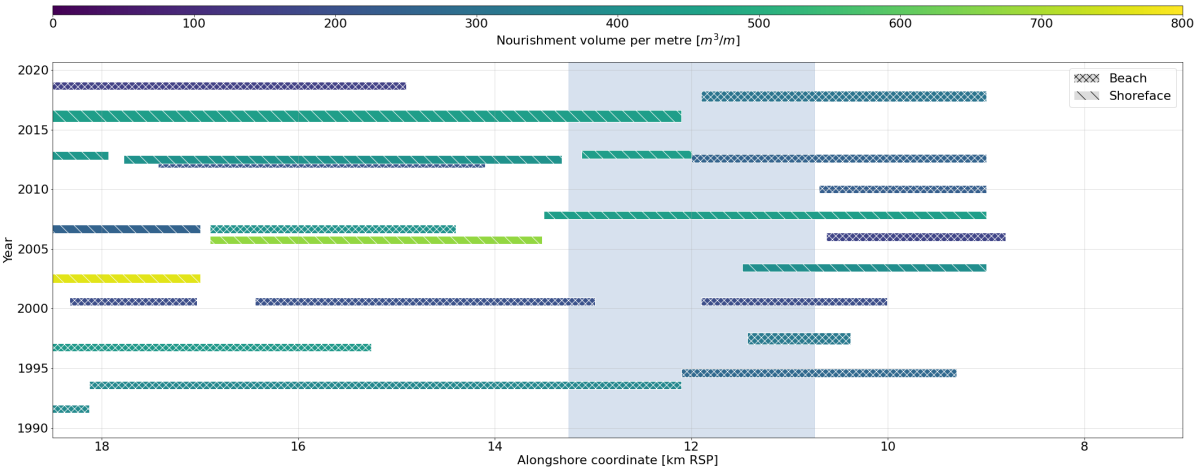

Figure 4.34: Overview of the nourishments in and around cluster 21. The colours indicate the nourishment volumes and the type of nourishment is indicated by the hatch of the boxes.

Figure 4.35 shows the bathymetry of the area. The tidal channel the Molengat and the shoal the Noordelijke Uitlopers Noorderhaaks (NUN) migrated landward until 1990. The landward migration of the tidal channel caused steepening of the foreshore and beach slope. After 1990, the location of the channel and the shoal remained constant. The incoming wave energy in the cluster is reduced by the shallow bed level of the NUN and the incoming wave direction is affected by wave refraction on the shoal. The refraction of waves created a divergence point for sediment transport around beach pole 13 at the northern part of the cluster.

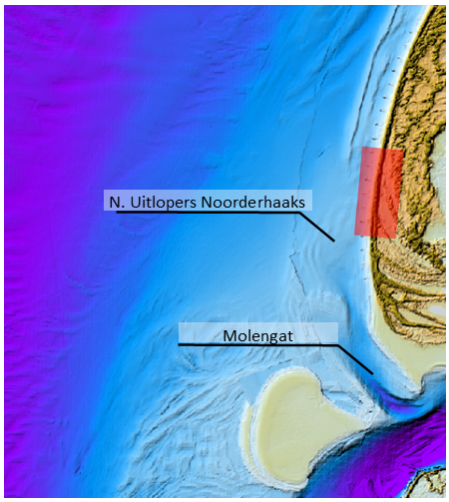

Figure 4.35: Map of the bathymetry around cluster 21 (highlighted in red). Obtained from Coastviewer (Deltares, 2018).

Figure 4.36 shows the development of the shoreline of the cluster. The shoreline migrated landward rapidly until 1990. After 1990, the average shoreline location did not show any significant change. The strongest landward migration was found in the central and southern parts of the cluster, which lies closer to the Texel inlet and the tidal channel.

The development of the dune volume in the cluster is shown in Figures 4.38 and 4.37a. It can be seen from the figures that the dune volume increased significantly since 1976 in the entire research area. The increase in dune volume was largest in the southern part of the cluster. The smallest dune volume increase was found at 12.49 km RSP transect, which directly crosses a beach pavilion.

Figure 4.37b shows the development of the dune heights in the cluster over time which increased significantly. The dune height showed a trend similar to the dune volume, with a larger increasing rate from around 1995. The dune height increase reduced around 2018 and remained constant since then. The development of the dune slope is shown in Figure 4.37c. The dunes in the cluster had a mild slope up to approximately 2000, after which it increased significantly to approximately 0.3.

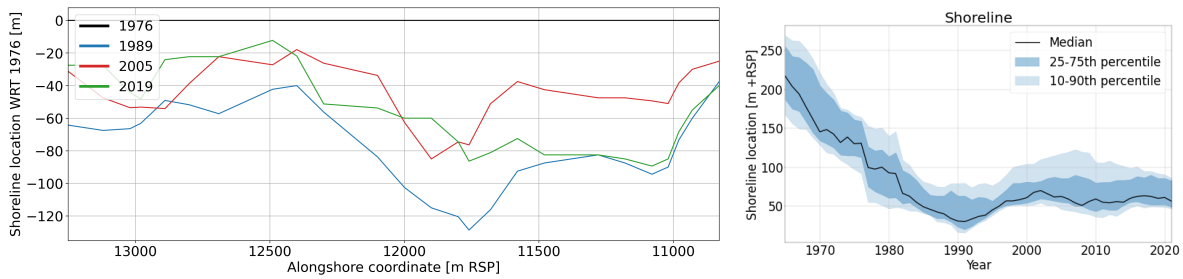

(a) (b)

Figure 4.36: Development of the shoreline location of cluster 21. Panel A shows a spatial plot of the shoreline location in four years relative to the shoreline location in 1976. Panel B shows the temporal development of the shoreline location of all transects in cluster 21.

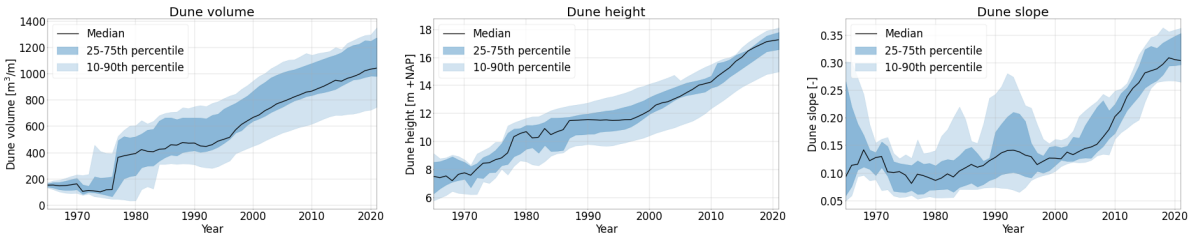

(a) (b) (c)

Figure 4.37: Temporal development of the dune volume (a), dune height (b) and dune slope (c) of all transects in cluster 21.

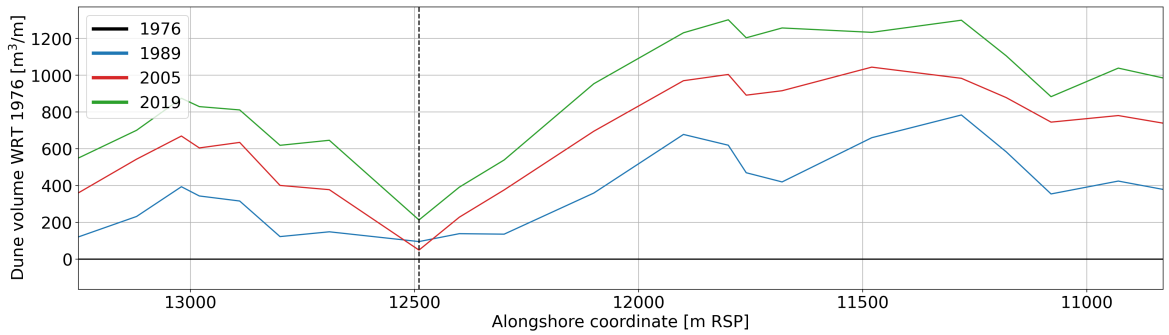

Figure 4.38: Spatial plot of the development of the dune volumes in cluster 21 over time for four different years relative to the dune volumes in 1976. The dashed line shows the location of the beach pavilion.

4.3.6. Cluster 24: De Koog (18.25-20.75km RSP)

This subsection describes the development of cluster 24, which is located on the coast of Texel at De Koog. Figure 4.39 gives an overview of the cluster, which stretches from 18.25 $km\ RSP$ to 20.75 $km\ RSP$. The red circles show the beach pavilions in the cluster and the red lines indicate the small beach houses. The cluster lies at a rather straight part of the coast with a North-West orientation.

The cluster received frequent nourishments since 1984 and an overview of the nourihsments is shown in Figure 4.40. Nourishments in this cluster started in 1984 and most early nourihsments were supplied on the beach. After 2000, most nourishments were supplied on the shoreface, including the largest nourishment in this area which was supplied in 2002.

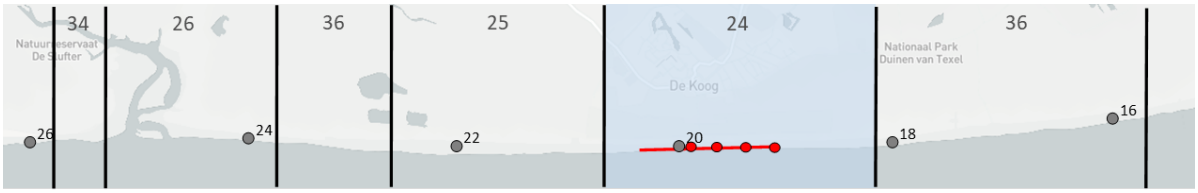

Figure 4.39: Overview of cluster 24 located in the central part of Texel. The cluster boundaries are indicated by the black lines and the cluster numbers are shown at the top of the figure. The numbered circles show the beach poles along the Dutch coast and the buildings on the beach are shown in red.

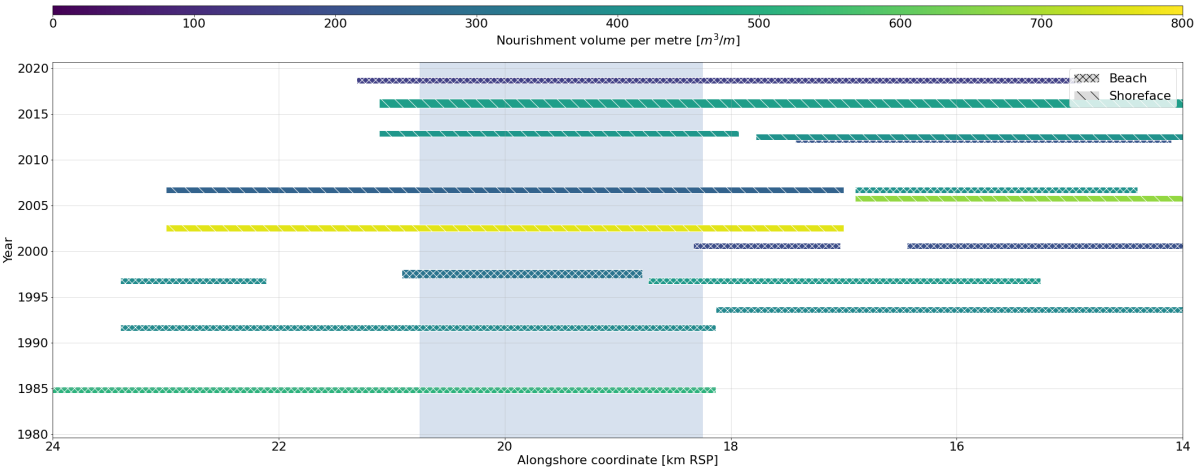

Figure 4.40: Overview of the nourishments in and around cluster 24. The colours indicate the nourishment volumes and the type of nourishment is indicated by the hatch of the boxes.

Figure 4.41 shows the alongshore differences in dune volume development of the cluster. The dune volumes increased in the entire cluster, but there are large alongshore differences. Dune volume increases were largest in the southern part of the cluster and a minimum increase is found at 19.92 $km\ RSP$. The transect at this location crosses a beach pavilion, a beach entrance and a restaurant on top of the dune and could therefore not grow naturally. The development of the dune volume over time is described by Figure 4.42a. The dune volumes in the cluster were relatively constant until 1990 and increased significantly after 1990. The beach width and slope of this cluster fluctuated around 80 metres and 0.035 respectively, which lies around the average of the research area. The dune volume increase did not show any correlation with the beach slope or width.

The development of the dune height is shown in Figure 4.42b. The dune height showed a development similar to the dune volume, with a large increase since 1990. The rate of increase in dune height was largest between 1990 and 2000 and was preceded by a rapid decrease around 1985. In the last three years, the dune height remained constant.

Figure 4.42c shows the development of the shoreline over time. The shoreline was retreating until 1982 and then showed a varying behaviour but with a mean increasing trend. The increasing trend starts around the same time as the nourishments. However, the yearly differences in shoreline location do not show a strong correlation with the supplied nourishments.

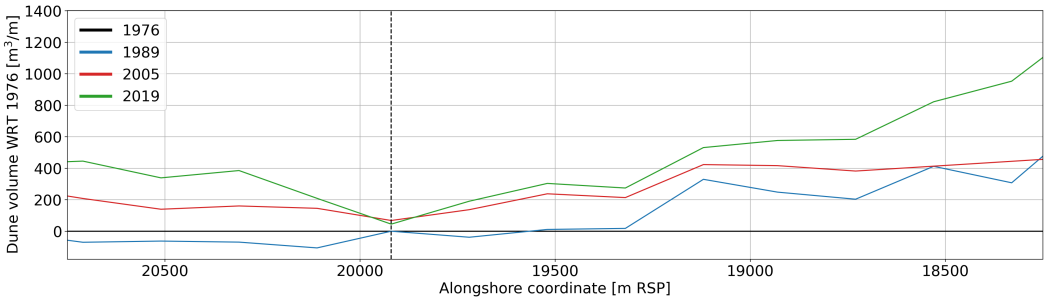

Figure 4.41: Spatial plot of the development of the dune volumes in cluster 24 over time for four different years relative to the dune volumes in 1976.

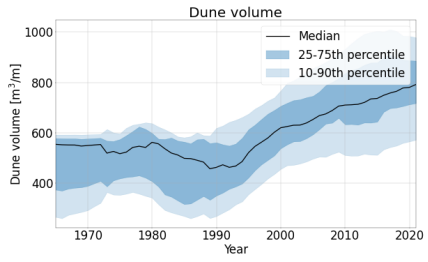

(a) Dune volume

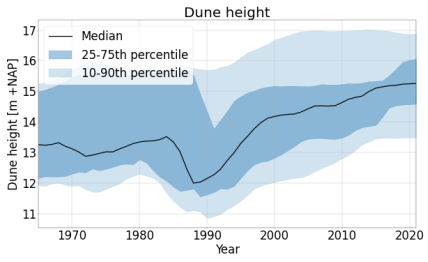

(b) Dune height

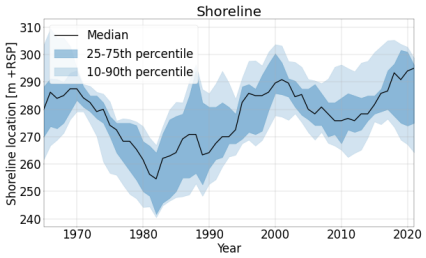

(c) Shoreline

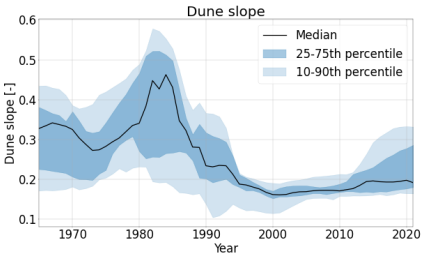

(d) Dune slope

Figure 4.42: Temporal development of the dune volume (a), dune height (b), shoreline location (c) and dune slope (d) of all transects in cluster 24.

4.3.7. Cluster 34: Three locations

This subsection describes cluster 34 which consisted of transects at three different locations in the research area. The three areas are located South of Callantsoog (coastal section 7: 14.25 - 15.75 $km\ RSP$), around Schoorl (coastal section 7: 29.25 - 31.25 $km\ RSP$) and North of the Slufter (coastal section 6: 25.25 - 25.75 $km\ RSP$). The three different locations are different in orientation and nourishment volumes, which is illustrated by Figures fig. 4.43 and fig. 4.44. Furthermore, the northern part of the cluster is influenced by the Slufter and lies close to the Eierlandse Dam while the other two parts lie in coastal section 7. There are no buildings on the beach in any part of this cluster.

Figure 4.43: Overview of cluster 34 that consists of three parts at different locations in the research area.

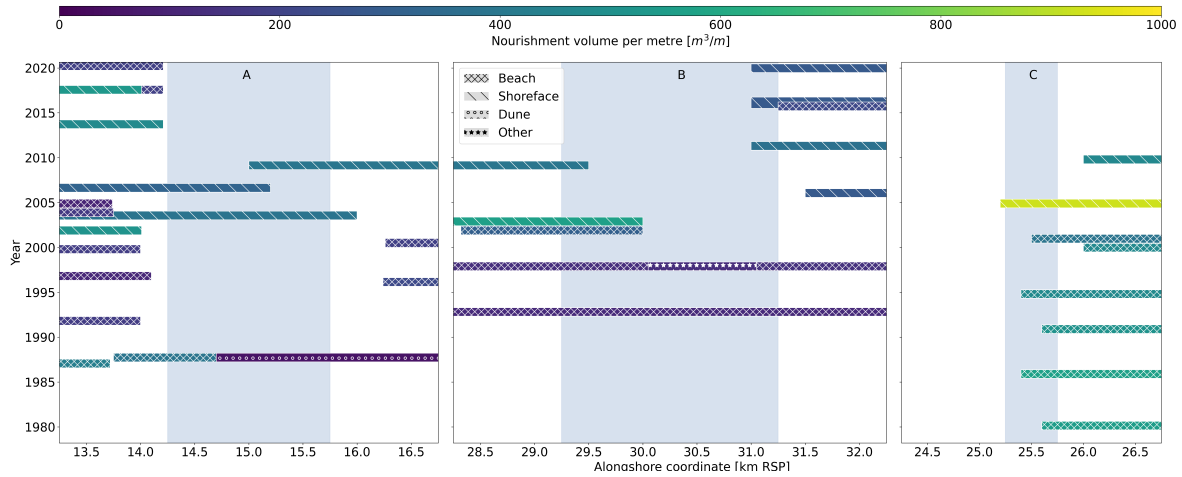

Figure 4.44: Overview of the nourishments in and around cluster 24. The colours indicate the nourishment volumes and the type of nourishment is indicated by the hatch of the boxes. Panel A and B are in coastal section 7 and panel C is in coastal section 6. The figures show the cluster highlighted in blue and a part of the adjacent coast.

While the three different locations lie in different morphological zones, the clustering algorithm categorised the transects into the same cluster. The clustering of the transects was done using the modified transects that were obtained with the smoothing operations. Figure 4.45a shows the smooth transects of the cluster for three different years and different colours were used for the three different parts of the cluster. Although the shape of the profiles of parts A and B differ a lot from the profiles of part C, the changes over time are similar. The profiles show a landward retreat of the most seaward dune between 1965 and 1995. Between 1995 and 2021, most seaward dunes remained around their 1995 location but increased in height.

After comparison of the modified profiles, the real profiles from the original dataset were compared by plotting the profiles of the same years in Figure 4.45b. The figures show that the shape of the profiles of part A and part B are quite similar, while the profiles of part C clearly deviate. The dune tops of the original profiles are higher than the dune tops of the smoothed profiles. The dune

tops were not aligned in the cross-shore direction and the averaging of the profiles in the alongshore direction smoothed out the dune tops. The transects of part C from the original dataset clearly showed a different development than the transects of parts A and B and were therefore left out of the following figures comparing the beach and dune development of parts A and B.

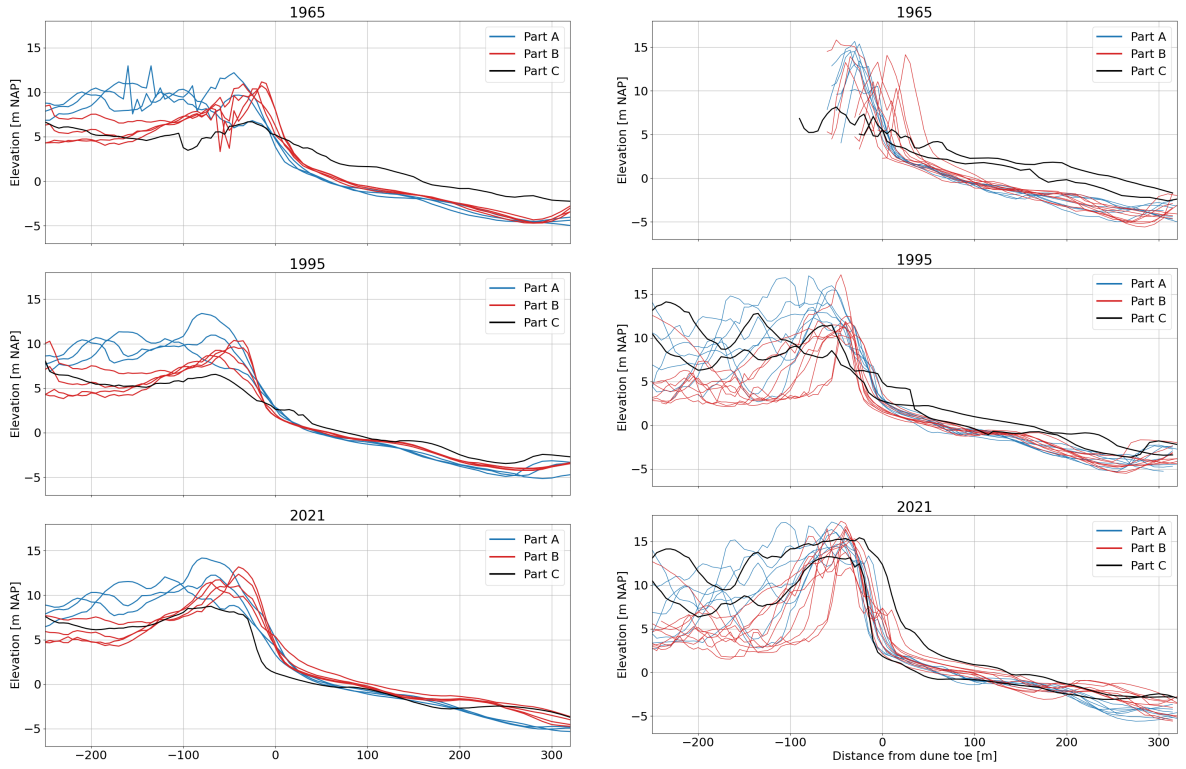

Figure 4.45: Overview of the profiles of the three parts of cluster 34 for the years 1965, 1995 and 2021. The profiles from the modified dataset are shown in panel (a) and the original profiles are shown in panel (b).

The development of the beaches and dunes of parts A and B were compared by plotting the characteristic parameters in time which is displayedin Figure 4.46. Both parts show an increase in dune volume from 1985. The strongest increase in dune volume is observed in part A around 1987 simultaneous with the dune nourishment that was supplied. After 1990, the dune volume of part B increased at a faster rate than the dune volumes in part B.

The two parts of the cluster show a difference in dune height development, the dune height of part A remained rather constant while the dune height of part B increased by approximately 6 metres since 1987. The profiles displayed in Figure 4.45a show that the volume increase in part A is caused by sediment depositions on the dune front, causing a seaward migration and steepening of the dune front slope. The sediment causing the volume increase in part B was deposited on the top and at the toe of the dune, causing an increase in dune height and the creation of embryo dunes.

The beach width and slope of both parts were similar around 1965. The beach slope in the cluster was steeper than the average slope in the research area and showed a clear decreasing trend from approximately 0.040-0.045 to approximately 0.030-0.035. The development of the beach width of part A showed a saw tooth signal with an increase around the nourishments in 1987, 2003, 2007 and 2009 and a decrease in the period afterwards. The effect of the nourishments in part B before 2000 is not clear and the volumes were all lower than 150 m^3/m. The beach width did show an increase around 2004, just after the larger nourishments that were supplied in 2002 in the northern half of part B.

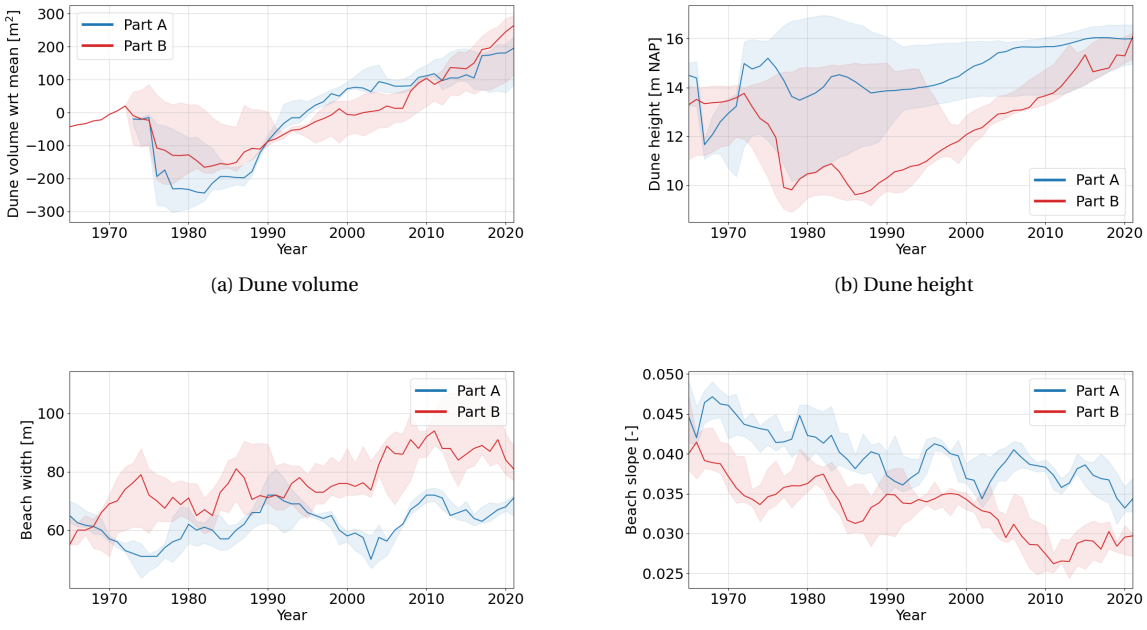

(a) Dune volume

(b) Dune height

(c) Beach width

(d) Beach slope

Figure 4.46: Temporal development of the dune volume (a), dune height (b), beach width (c) and the beach slope (d) of all transects in part A (blue) and part B (red) of cluster 34.

4.3.8. Overall findings

The relationship between different drivers and the beach and dune development was investigated for different clusters. This subsection presents the similarities and differences in relationships of the drivers and the development that were found in the investigated clusters.

The effect of the beach slope and width on the development of the dune volume was investigated in several clusters. The correlation between the beach width or slope and the dune volume changes was investigated for clusters 2, 12, 13, and 24. For all four clusters, there was no clear correlation between the beach width and slope and the development of the dune volume. The dune volume change of every year and transect was calculated and plotted against the beach width and beach slope of the profile of the same year and transect, which is shown in Figure 4.47. Both figures show that the range of dune volume change is very large for every value of the beach width and slope. The mean dune volume change of very large beach widths (>200m) is slightly larger than the total mean of 10 $m^2/year$ and the mean dune volume change for small beach widths (<60m) is slightly lower than the mean. Extreme values of the beach slope do not show large deviations in dune volume change from the mean volume change.

The relationship between the change in beach width and shoreline location and the supplied nourishments was investigated in all clusters. In every cluster, the nourishments either slowed down an erosion trend or caused an accretion trend of the beach. Parts of the coast that received frequent nourishments showed a sawtooth signal, where the beach width increased due to (large) nourishments and the beach width decreased when no or small nourishments were supplied. This effect could be clearly seen in clusters 12, 13 and 24.

The effect of the beach pavilions and the small beach houses was investigated in the highlighted clusters and using the data of the entire research area. The effect of the large beach pavilions on the development of the dune height and volume was clearly visible for every transect that directly crossed a pavilion as was shown for clusters 12, 21, 24 and 33. The effect of the small beach houses was not visible from the figures. Figure 4.48 shows the development of the dune height and volume

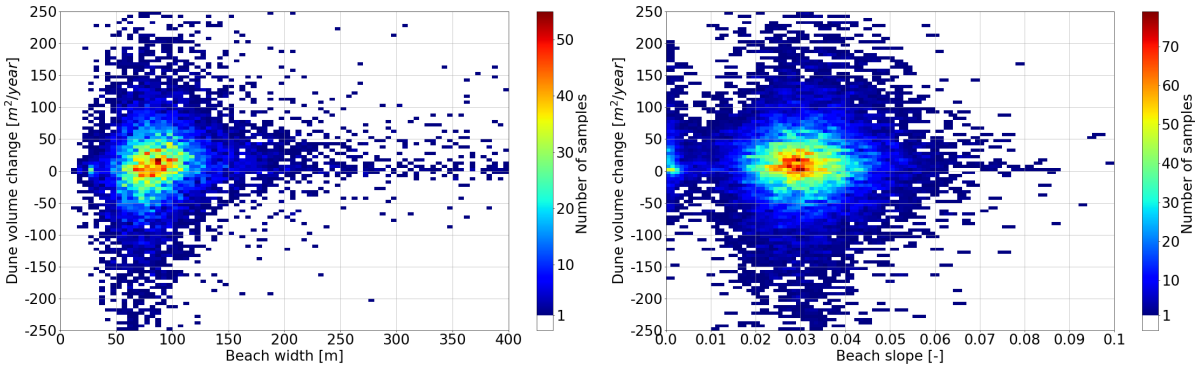

(a) (b)

Figure 4.47: Scatter plot of the dune volume change against the beach width (a) and against the beach slope (b). The figure shows the occurrences of profiles that experienced a certain dune volume change (vertical axis) while the profile had a certain beach width or slope (horizontal axis), using all available profiles in the dataset.

of the entire research area with respect to the temporal mean value of each transect. The figure shows different graphs for transects that cross beach pavilions, transects that cross small beach houses and transects without buildings. The graph for the transects that cross a beach pavilion shows a clear difference from the transects without buildings for both the development of the dune volume and height. The transects that cross small beach houses do not show any significant difference in development from the transects without buildings.

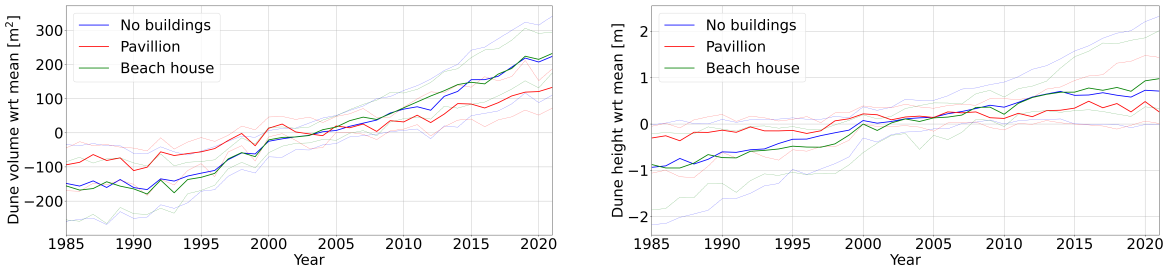

(a) Dune volume (b) Dune height

Figure 4.48: Temporal development of the dune volume (a) and the dune height (b) of all transects in the research area. The figure shows different graphs for transects with no buildings on the beach (blue), transects that cross a large buildling on the beach (red) and transects that cross small beach houses (green). The volumes and heights of the transects are relative to their mean temporal value.

Most beach pavilions in the research area do not have a fixed location and were moved approximately once in every 5 years to allow for seaward migration of the dunes. The beach pavilions at Castricum do have a fixed location and the difference in dune development of this location was compared to the other locations with beach pavilions. The transect at 44.75 $km\ RSP$ directly crossed a large beach pavilion at Castricum and the development of the dune front and beach between 1990 and 2020 is shown in Figure 4.49. The graphs show that the profile of the dune at Castricum stays similar and the dune front does not show a landward or seaward migration. The other transects showed a seaward migration of the dune toe with an average of 19 metres between 1990 and 2020. In addition, the dune fronts of most transects showed a similar seaward migration, with the exception of Castricum and two other transects at 27.16 and 38.75 $km\ RSP$. Satellite images of the transects showed that both pavilions have an access route for supplies at the back of the buildings where sand is removed by bulldozers to maintain the access route.

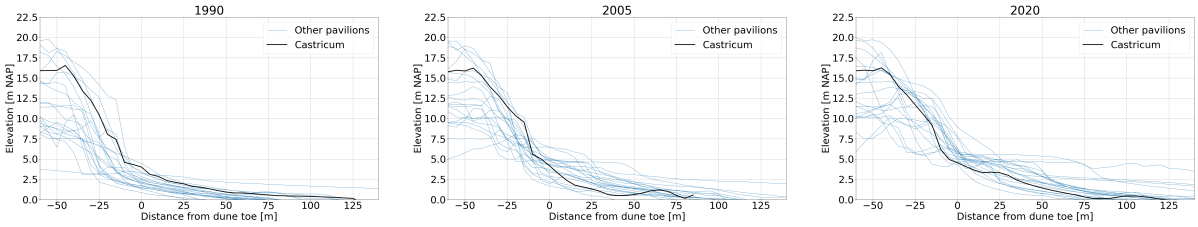

(a) (b) (c)

Figure 4.49: Comparison of the development of the dune fronts of the transects crossing a beach pavilion (blue) with the transect at Castricum (black). The graphs show part of the profiles around the dune toe for 1990 (a), 2005 (b) and 2020 (c).

At several locations in the research area, reed fences have been placed to trap sediment. The dune development of one of these places was investigated at 12 *km RSP* near Callantsoog. The aerial picture of 2013 in Figure 4.50a, showed that several reed fences were placed perpendicular to the coastline. The reed fences were no longer visible in aerial pictures after 2015. The graphs in Figures 4.50b and 4.50c show the elevation of the two highlighted transects, between 2005 and 2020, relative to their temporal mean profiles. Both graphs show a strong increase in elevation at the dune front. The increase in elevation of transect 7001258 between 2008 and 2014 is strongest around -80m RSP, which is at the same location as the reed fences. The elevation increase of transect 7001243 is strongest more landward around -110m RSP.

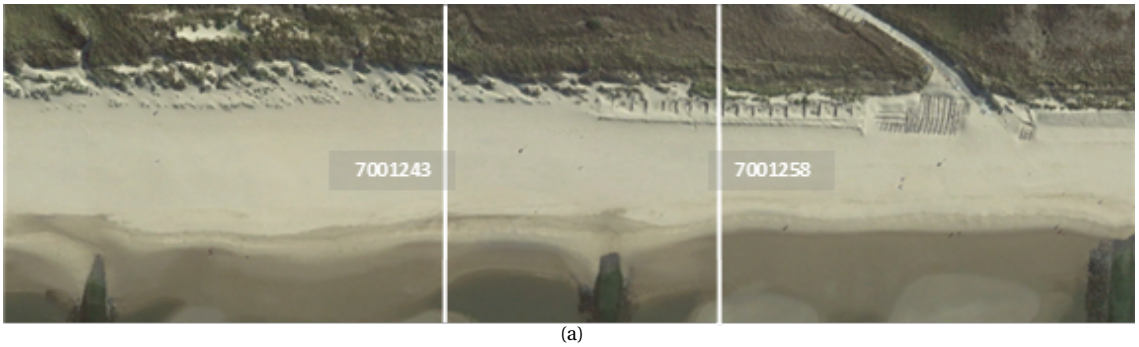

(a)

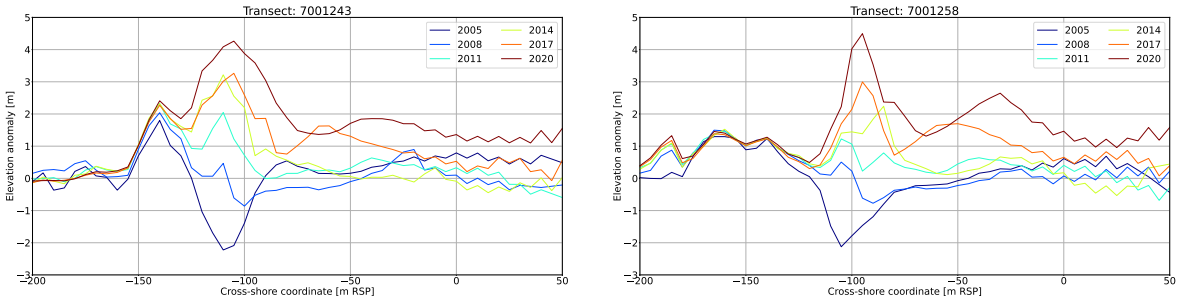

(b) (c)

Figure 4.50: Aerial of the beach near Callantsoog (a), where reed fences were placed to trap sediment. The reed fences can be seen around the dune toe of transect 7001258. The two graphs show the elevation near the dune toe, relative to the temporal mean profile of transects 7001243 (b) and 7001258 (c).

5
Discussion

This section gives a discussion of the results that were presented in Chapter 4. Section 5.1 presents the discussion of the spatial modes and temporal indices that were found using the principal component analysis. The results of the clustering algorithm and the spatial distribution of the clusters are discussed in Section 5.2. The observed beach and dune developments in the clusters were compared with the natural and human drivers and Section 5.3 gives a discussion of the found relationships. Finally, Section 5.4 gives a discussion on the future developments.

5.1. Spatial and temporal decomposition

The results of the spatial and temporal decomposition are described in Section 4.1. The importance of the different modes was described in Table 4.1 and it showed that the explained variance ratio of the different modes decreased rapidly. The first mode described approximately 50% of the variability in elevation in the research area. By using the first twelve modes, the amount of input data for the clustering algorithm could be reduced while preserving 95% of the elevation variability. The reduction of input data decreased the computation time of the clustering algorithm while preserving most of the information in the dataset. The computation time was not a very large issue for this research, but this research demonstrated that the method efficiently reduced the amount of data without losing relevant information and it could be used to reduce the computation time.

Besides the reduction of data, the spatial and temporal decomposition gave insight into the morphological changes in the research area. The temporal indices showed the dominant trends in the dataset, where the first mode showed a rather monotone increasing trend and the second mode had a trend break in 1990. The increasing trend of the first mode showed that in most areas, the beach and dune front increased in height. The mode also showed several locations that mostly experienced erosion, like the coast at Heemskerk and the foreshore of the southwestern corner of Texel, which agrees with the developments described in Chapter 2. The second mode changed in trend in 1990, which was the year that the dynamic preservation policy was adopted. The change in trend from 1990 could be explained by the nourishments, which is found to be the main driver of the shoreline migration. The lower modes showed a cyclic behaviour, which might describe the migration of sand banks and sand waves.

The derived spatial modes and temporal indices do not necessarily contain any physical meaning. The different modes seem to compensate each other at certain locations, when the first mode shows an increasing trend but the second mode showed a decreasing trend before 1990 and an increasing trend 1990, the resulting elevation of the two modes is constant before 1990 and increases rapidly after 1990. As the dataset was decomposed into 57 modes, the combination of the different modes can be very complex and the first three modes might not describe the actual development of a location very well. Additionally, the linear trend of the first mode could be enhanced by the linear interpolation used to fill the missing data of the original dataset.

5.2. Coastal categorisation

This subsection gives a discussion of the coastal categorisation and its results that are shown in Section 4.2. The outcomes of the categorisation depended on the number of clusters that were selected, which was determined using two internal evaluation methods and manual inspections of the profile development. The final number of clusters was based on a subjective judgement of the results and a significantly different result with a similar score would be obtained when the number of clusters was slightly changed. Several cluster boundaries shifted when the number of clusters changed which was illustrated by the low silhouette scores shown in Figure 4.5. Although the optimal number of clusters remains debatable the final results that were obtained showed a similar temporal behaviour of the transects in the clusters, which was the aim of the coastal categorisation.

The number of samples in this research was low compared to the number of features and clusters. Clustering algorithms are usually applied on datasets that have significantly more samples than clusters and more samples per cluster than features. Due to a large number of features, the silhouette scores for different numbers of clusters displayed in Figure 4.2 did not exceed 0.26, while a larger score was desired.

The coastal categorisation worked well on the modified dataset, with small intra-cluster distances between the coastal profiles. However, due to the smoothing operation in the alongshore direction, several local deviations were flattened out by taking average values with the neighbouring transects. Transects that showed large deviations, for example at the locations of beach pavilions, were not accurately represented by the transect in the modified dataset. In addition, smoothing in the alongshore direction made the boundaries between different areas less distinct, which could be one of the reasons for the low silhouette scores at the boundaries of a cluster.

Although local differences were smoothed out, some distinct boundaries between subsections of the coast were found by the coastal categorisation. Cluster 33, which was described in more detail in Subsection 4.3.1, enclosed cluster 2 with a large northern part of the cluster and a smaller part south of cluster 2. The transects in the two parts of cluster 33 showed a similar behaviour that was different from the observed developments in cluster 2. The coastal categorisation placed the transects near Callantsoog in clusters 12 and 13, where the differences in dune development were apparent. Clusters 12 and 13 both showed an increase in dune volume, but the dune volume increase in cluster 13 was found in the embryo dunes which were not formed in cluster 12. Furthermore, cluster 12 was largely influenced by buildings on the beach, which were not present in cluster 13.

The coastal categorisation grouped several transects in three different sections of the research area into cluster 34. Subsection 4.3.7 showed the coastal profiles of the three sections for three different years. Parts A and B of the cluster had a similar profile shape while the profile of part C was clearly different. The changes over time were quite similar with a landward migration before 1995 and a seaward migration after. Most of the weight of the features was put on the EOFs that described the elevation changes, therefore the profiles in a cluster could have a very different shape. However, a higher weight on the features that described the profile shape in this research resulted in clusters with a very similar shape but different temporal development.

Improvements

The number of samples could be increased by using the full surface elevation survey to derive transects with a smaller spacing. The data has a resolution of a few metres and the spacing could therefore be reduced to 20 metres, increasing the sample size by a factor of 25. Using the entire Dutch coastline for the coastal categorisation, instead of only the research area would increase the length of the coastline from 84 kilometres to approximately 350 kilometres. Using both options would yield approximately 17500 samples.

The number of features of the input data could also be reduced using several approaches. When

the number of samples is increased to 17500 and the number of clusters remains at 36, on average there would be 486 samples per cluster which are still less than the 1495 features. Figure 4.3 showed the results of the internal evaluation methods for a model with a reduced number of features. The number of features was reduced by selecting only the first 6 EOFs and by reducing the cross-shore resolution to 25 metres. The silhouette scores improved by approximately 0.05 to a maximum of 0.03, which is still lower than desired.

The number of features could be further reduced when development is not described by the derived EOFs. The development of the transects could be described by the characteristic parameters and optionally some binary features like the presence of a pavilion or blow-out and type of beach (dynamic or fixed) could be added. The temporal behaviour of the characteristic parameters is complex but could be represented by the best fit of low-order polynomials producing several features for each characteristic parameter. A principal component analysis could also decompose the temporal variation of a characteristic parameter of the coastline into several components.

Using a smaller spacing of the transects would solve the problem that several points of interest with small-scale deviations are not represented in the input data. Decreasing the spacing to 20 metres would be sufficient to have transects at every pavilion or blow-out. When data is missing for several locations, the smoothing operations should be improved so that the shape of the profile and properties like dune height and slope are preserved.

5.3. Relationships characteristic variables and drivers

The relationships between the development of the characteristic variables and the drivers were investigated in several highlighted clusters, as well as in the entire research area which was presented in Section 4.3. This section discusses the findings of the beach and dune development, its drivers and their relationships. A discussion of the results of each highlighted cluster can be found in Appendix B.

Increases in dune volume are caused by the aeolian transport of sediment from the beach into the dune and therefore the beach width and slope were expected to influence the changes in dune volume. The effect of the beach width and slope on the dune volume change was investigated for clusters 12, 13, 15 and 24, as well as the correlation for the entire research area displayed in Figure 4.47. The expected effect on the dune volume change was not supported by the data analysis which showed a large spread in volume changes for every beach width and slope. The distribution of the measured values for the beach slope and width of the entire dataset was shown in Figure 4.9. The 10th and 90th percentile for the beach slope were found at 0.0156 and 0.0485 respectively, which results in a factor for the transport rate of 1.0238 and 1.0787. The difference between the upper and lower value of the 10-90th percentile range is quite small and transport rates were therefore expected to be dominated by other varying conditions. The 10th and 90th percentile of the beach width were found at 50 metres and 170 metres respectively. A limited fetch length is required to reach the transport capacity and as the dune volume changes showed no correlation with the beach width it is expected that the required fetch length is less than 50 metres.

The effect of the nourishment on the shoreline position and beach width was clear in several clusters. Clusters 12 and 13 both showed a strong response of the beach width to the large nourishments, with large increases between 2002 and 2007 and between 2014 and 2020. During the period in which the nourishment volumes were low, the beach width rapidly decreased, creating a saw tooth signal. The decreasing trend of the beach width in cluster 15 was also turned into a short increasing trend after the nourishment in 2009. The nourishments in cluster 33 were only supplied in parts of the cluster. The parts that received shoreface nourishments did show a strong seaward migration of the shoreline which demonstrates the effectiveness of the nourishments. The results in all clusters showed that the nourishments have a strong effect on the beach width and shoreline lo-

cation. However, parts of the coast that received frequent nourishment showed faster erosion rates when no nourishments were supplied than the erosion rates of areas that did not receive frequent nourishment. The nourished coastline is further away from its equilibrium profile, causing faster erosion rates.

Several highlighted clusters had buildings on the beach that blocked the aeolian transport. The buildings on the beach were divided into two categories, small beach houses that are placed in rows with small gaps between the buildings and the remaining larger buildings. The effect of the larger buildings could be seen in the development of the dune volume in clusters 13, 21 and 33. The dune volume changes behind the buildings compared to the adjacent coast were significantly smaller. The effect of the small beach houses was not visible. The smaller buildings allowed for sediment transport between the beach houses so that the dunes could grow. The graphs in Figure 4.48 illustrated the difference between profiles without buildings and profiles with small or larger buildings. The smaller beach houses do not show any effect on the dune volume or height development.

The larger buildings are regularly moved due to their effect on the dune development. Figure 4.49 compared the dune front development of transects with buildings that are moved to a transect at Castricum where the buildings are not moved. The seaward movement of the buildings allows for the dune toe to grow in the seaward direction. Although the transport to the dunes is partially blocked by the buildings, regularly moving them seaward allowed for dune volume increase mainly around the dune toe. At several villages like Egmond aan Zee, Bergen aan Zee and Callantsoog there is no room at the landward side of the dunes to grow, which requires a seaward migration of the dune front to grow and guarantee safety in the future.

The effect of blow-outs was visible in cluster 2, which was the only highlighted cluster where the transects crossed blow-outs. Two transects that crossed a blow-out showed a large increase in dune volume behind the most seaward dune. The main wind direction comes from the southwest which is also visible in the orientation of the blow-outs. Because of the wind direction, sediment that is transported behind the dune through the blow-out comes from the coast just south of the blow-out. The adjacent coast just south of the blow-out at transect 4900 did show erosion which could be caused by the blow-out (see Figure 4.20). The blow-outs affect the airflow and could cause slight erosion of the dunes next to it, the erosion volumes were however much smaller than the accretion volume in the dunes behind the blow-out. When there is enough room for dunes to grow on the landward side of the most seaward dune, blow-outs can significantly increase the dune volume and flood safety.

The effects of the maintenance works of HHNK were investigated separately at several locations. Reed fences were placed near Callantsoog which trapped sediment from aeolian transport. Reed fences are used to trap the sediment at the desired location, which in this case was the dune toe. Development of the coastal profile showed that a lot of sediment was trapped between the reed fences and therefore the dune migrated seaward. A comparison with the adjacent transect showed that the fences did not cause any significant effect on the net dune volume change, only a change in the cross-shore location of the sediment deposition. The reed fences showed to be effective to trap sediment in the required location, but the effects on the net volume increases could not be accurately assessed from one case.

Several clusters that were not investigated thoroughly showed a very different behaviour than the adjacent coast due to coastal structures or tidal channels. The transects in these clusters were grouped in many different weight configurations and were also placed close to each other on the lattice of Figure 4.6. This was the case for the transects near the Eierlandse dam, which created very wide beaches at the northern part of Texel, the transects near the Texel inlet and the transects close to the breakwater of IJmuiden. The two coastal structures and the tidal inlet governed most of the developments in their proximity.

The largest and most monotone increases in the dune volume of the highlighted clusters were

found in clusters 15 and 21. Cluster 15 showed a constant increase over the entire time span, while cluster 21 had a trend break in the rate of change around 1991. Both clusters had a beach width and slope around the median value of the research area. Figures 4.28 and 4.35 showed the bathymetry near the clusters. Both clusters have shoals close to the coastline which could affect the incoming wave energy. The ebb-tidal delta of the Texel inlet has shoals in the north-northwest direction of cluster 15, which is the main direction of larger storms. The shallow sea bed causes dissipation of energy from the incoming waves, limiting the wave attack on the dunes behind it. The shoals of the ebb-tidal delta lie southwest of cluster 21 and do not reduce the incoming wave energy during large storms from the north-northwest. The cluster does have a shallow foreshore and the shoals of the ebb-tidal delta reduce the incoming wave energy from the west. Reduction of the incoming wave energy in these two clusters reduced the erosion volumes and allowed for a rapid dune volume increase.

5.4. Future developments

Several predictions for the future development of the natural drivers were presented in Section 2.4. The sea-level rise showed a rather constant rate before 1993 which has increased by 33% after 1993. The increased rate could cause more shoreline retreat, which has been effectively countered by the nourishments. The increased rate of the sea-level rise requires larger nourishment volumes. However, the median dune height increase of the research area between 1993 and 2021 is approximately one metre, which increased at a much faster rate than the sea-level.

The amount of storms and the corresponding surge levels are not expected to increase in the future. Large storm surge levels are the major reason of dune erosion as the waves can directly hit the dune toe when the water level is high. The frequency of storms coming from the west-southwest is expected to increase, but wind from the west-southwest creates lower storm surge levels due to the shorter fetch length. Therefore the erosion volumes during storms are not expected to increase in the future.

The effect of the human drivers on the beach and dune development plays an important role. The beach and dune development under the current management strategy are mainly governed by the additional available sand due to nourishment. The human activities disturb the natural development of the coastline, which makes it harder to predict the future development of the coast. The buildings on the beach showed a clear effect on the dune development. The parts of the dunes that are affected by these buildings showed hardly any volume increase and might become weak spots with the future sea levels if they are not regularly moved.

6

Conclusions and Recommendations

The aim of this research was to get more insight into the developments of the beaches and dunes in the management area of HHNK. This research focused on the relationship between characteristic parameters that describe the coastal profile and natural and human drivers. Section 6.1 describes the conclusions of the research and gives answers to the research questions. Section 6.2 gives recommendations for further research.

6.1. Conclusions

The main goal of the research was to gain insight into the beach and dune development of the Dutch coast by analysing the JarKus data set and relating the outcomes to physical processes. The first step of this research identified the main drivers of beach and dune development. A literature study provided information on the relevant drivers for the research area which were further investigated by comparing the observed development of several clusters with the drivers. Tidal inlets and coastal structures showed a strong effect on the surroundings and caused large spatial differences in morphological development. Both drivers mainly showed a local effect and did not influence the more distant coastlines. After 1990, shoreline migration was found to be mainly governed by noursihment, which is the main driver for the development in the research area. The growth of dunes in the research area depends on the supply of sand by aeolian transport and the erosion of sand during storms. Several factors influence the erosion volumes during storms, including the storm conditions and the bathymetry of the foreshore. According to literature, aeolian transport is influenced by the beach width and slope, but no correlation between these variables was found. Buildings on the beach and blow-outs had a local effect on the dune volume changes.

After identifying the natural and human drivers, the transects of the research area were categorised based on their morphological development. An overview of the spatial distribution of the clusters was given in Section 4.2. The coastal categorisation method was able to identify different alongshore locations that showed a similar development of the beaches and dunes of the modified profiles. Modifications of the dataset smoothed out small-scale details in the profiles, which made it less suitable to investigate the effect of small-scale processes. When the number of clusters was changed, the boundaries of the clusters shifted and other locations were grouped, but all transects within a cluster showed a similar development of the beaches and dunes until the number of clusters became too small (<36). Therefore, several different categorisations could provide a solid answer to the second research question. Several locations were clustered together regardless of the number of clusters which were located near a structure or inlet that produced unique morphological conditions, like the coast near IJmuiden and De Hors among others.

The third research question focused on the relationship between the observed developments and the identified drivers. The strongest relationship was found between the nourishments and the shoreline migration. The increased sand volumes due to nourishments effectively maintained

the shoreline and the effect of the nourishments over time agreed with the research of Brand et al. (2022). The beach width and slope were expected to show a relationship with the dune volume increases, but no correlation was found for the investigated clusters. The beach width was assumed to be predominantly larger than the critical fetch length and therefore large enough to reach the aeolian transport capacity. The fluctuations of the beach slope in time did not show any effect on the dune volume changes in contrast with the findings of de Vries et al. (2012), who found a small correlation between the beach slope and dune volume changes. The fluctuations in the beach slope of the investigated clusters were assumed to be too small to cause significant changes in dune volume change compared to the annual variations in wind climate and erosive events. The effect of the tidal cycles was mainly found on a local scale, where the migration of the tidal channels influenced the shoreline location. The shoals of the ebb-tidal delta reduced the incoming wave energy at the adjacent coasts which reduced the erosion volumes during storms. Buildings on the beach and blow-outs showed a relationship with the local dune volume changes, but no effect on the adjacent coastline. Aeolian transport was blocked by the buildings hindering the dune growth, while blow-outs allowed for more aeolian transport from the beach to the back of the dune increasing the dune volume locally.

The future coastal development of the research area is hard to predict due to the large number of drivers that affect the development. The results showed that the developments in the research area greatly depend on nourishment. The nourishments are designed based on observations and disturb the natural development of the Dutch coast, which made it impossible to predict future developments in the research area. However, some predictions for future changes in natural drivers were available. The rate of sea-level rise is expected to increase which increases the required nourishment volumes to counter the shoreline retreat. Furthermore, the change in wave direction of the extreme events is expected to change, which could make certain areas that are now shielded by shoals during extreme events, like cluster 15, more vulnerable. There are no predicted changes in the occurrences of extreme events that could increase the erosion volumes at the other parts of the coastline. The large sediment availability caused by frequent nourishment facilitated the large dune volume changes throughout the research area, which showed an increasing rate after 1990.

The last research question concerned the added value of this research on the management strategy of the Hoogheemraadschap Hollands Noorderkwartier. The coastal categorisation was done to get insight into which regions showed a similar development of the dunes and beaches. The algorithm eventually produced 36 clusters of transects with a similar development of the modified profiles. The clusters do give insight into the long-term and large-scale developments like an increase or decrease of dune volume and the migration of the shoreline. However, most maintenance and management work of HHNK consists of smaller-scale activities that were smoothed out by the data modifications. Several improvements of the coastal categorisation were proposed to include smaller-scale developments in the method. Furthermore, some effects on smaller scales were investigated within the clusters. The results supported the hypothesis that large buildings on the beach hinder the dune growth. The dunes behind smaller beach houses did not show any significant difference in development from the undisturbed coastline and the current regulations for the beach houses would allow for sufficient dune growth. Relocation of the larger buildings on the beach in the cross-shore direction allows for a seaward migration of the dune front, while relocation in the alongshore direction could allow for more natural growth of the dune volume. The dunes located at blow-outs showed a large increase in dune volume behind the most seaward dune, but this is only possible if enough space is available on the landward side of the dune. Reed fences trapped sediment at the desired location but did not cause a net dune volume increase.

6.2. Recommendations

This section gives several recommendations for improvements of the used methods and possibilities for further research on the development of the beaches and dunes along the Dutch coast. The research used a coastal categorisation to partition transects of the HHNK area, which comprises only a part of the Dutch coast and the JarKus measurements. The annual surface elevation data is available for the entire Dutch coast and the categorisation could therefore be extended to cover the entire coastline.

Besides changing the spatial scale, changes can be made to the temporal scale. The developments in the research area showed different behaviour before and after 1990. This research investigated the similarities in both the period before 1990 as well as after 1990, while the development changed significantly. By using the measurements after 1990, only the development of the transects under the current management strategy is compared which better resembles the development in future scenarios.

Analysis of the relationships between characteristic variables and the drivers used both a quantitative analysis and a qualitative analysis. The quantitative analysis was mainly performed between the different characteristic variables and not with the drivers. Including more data on the drivers like annual wind and wave climate variations and storm surge levels could give better insight into the relationships between these drivers and the observed developments. Furthermore, the effect of more maintenance works could be investigated to study their effect on the beach and dune development. To study the effect of the measures, the dates and locations where the maintenance works are performed should be known.

Finally, several improvements of the model were proposed to get better results in the coastal categorisation phase. Modification of the data to fill missing values significantly changed the profile shapes and characteristics. Improvements in the data modification method could preserve the profile shape and small-scale characteristics. Additionally, the coastal categorisation could be improved by increasing the number of samples and reducing the number of features so that the number of samples is significantly larger than the number of features. The number of samples could be increased by using the full elevation survey data of the entire Dutch coastline and smaller spacing between the transects. The number of features could be reduced by using fewer EOFs or by using a different set of features such as features based on the characteristic variables. However, an analysis of the relationships between the drivers and the beach and dune development in the HHNK area does not require the coastal categorisation phase and it is recommended to use the categorisation only on a larger scale.

References

P. Athanasiou, A. van Dongeren, A. Giardino, M. Vousdoukas, J.A.A. Antolinez, and R. Ranasinghe (2021). A clustering approach for predicting dune morphodynamic response to storms using typological coastal profiles: A case study at the dutch coast. *Frontiers in Marine Science*, 8. ISSN 22967745. doi: 10.3389/fmars.2021.747754.

F. Baart, G. Rongen, M Hijma, H. Kooi, R. de Winter, and R. Nicolai (2019). Zeespiegelmonitor 2018. de stand van zaken rond de zeespiegelstijging langs de nederlandse kust.

M.A.J. Bakker, S. Van Heteren, L.M. Vonhgen, A.J.F. Van Der Spek, and B. Van Der Valk (2012). Recent coastal dune development: Effects of sand nourishments. *Journal of Coastal Research*, 28:587–601. ISSN 07490208. doi: 10.2112/JCOASTRES-D-11-00097.1.

W. Bodde, R. Huiskes, S. IJff, H. Kramer, L. Kuiters, G. Lagendijk, J. Leenders, S. Ouwerkerk, M. Scholl, M. Smit, N. Smits, R. Stuurman, B. vd Valk, A. Verheijen, D. de Vries, and C. Wegman (2019). Innovatieproject hondsbossche duinen eindrapportage, definitief 0.1.

M. Boers (1999). Suppleties bij egmond en bergen. *RIKZ-99.030*.

E. Brand, G. Ramaekers, and Q.J. Lodder (2022). Dutch experience with sand nourishments for dynamic coastline conservation – an operational overview. *Ocean and Coastal Management*, 217. ISSN 09645691. doi: 10.1016/j.ocecoaman.2021.106008.

P. Bruun (1962). Sea-level rise as a cause of shore erosion. *Journal of the Waterways and Harbors division*, 88(1):117–130.

J. Cleveringa (2001). Zand voor zuidwest texel technisch advies rikz over vier mogelijke ingrepen in het zeegat van texel.

J. Andrew G. Cooper and Orrin H. Pilkey (2004). Sea-level rise and shoreline retreat: time to abandon the bruun rule. *Global and Planetary Change*, 43(3-4):157–171. doi: 10.1016/j.gloplacha.2004.07.001. URL `https://doi.org/10.1016/j.gloplacha.2004.07.001`.

S. de Vries, H.N. Southgate, W. Kanning, and R. Ranasinghe (2012). Dune behavior and aeolian transport on decadal timescales. *Coastal Engineering*, 67:41–53. ISSN 0378-3839. doi: https://doi.org/10.1016/j.coastaleng.2012.04.002. URL `https://www.sciencedirect.com/science/article/pii/S0378383912000725`.

S. de Vries, H.N. Southgate, W. Kanning, and R. Ranasinghe (2012). Dune behavior and aeolian transport on decadal timescales. *Coastal Engineering*, 67:41–53. ISSN 03783839. doi: 10.1016/j.coastaleng.2012.04.002.

R.C. De Winter and B.G. Ruessink (2017). Sensitivity analysis of climate change impacts on dune erosion: case study for the dutch holland coast. *Climatic Change*, 141(4):685–701.

R.C. De Winter, F. Gongriep, and B.G. Ruessink (2015). Observations and modeling of alongshore variability in dune erosion at egmond aan zee, the netherlands. *Coastal Engineering*, 99:167–175.

Deltares (2013). Voorbeelden van dynamisch kustbeheer.

Deltares (2018). Coastviewer. https://www.openearth.nl/coastviewer-static/.

E. Diamantidou, G. Santinelli, A. Giardino, J. Stronkhorst, and S. De Vries (2020). An automatic procedure for dune foot position detection: Application to the dutch coast. *Journal of Coastal Research*, 36:668–675. ISSN 15515036. doi: 10.2112/JCOASTRES-D-19-00056.1.

O. Durán, P. Claudin, and B. Andreotti (2011). On aeolian transport: Grain-scale interactions, dynamical mechanisms and scaling laws. *Aeolian Research*, 3(3):243–270.

E.P.L. Elias and A. Bruens (2013). Beheerbibliotheek Noord-Holland.

E.P.L. Elias and J. Cleveringa (2003). Morfologische analyse van de ontwikkeling van het nieuwe schulpengat en de aangrenzende kust. *Rapportnr.: 2003.040*.

E.P.L. Elias and Ad J.F. Van Der Spek (2006). Long-term morphodynamic evolution of texel inlet and its ebb-tidal delta (the netherlands). *Marine Geology*, 225:5–21. ISSN 00253227. doi: 10.1016/j.margeo.2005.09.008.

E.P.L. Elias and A.J.F. van der Spek (2017). Dynamic preservation of texel inlet, the netherlands: understanding the interaction of an ebb-tidal delta with its adjacent coast. *Netherlands Journal of Geosciences*, 96(4):293–317. doi: 10.1017/njg.2017.34.

E.P.L. Elias, C. van Oeveren, and A. Bruens (2014). Beheerbibliotheek Texel feiten en cijfers ter ondersteuning van de jaarlijkse toetsing van de kustlijn.

I. Fairley, M. Davidson, K. Kingston, T. Dolphin, and R. Phillips (2009). Empirical orthogonal function analysis of shoreline changes behind two different designs of detached breakwaters. *Coastal Engineering*, 56:1097–1108. ISSN 03783839. doi: 10.1016/j.coastaleng.2009.08.001.

A. Giardino, J. Mulder, J. Ronde de, and J. Stronkhorst (2011). Sustainable development of the dutch coast: Present and future. *Journal of Coastal Research*, (61 (10061)):166–172.

V. Gornitz. Storm surge. In *Encyclopedia of Coastal Science*, pages 912–914. Springer Netherlands (2005). doi: 10.1007/1-4020-3880-1_298. URL https://doi.org/10.1007/1-4020-3880-1_298.

C. Hallin, B.J.A. Huisman, M. Larson, D.R. Walstra, and H. Hanson (2019). Impact of sediment supply on decadal-scale dune evolution — analysis and modelling of the kennemer dunes in the netherlands. *Geomorphology*, 337:94–110. ISSN 0169-555X. doi: https://doi.org/10.1016/j.geomorph.2019.04.003. URL https://www.sciencedirect.com/science/article/pii/S0169555X19301436.

C.J. Hapke, N.G. Plant, R.E. Henderson, W.C. Schwab, and T.R. Nelson (2016). Decoupling processes and scales of shoreline morphodynamics. *Marine Geology*, 381:42–53. ISSN 00253227. doi: 10.1016/j.margeo.2016.08.008.

J. Hardisty and R.J.S. Whitehouse (1988). Evidence for a new sand transport process from experiments on saharan dunes. *Nature*, 332(6164):532–534. doi: 10.1038/332532a0. URL https://doi.org/10.1038/332532a0.

HHNK (2018). Waterprogramma 2016-2021.

HHNK (2021). Waterplan 2022-2027.

C. Hinton and R.J. Nicholls (1998). Spatial and temportal behavior of depth of closure along the holland coast. *Coastal Engineering Proceedings*, (26).

P. Hoekstra and A. Stolk (1990). The dutch coastal zone: An outline of physical processes and coastal morphodynamics. *Journal of Coastal Research*, pages 358–375. ISSN 07490208, 15515036. URL http://www.jstor.org/stable/44868645.

B.M. Hoonhout and J. Van Thiel de Vries (2013). Invloed van strandbebouwing op zandverstuiving, adviezen voor vergunningverlening. *Deltares, Delft*.

C. Houser, C. Hapke, and S. Hamilton (2008). Controls on coastal dune morphology, shoreline erosion and barrier island response to extreme storms. *Geomorphology*, 100(3-4):223–240.

J.D. Iversen and K.R. Rasmussen (1999). The effect of wind speed and bed slope on sand transport. *Sedimentology*, 46(4):723–731. doi: 10.1046/j.1365-3091.1999.00245.x. URL https://doi.org/10.1046/j.1365-3091.1999.00245.x.

N.L. Jackson and K.F. Nordstrom (2011). Aeolian sediment transport and landforms in managed coastal systems: A review. *Aeolian Research*, 3:181–196. ISSN 18759637. doi: 10.1016/j.aeolia.2011.03.011.

L. Jänicke, A. Ebener, S. Dangendorf, A. Arns, M. Schindelegger, S. Niehüser, I.D. Haigh, P. Woodworth, and J. Jensen (2021). Assessment of tidal range changes in the north sea from 1958 to 2014. *Journal of Geophysical Research: Oceans*, 126(1). doi: 10.1029/2020jc016456. URL https://doi.org/10.1029/2020jc016456.

KNMI (2022a). Zware stormen in nederland sinds 1910. https://www.knmi.nl/nederland-nu/klimatologie/lijsten/zwarestormen. Accessed: 24-08-2022.

KNMI (2022b). Klimaatviewer; windroos de kooy. https://www.knmi.nl/klimaat-viewer/grafieken-tabellen/windrozen/windroos-de-kooy.

D.L. Kriebel and R.G. Dean (1993). Convolution method for time-dependent beach-profile response. *Journal of Waterway, Port, Coastal, and Ocean Engineering*, 119:204–226. doi: 10.1061/(ASCE)0733-950X(1993)119:2(204).

M. Larson, M. Capobianco, H. Jansen, G. Rózyński, H.N. Southgate, M. Stive, K.M. Wijnberg, and S. Hulscher (2003). Analysis and modeling of field data on coastal morphological evolution over yearly and decadal time scales. part 1: Background and linear techniques.

C. Laustrup, H.T. Madsen, P. Sorensen, and I. Broker (1996). Comparison of beach and shoreface nourishment Torsminde Tange, Denmark. *Coastal Engineering Proceedings*, 1(25). doi: 10.9753/icce.v25.\%p. URL https://icce-ojs-tamu.tdl.org/icce/index.php/icce/article/view/5441.

J.K. Leenders, C. Wegman, W. Bodde, and A. Verheijen (2018). Optimalisatie veiligheidsontwerp hondsbossche duinen.

T. Louters and F. Gerritsen (1994). The riddle of the sands: A tidal systems answer to a rising sea level.

T. Soni Madhulatha (2012). An overview on clustering methods. *CoRR*, abs/1205.1117. URL http://arxiv.org/abs/1205.1117.

J.K. Miller and R.G. Dean (2007). Shoreline variability via empirical orthogonal function analysis: Part ii relationship to nearshore conditions. *Coastal Engineering*, 54:133–150. ISSN 03783839. doi: 10.1016/j.coastaleng.2006.08.014.

J.P.M. Mulder, S. Hommes, and E.M. Horstman (2011). Implementation of coastal erosion management in the netherlands. *Ocean & Coastal Management*, 54(12):888–897. ISSN 0964-5691. doi: https://doi.org/10.1016/j.ocecoaman.2011.06.009.

KF Nordstrom and SM Arens (1998). The role of human actions in evolution and management of foredunes in the netherlands and new jersey, usa. *Journal of Coastal Conservation*, 4(2):169–180.

A.P. Oost and P.A.H. Kleine Punte (2003). Autonome morfologische ontwikkeling westelijke waddenzee: Een doorkijk naar de toekomst. *Rapportnr.: 2004.021*.

N.G. Plant, E.R. Thieler, and D.L. Passeri (2016). Coupling centennial-scale shoreline change to sea-level rise and coastal morphology in the gulf of mexico using a bayesian network. *Earth's Future*, 4(5):143–158. doi: 10.1002/2015ef000331. URL https://doi.org/10.1002/2015ef000331.

D.W. Poppema and J.P.M. Mulder (2020). The effect of buildings on the morphological development of the beach-dune system literature report. ISSN 1568-4652.

D.W. Poppema, K.M. Wijnberg, J.P.M. Mulder, and S.J.M.H. Hulscher (2022). Deposition patterns around buildings at the beach: Effects of building spacing and orientation. *Geomorphology*, 401: 108114.

R. Ranasinghe, D. Callaghan, and M.J.F. Stive (2012). Estimating coastal recession due to sea level rise: Beyond the bruun rule. *Climatic Change*, 110:561–574. ISSN 01650009. doi: 10.1007/s10584-011-0107-8.

H. Ridderinkhof (1988). Tidal and residual flows in the western dutch wadden sea i: Numerical model results. *Netherlands Journal of Sea Research*, 22(1):1–21. ISSN 0077-7579. doi: https://doi.org/10.1016/0077-7579(88)90049-X. URL https://www.sciencedirect.com/science/article/pii/007775798890049X.

Rijkswaterstaat (2020). Kustgenese 2.0: kennis voor een veilige kust.

Rijkswaterstaat (2021). Kustlijnkaarten 2021. https://puc.overheid.nl/doc/PUC_629858_31.

D.J.A Roelvink, A. Reniers, A. van Dongeren, J.S.M. van Thiel de Vries, R. McCall, and J. Lescinski (2009). Modelling storm impacts on beaches, dunes and barrier islands. *Coastal Engineering*, 56: 1133–1152. ISSN 03783839. doi: 10.1016/j.coastaleng.2009.08.006.

A.B. Smith, D.W.T. Jackson, J.A.G. Cooper, and L. Hernández-Calvento (2017). Quantifying the role of urbanization on airflow perturbations and dunefield evolution. *Earth's Future*, 5:520–539. ISSN 23284277. doi: 10.1002/2016EF000524.

R.C. Steijn and C. Jeuken (2000). Vier mogelijke beheersingrepen in het zeegat van texel : morfodynamische modelberekeningen. URL https://puc.overheid.nl/rijkswaterstaat/doc/PUC_40855_31/.

M.J.F. Stive, S.G.J. Aarninkhof, L. Hamm, H. Hanson, M. Larson, K.M. Wijnberg, R.J. Nicholls, and M. Capobianco (2002). Variability of shore and shoreline evolution. *Coastal Engineering*, 47:211–235. URL www.elsevier.com/locate/coastaleng.

STOWA (2010). Hoe verder met dynamisch kustbeheer?

J. Sündermann and T. Pohlmann (2011). A brief analysis of north sea physics. *Oceanologia*, 53(3): 663–689. doi: 10.5697/oc.53-3.663. URL https://doi.org/10.5697/oc.53-3.663.

T.J. Van Heuvel (1999). Evaluatie van zeewaarste kustverdediging. *RIKZ-99.009*.

C.O. Van Ijzendoorn (2021). Jarkus analysis toolbox. https://github.com/christavanijzendoorn/JAT.

C.O. van IJzendoorn, S. de Vries, C. Hallin, and P.A. Hesp (2021). Sea level rise outpaced by vertical dune toe translation on prograding coasts. *Scientific Reports*, 11. ISSN 20452322. doi: 10.1038/s41598-021-92150-x.

M.E.B. van Puijenbroek, J. Limpens, A.V. de Groot, M.J.P.M. Riksen, M. Gleichman, P.A. Slim, H.F. van Dobben, and F. Berendse (2017). Embryo dune development drivers: beach morphology, growing season precipitation, and storms. *Earth Surface Processes and Landforms*, 42(11):1733–1744.

L.C Van Rijn (1997). Sediment transport and budget of the central coastal zone of holland. *Coastal Engineering*, 32(1):61–90.

A. van Rooijen and J.S.M. van Thiel de Vries (2014). Stormgedreven morfodynamiek van de slufter, texel. doi: 10.13140/RG.2.1.4924.7849. URL https://www.researchgate.net/publication/280067301.

W.A.C. van Santen (1999). Morphodynamics of the nieuwe schulpengat area, texel inlet, the netherlands.

H.J. Verhagen and H. van Rossum (1990). Strandhoofden en paalrijen. evaluatie van hun werking.

T. Vermaas (2012). Analyse bruikbaarheid gecombineerde hoogtedata hollandse kust: pilotstudie naar het combineren van hoogtedata uit verschillende bronnen.

Z.B. Wang, P. Hoekstra, H. Burchard, H. Ridderinkhof, H.E. De Swart, and M.J.F. Stive (2012). Morphodynamics of the wadden sea and its barrier island system. *Ocean & Coastal Management*, 68:39–57. ISSN 0964-5691. doi: https://doi.org/10.1016/j.ocecoaman.2011.12.022. URL https://www.sciencedirect.com/science/article/pii/S0964569112000026. Special Issue on the Wadden Sea Region.

Z.B. Wang, E.P.L. Elias, A.J.F. van der Spek, and Q.J. Lodder (2018). Sediment budget and morphological development of the dutch wadden sea: impact of accelerated sea-level rise and subsidence until 2100. *Netherlands Journal of Geosciences*, 97(3):183–214. doi: 10.1017/njg.2018.8.

C. Wegman and J. Leenders (2020). Profielverandering door suppleties en zeespiegelstijging, kustlijn hollands noorderkwartier. HKV.

R.C. De Winter, A. Sterl, J.W. De Vries, S.L. Weber, and G. Ruessink (2012). The effect of climate change on extreme waves in front of the dutch coast. *Ocean Dynamics*, 62:1139–1152. ISSN 16167341. doi: 10.1007/s10236-012-0551-7.

M. Wittebrood, S. de Vries, P. Goessen, and S. Aarninkhof (2018). Aeolian sediment transport at a man-made dune system; building with nature at the hondsbossche dunes. *Coastal Engineering Proceedings*, (36):83–83.

M. Yedla, S.R. Pathakota, and T.M. Srinivasa (2010). Enhancing k-means clustering algorithm with improved initial center. *International Journal of computer science and information technologies*, 1(2):121–125.

N.C. Zwarenstein Tutunji (2021). Classification of coastal profile development in the hoogheemraadschap hollands noorderkwartier area. using advanced data analysis techniques. URL http://resolver.tudelft.nl/uuid:3d95c3a6-76a7-44c6-bbbb-99412fd028ab.

Appendices

A

PCA Results

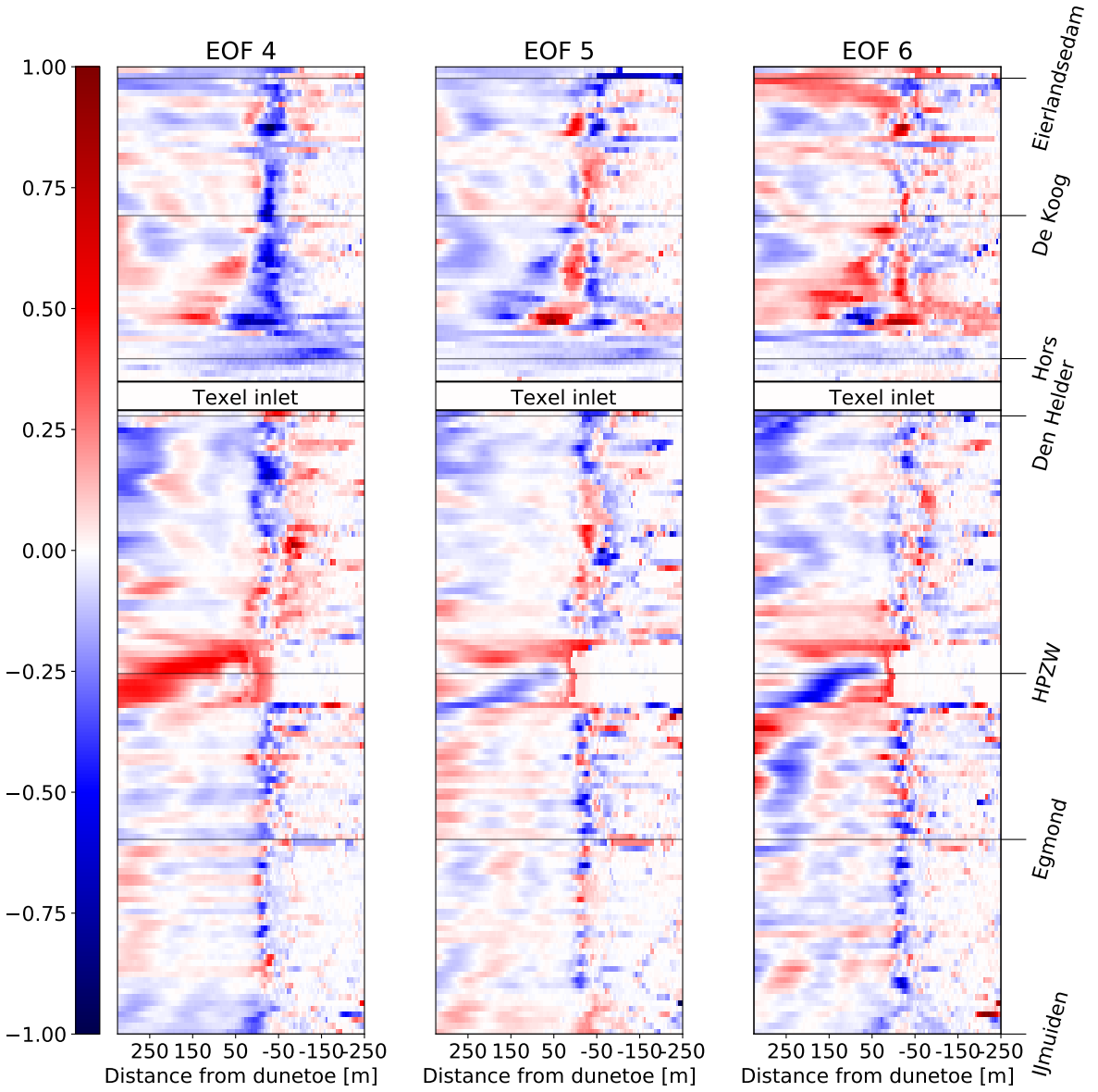

(a)

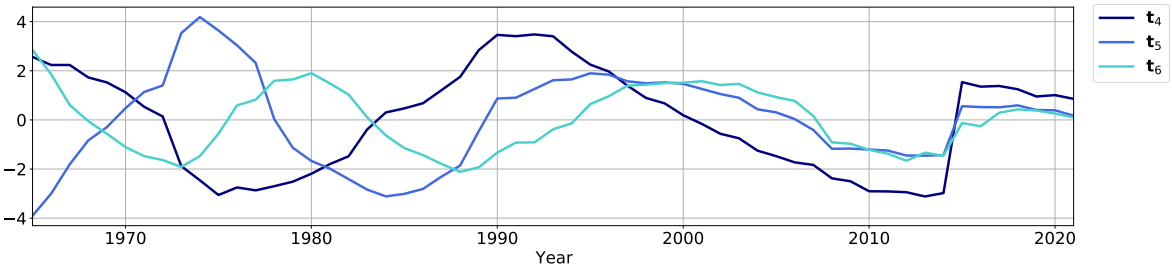

(b)

Figure A.1: Spatial modes 4, 5 and 6 (a) showing the spatial distribution of elevation variance in the different modes across the research area. The elevation variance within the mode of every location is directly proportional to the corresponding temporal index with a proportionality coefficient equal to the values indicated by the colours. Temporal indices 4, 5 and 6 (b) show the temporal development of the elevation of each mode.

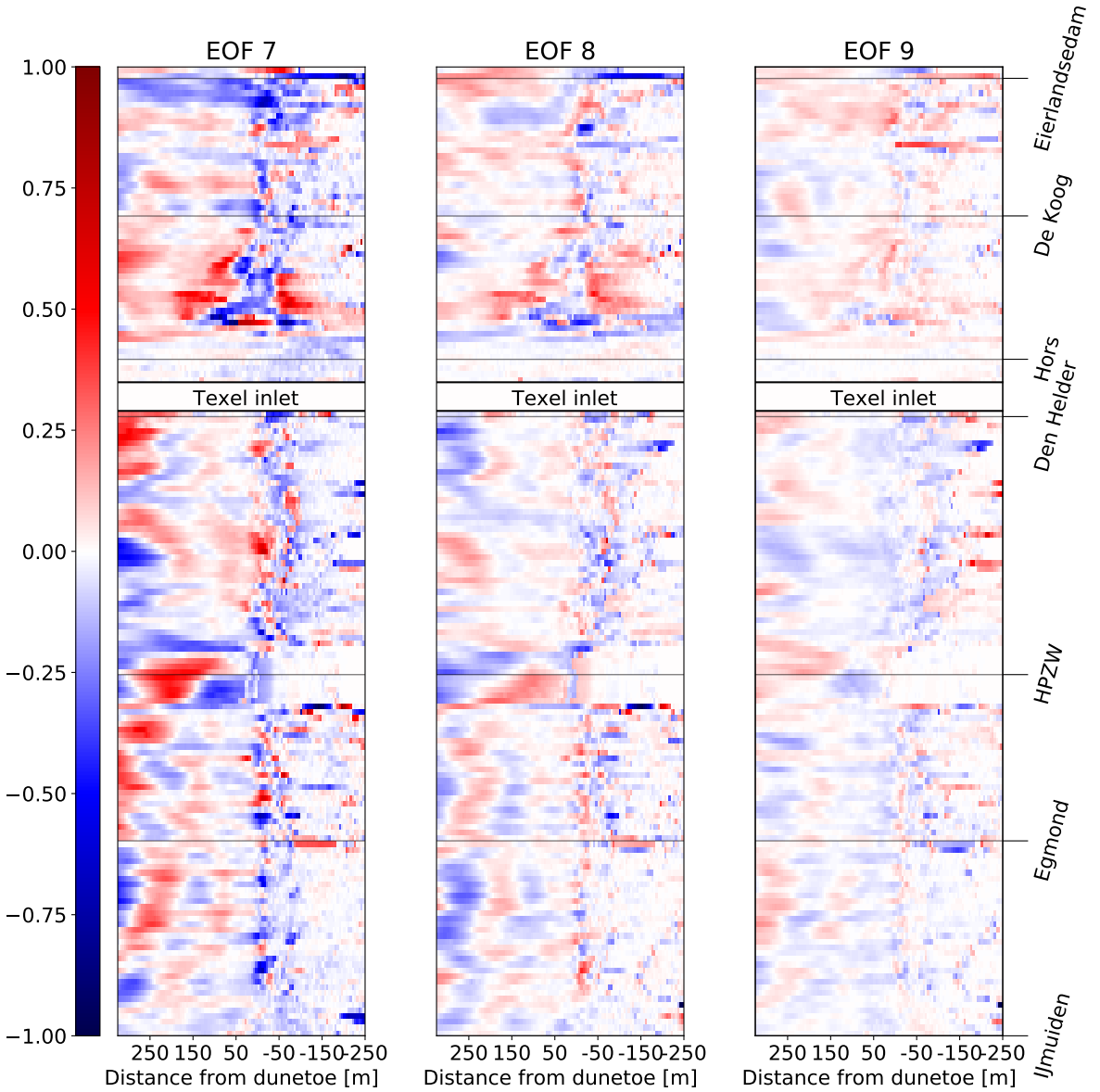

(a)

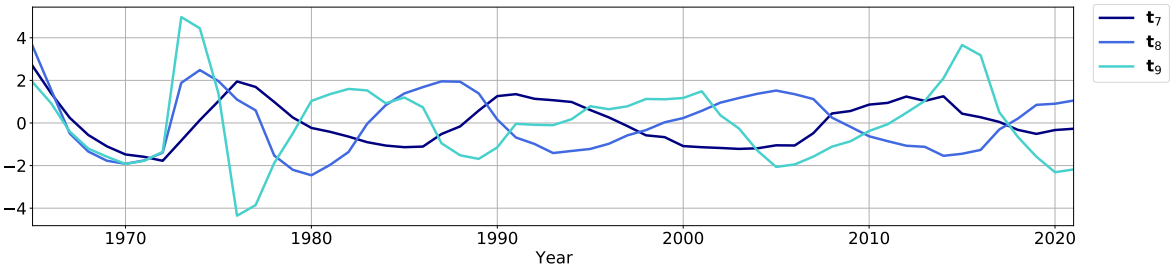

(b)

Figure A.2: Spatial modes 7, 8 and 9 (a) showing the spatial distribution of elevation variance in the different modes across the research area. The elevation variance within the mode of every location is directly proportional to the corresponding temporal index with a proportionality coefficient equal to the values indicated by the colours. Temporal indices 7, 8 and 9 (b) show the temporal development of the elevation of each mode.

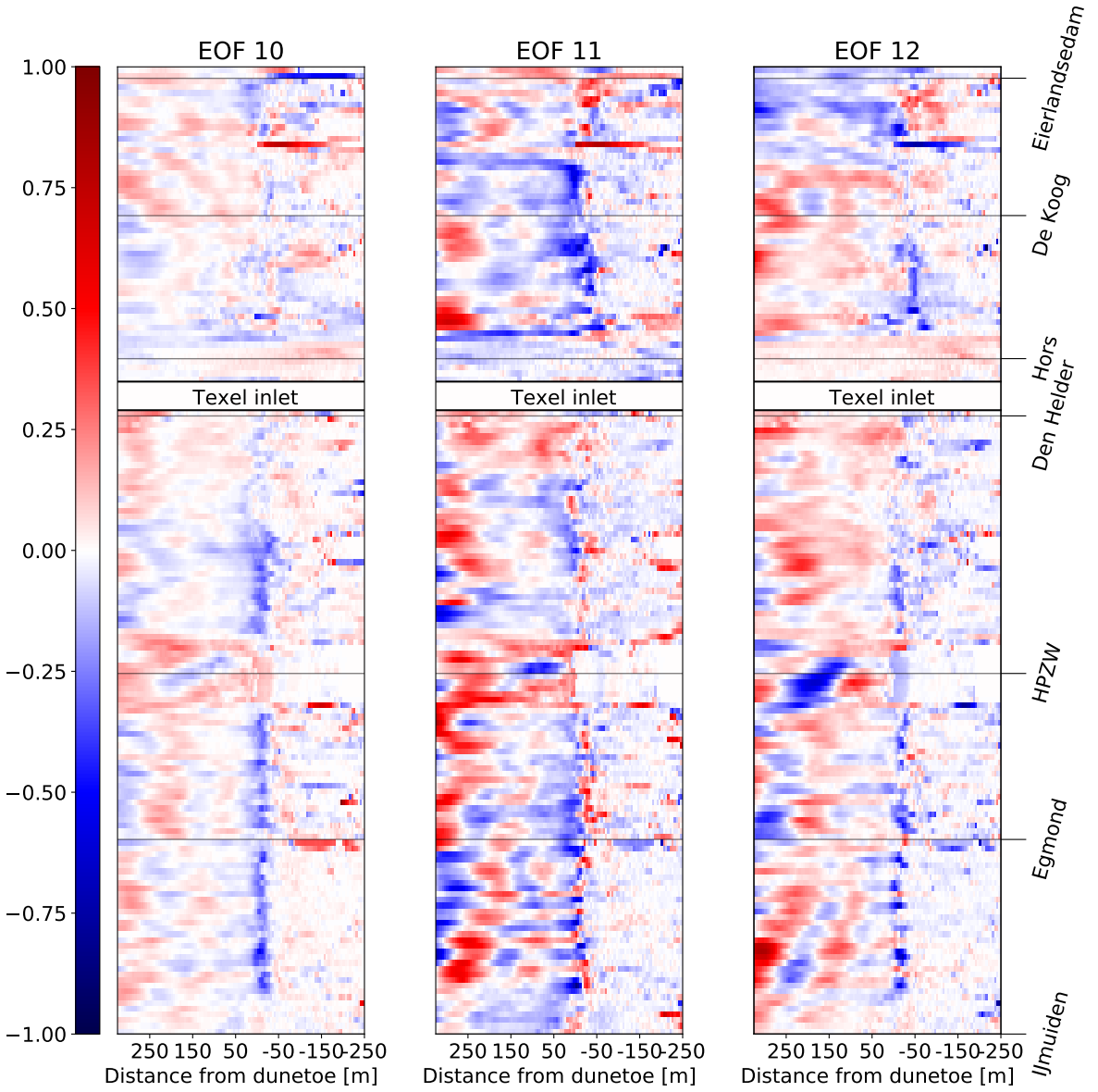

(a)

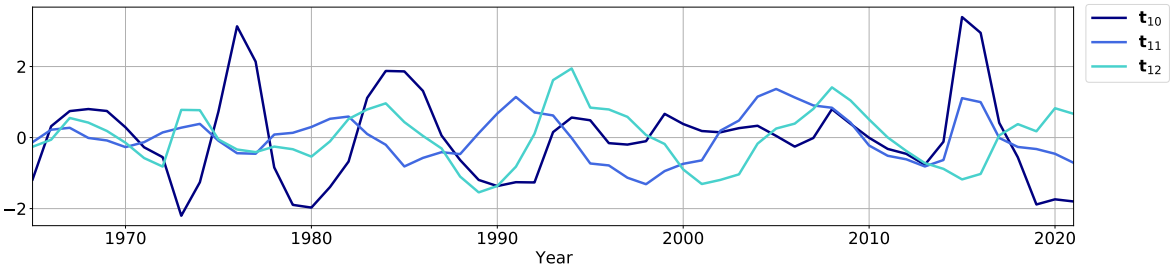

(b)

Figure A.3: Spatial modes 10, 11 and 12 (a) showing the spatial distribution of elevation variance in the different modes across the research area. The elevation variance within the mode of every location is directly proportional to the corresponding temporal index with a proportionality coefficient equal to the values indicated by the colours. Temporal indices 10, 11 and 12 (b) show the temporal development of the elevation of each mode.

B

Highlighted clusters discussion

This appendix gives a discussion of the clusters that were selected to investigate the relationships between different characteristic parameters that describe the coastal profiles and the drivers. The clusters were selected to obtain a set of clusters with a difference in morphological behaviour, nourishment volumes, dune types, location and orientation. Section 4.3 gives a detailed description of the development of these highlighted clusters and some of the relevant drivers in the area. The results of the clusters are discussed in the following sections, following the same order as the results.

B.1. Cluster 33: Egmond - Wijk aan Zee (38.25-47.75 & 50.75-51.75km RSP)

This cluster covering the southern part of the research area showed both dune growth and seaward migration of the shoreline and dune toe. The seaward migration of the shoreline was strongest between 2005 and 2019 at the locations where nourishments were supplied. The supplied volumes of sand have effectively moved the shoreline seaward since 2005 at the locations where the trend from 1979 to 1999 was erosive, around 44 $km\ RSP$.

The dunes have grown in volume and height in most parts of the research area. The dataset does not show a strong correlation between the dune growth and the beach width and slope, while the beach width and slope were expected to influence the aeolian transport and therefore on the dune growth. The beach widths of this cluster mainly lie in the range of 60 to 110 metres, which is around the average of 85 metres of the entire research area. The beach width is assumed to be sufficiently wide to reach transport capacity and therefore no effect of the variations in beach width were found.

There are many buildings on the beach in this cluster as was shown in Figure 4.10. Two transects in this cluster crossed beach pavillions indicated by the dashed lines in Figures 4.13 and 4.14. The dunes at these two transects were growing between 1979 and 2005, but showed a constant volume and a decrease in height between 2005 and 2019. The buildings on these transects block the aeolian transport of sand onto the dunes, which could be the main cause of the decrease in volume and halt in vertical growth.

B.2. Cluster 2: Heemskerk (47.75-50.75km RSP)

The results of cluster 2 are shown in Subsection 4.3.2 and showed a large landward migration of the dune toe. The erosive trend of this coastline is probably caused by the breakwater of IJmuiden, which blocks the alongshore transport south of this cluster. The net transport direction along the Dutch coast is to the North, but sediment can not pass the port of IJmuiden. The breakwaters of IJmuiden block the incoming wave energy from the West-southwest direction, causing a lower transport flux into the cluster from the southern boundary. Cluster 2 is not shielded by the breakwaters and therefore transport fluxes caused by the waves increase in this area which causes erosion in the

cluster. The landward migration of the shoreline and dune toe could be increased by the sea-level rise, which causes a landward migration to obtain a profile in equilibrium with the new water level.

The erosive trends were countered by nourishments in most subsections of the research area. Nourishment volume and frequency were below average in cluster 2, which could be one of the reasons that the landward migration did not halt in this cluster. The effect of the largest nourishment, a foreshore nourishment in 2012 spanning a large part of the cluster, can be seen clearly from the development of the beach width. The beach width shows a large jump around 2014, two years after the foreshore nourishment. Figure 2.17b showed that most of the foreshore nourishment volume is present on the beach 3 to 4 years after the nourishment. The foreshore nourishment is therefore expected to be the main factor for the increased beach width. The dune toe shows some seaward migration in 2017, which could be caused by the beach nourishment.

The dune volumes in the cluster showed large alongshore differences. Two transects showed a large increase in dune volume while the other transects remained rather constant or decreased in volume. The two transects with a large volume increase directly crossed blow-outs in the dunes. The blow-outs caused a local increase in dune volume as sediment could be transported through the blow-outs, on the landward side of the primary dune. Sediment deposition at the landward side of the dune can hardly erode as there is no wave attack. The adjacent dunes did not show any changes in behaviour that could be explained by the blow-outs.

The beach slope and width of this cluster were varying around the average values of the research area and were therefore expected to be of minor importance to the difference in dune development of this cluster compared to the other clusters. The cluster did have a steep dune slope, which could be one of the reasons that the dunes did not increase in height. The steep dune slopes presumably made the dunes more susceptible to dune erosion during storms. The largest dune erosion volumes are caused by avalanching of the dune front when the slope gets too steep. The steep slope of the dunes could lower the required incoming wave energy for avalanching to take place.

B.3. Clusters 12 and 13: Callantsoog (12.75-14.25 & 11.25-12.75km RSP)

This section describes the development of the beaches and dunes of clusters 12 and 13. Clusters 12 and 13 cover the coast near Callantsoog in the northern part of the Noord-Holland coast. Both clusters had a narrow beach until 2000, with a width of approximately 50 to 60 metres. An increase in beach width was observed from 2000, which is probably caused by the large nourishment volumes that were supplied in the area. Significant erosion was observed between 2008 and 2012 and no nourishments were supplied in those years, which indicates that the nourishments are necessary to maintain the coastline.

The dune volumes increased in both clusters from 1987 and the large decrease in 1985 for cluster 13 was caused by the change in transects for which the data was measured. The rate of increase in dune volume was constant for cluster 12 but increased in cluster 13. The dune volume increases were lowest in the areas where buildings on the beach were present. The buildings on the beach blocked the aeolian tranpsort of sand into the dunes and therefore limited the dune growth. The area with the embryo dunes showed the largest increase in dune volume between 2007 and 2019. Growth of embryo dunes can only occur if there are no large erosion events where waves attack the newly formed dunes van Puijenbroek et al. (2017). The wider beach and milder beach slope could have reduced the erosion volumes by dissipating more wave energy. Furthermore, there were no large storms (≥ 10 Beaufort) between 2007 and 2013 at the Dutch coast (KNMI, 2022a), which allowed for the embryo dunes to grow.

B.4. Cluster 15: Julianadorp (6.25-9.75km RSP)

The developments of the beaches and dunes of cluster 15 are described in Subsection 4.3.4. Both the dune volume and dune height increased significantly throughout the investigated period. The beach slope and width were expected to influence the dune growth as they influence the aeolian transport. The beach slope directly affects the transport capacity and the beach width only affects the transport rate when the fetch length is not sufficient to reach the full transport capacity of the wind. However, the development of the dunes did not show any correlation with the beach width or the beach slope. The beach width in this cluster was above the average of the research area and could be larger than the required fetch length to reach full transport capacity, limiting its effect on the dune growth. The beach slope varied between 0.0275 and 0.0375, which results in a factor for the critical velocity varying between 1.023 and 1.032 and for the transport rate varying between 0.722 and 0.644. The difference in aeolian transport caused by the slope and width of the beach will therefore be small compared to the differences caused by the annual variations in wind climate.

Changes in dune volume and height are not only governed by the aeolian transport, which causes dune growth, but also by the erosive events. Dune erosion occurs when waves reach the dune toe, which typically occurs during storms. The wide beach of this cluster reduces the incoming wave energy on the dune front. The main wave direction during extreme events in the research area comes from the North-northwest. Waves approaching this cluster from the NNW direction cross the shoal of the ebb-tidal delta of the Texel inlet, which could significantly reduce the incoming wave energy and therefore reduce the erosion of the dunes. The reduction of the wave energy by these shoals could be the main contributing factor to the large increase in dune volume of this cluster. The predicted change in wave direction during extreme events, from the North-northwest to the West-southwest (Winter et al., 2012), could increase the erosion volumes during storms in the future.

Landward migration of the tidal channel Nieuwe Lands Diep caused erosion of the beach of cluster 15. The beach width showed a decrease from 110 to 80 between 1965 and 1990. After 1990 the beach width remained rather constant, which could be caused by the stabilisation of the location of the Nieuwe Schulpengat and the Franse Bankje. The beach width showed an increase after 2009 for about 6 years, caused by the foreshore nourishments over the entire cluster. The effect of the nourishment is visible for about 6 to 7 years, which agrees with the expected development over time of foreshore nourishment volumes shown in Figure 2.17b.

The dune height is increasing rapidly along with the dune volume in this cluster, which is in contrast to the other investigated clusters of the Noord-Holland coast. The dune heights in clusters 12 and 13 remained constant while dune volumes increased. The difference in dune height increase could be caused by the differences in dune slope. Cluster 15 had a mild dune slope compared to the other investigated clusters along the Noord-Holland coast. When the dune slope increases, sediment particles require a larger force to be transported up the slope and might be deposited on the dune front, limiting the growth in the dune height. The investigated clusters of the Texel coast, with milder dune slopes, showed a similar increase in dune height.

B.5. Cluster 21: South West Texel (10.75-13.25km RSP)

The development of cluster 21 was described in Subsection 4.3.5. the shoreline of the cluster showed a large retreat until 1990. The retreat of the shoreline can be explained by the movement of the tidal channel that showed a landward migration. Nourishments in this area started around 1990 and have effectively maintained the shoreline at a constant location.

The dune volume in the area showed a large increase over the entire period, even when the shoreline was retreating. The beach width and slope of the cluster fluctuated around values that are

average for the research area. The amount of sand that could be transported into the dunes is therefore expected to not be limited by these factors. The main reason for the dune growth in therefore expected to be the lack of large erosion events. The shoal in front of the cluster protects the coast from waves coming from the west and southwest direction. Which is the main wave direction in the area. The shoal does not extend far enough to shield the coast from the North-northwest direction where the waves during most extreme events come from, but the offshore area is relatively more shallow than for other parts of the research area.

The dune volume increased in every part of the cluster, but the increase in dune volume was significantly smaller at 12 $km\ RSP$. The difference in volume change is probably caused by the presence of the beach pavilion at this location. The beach pavilion blocked the aeolian transport of sand into the dunes and therefore limited the dune growth of this transect. The small beach houses around the pavilion do not remain on the beach during the entire year, which could be one of the reasons that no reduction in dune growth was seen here. Furthermore, the beach houses are smaller in width and height and there is some space in between the houses which allows for aeolian transport into the dunes.

The dune height of this cluster showed a strong increase similar to the dune volume. The rate at which the dune height increased, reduced in the last five years, while the dune volume kept increasing at a similar rate. The dune slope increased significantly since 2005 from a very mild to an average slope. The increase in dune slope could be the reason for the reduction in the rate of change of the dune height. When the dune slope increases, sediment particles require a larger force to be transported up the slope and might be deposited on the dune front, limiting the growth in the dune height.

B.6. Cluster 24: De Koog (18.25-20.75km RSP)

Subsection 4.3.6 described the developments of cluster 24 that covers a part of the Texel coast, at De Koog. The dune volume increased in the entire cluster between 1976 and 2019. The dune volume increase was largest in the southern part of the cluster. This part of the cluster has less influence of human activities and buildings on the beach. The dune volume increase at the highlighted transect in Figure 4.41 was significantly lower than in the other parts of the cluster. This transect crosses a beach pavilion, the beach entrance and a restaurant on top of the dune, which made the dune growth practically impossible. The dune volume increases from 2005 to 2019 are smallest between 19 $km\ RSP$ and 20 $km\ RSP$, which could be caused by the small beach houses that are present in this part of the cluster.

The median dune volume of the cluster remained constant until 1980. The dune volume slightly decreased with about 100 m^3/m until 1992 and the dune slope during this period was steep with a median dune slope larger than 0.4. The decrease in volume was accompanied by a relatively larger decrease in dune height. The steep dune slope might have made the dune more susceptible to wave attack, as dune erosion mainly occurs in the form of avalanching when the dune becomes to steep. The median dune volume and height increased after 1990. The increase did not show a relation with the beach width or slope. The beach width and slope oscillated around values that were average for the research area. The beach slope varied between 0.03 and 0.04, which resulted in a aeolian transport reduction factor varying between 0.701 and 0.626. The maximum difference in the reduction factor of 12% was expected to be negligible to the annual variations in wind climate and erosive events.

The development over time of the shoreline of this cluster was shown in Figure 4.42c. The shoreline showed a landward migration until 1980. The shoreline migration changed direction around 1982, just before the first nourishment in the area. The change in direction was shown ahead of

the first nourishment due to the moving average that was applied to remove the seasonal fluctuations from the data. The actual seaward shoreline migration started after the first nourishment and showed a strong correlation with later nourishments. The supplied sediment effectively restored the former shoreline location.